BIOLOGICAL DAMAGE OF UV RADIATION IN ENVIRONMENTS OF F-TYPE STARS

by

SATOKO SATO

Presented to the Faculty of the Graduate School of
The University of Texas at Arlington in Partial Fulfillment
of the Requirements
for the Degree of

DOCTOR OF PHILOSOPHY

THE UNIVERSITY OF TEXAS AT ARLINGTON
May 2014

I dedicate this to my daughter Akari Y. Sato.

Acknowledgements

First of all, I would like to thank my supervising professor Dr. Manfred Cuntz. His advice on my research and academic life has always been invaluable. I would have given up the Ph.D. bound program without his encouragement and generous support as the supervising professor during a few difficult times in my life. I would like to thank Dr. Wei Chen, Dr. Yue Deng, Dr. Zdzislaw E. Musielak, and Dr. Sangwook Park for their interest in my research and for their time to serve in my committee.

Next, I would like to acknowledge my research collaborators at University of Guanajuato, Cecilia M. Guerra Olvera, Dr. Dennis Jack, and Dr. Klaus-Peter Schröder, for providing me the data of F-type evolutionary tracks and UV spectra.

I would also like to express my deep gratitude to my parents, Hideki and Kumiko Yakushigawa, for their enormous support in many ways in my entire life, and to my sister, Tomoko Yakushigawa, for her constant encouragement to me. I am grateful to my husband, Makito Sato, and my daughter, Akari Y. Sato. Their presence always gives me strength. I am thankful to my parents-in-law, Hisao and Tsuguho Sato, and my grand-parents-in-law, Kanji and Ayako Momoi, for their financial support and prayers. I would like to thank God for His guidance and my friends at Japanese Baptist Church of North Texas for their kindness and support with prayers during the years in college and graduate school.

Finally, I would like to acknowledge all of my teachers and friends that I have known throughout my education. I believe their influence in my life in varying degrees made me who I am, and enabled me to achieve a Ph.D. degree.

April 14, 2014

Abstract

BIOLOGICAL DAMAGE OF UV RADIATION IN ENVIRONMENTS OF F-TYPE STARS

Satoko Sato, Ph.D.

The University of Texas at Arlington, 2014

Supervising Professor: Manfred Cuntz

I investigate the general astrobiological significance of F-type main-sequence stars with special consideration to stellar evolutionary aspects due to nuclear evolution. DNA is taken as a proxy for carbon-based macromolecules following the assumption that exobiology is most likely based on hydrocarbons. The DNA action spectrum is utilized to represent the relative damage of the stellar UV radiation. Planetary atmospheric attenuation is taken into account in the form of parameterized attenuation functions. My work is motivated by previous studies indicating that the UV environment of solar-like stars is one of the most critical elements in determining the habitability of exoplanets and exomoons. It contributes further to the exploration of the exobiological suitability of stars that are hotter and emit much higher photospheric UV fluxes than the Sun. I found that the damage inflicted on DNA for planets at Earth-equivalent positions is between 2.5 and 7.1 times higher than for solar-like stars, and there are intricate relations for the time-dependence of damage during stellar main-sequence evolution. If atmospheric attenuation is included, however, less damage is obtained in alignment to the attenuation parameters. Also,

the outer part of late F-type stars have similar UV conditions to Earth. Therefore, F-type circumstellar environments should not be excluded from candidates for habitable places on the grounds of higher stellar UV emission than the Sun. Besides the extensive theoretical component of this study, emphasis is furthermore placed on applications to observed planetary systems including CoRoT-3, WASP-14, HD 197286, HD 179949, υ And, and HD 86264.

Table of Contents

Acknowledgements iv

Abstract v

List of Illustrations ix

List of Tables xii

1. Introduction 1

2. Previous Results 9

2.1 Previous Results by Cockell (1999) 9

2.2 UV Habitable Zone Based on Buccino et al. (2006) 11

3. Theoretical Approach 14

3.1 Stellar Habitable Zones 14

3.2 The DNA Action Spectrum 21

3.3 Planetary Atmospheric Attenuation 23

4. Application to F-type Stars 27

4.1 Background Information of F-type Stars 27

4.1.1 Properties of F-type Main-sequence Stars 27

4.1.2 Stellar Radiation from F-type Main-sequence Stars 28

4.1.3 Evolution of F-type Main-sequence Stars 32

4.1.4 Beyond F-type Stars: Effects of Nuclear and Magnetic Evolution in Other Types of Main-sequence Stars 37

4.2 Habitability around General F-type Main-sequence Stars 42

4.2.1 Stellar Case Studies 42

4.2.2 Habitability in Consideration of F-star Evolution 57

5. Application to Known F-type Planetary Systems 66
5.1 Selection of F-type Planetary Systems 66
5.1.1 Example (1): CoRoT-3 Planetary System 67
5.1.2 Example (2): WASP-14 68
5.1.3 Example (3): HD 197286 69
5.1.4 Example (4): HD 179949 70
5.1.5 Example (5): υ And 71
5.1.6 Example (6): HD 86264 73
5.2 Habitability around the Planetary Systems 76
6. Summary and Conclusions 82
Bibliography 88
Biographical Statement 97

List of Illustrations

Figure		Page
1.1	Typical size and color of a main-sequence star in each spectral type between O and M-type (LucasVB, 2006).	2
1.2	Illustration of the climatological habitable zones for a Sun-like star (middle) and stars hotter (top) and cooler (bottom) than the Sun. .	3
1.3	Formation of a pyrimidine dimer, an example of DNA damage caused by UV-B (Gerriet41, 2008).	4
1.4	Artist's concept of fictional exomoons around the observed exoplanet, υ And d, in the climatological habitable zone of υ And (Lucianomendez, 2011).	7
2.1	Evolution of UV habitable zone and climatological habitable zone around the Sun (Buccino et al., 2006).	13
3.1	Probability distribution for occurrence of various kinds of surface and subsurface liquids as a function of distance from the Sun (Bains, 2004).	16
3.2	DNA action spectrum following Horneck (1995) and Cockell (1999).	22
3.3	Plots of Equation (3.6) for six combinations of A, B, and C.	25
3.4	Plots of Equation (3.7) for $N = 3$, 5, and 9.	26
4.1	The climatological habitable zones around F0 V, F2 V, F5 V, F8 V, and G0 V stars.	29
4.2	Stellar flux from F0 V, F2 V, F5 V, F8V, and G0 V stars.	30

4.3 Comparison between the Kitt Peak Solar Atlas spectrum (thick curve) and the solar NLTE model (thin curve) between 0.3 and 1.3 μm. 30
4.4 Overview of the studies in biological damage caused by stellar UV radiation. 32
4.5 Evolutionary tracks of stars having ZAMS masses of 1.0 $M_{\odot}$, 1.2 $M_{\odot}$, 1.3 $M_{\odot}$, 1.4 $M_{\odot}$, and 1.5 $M_{\odot}$. 38
4.6 Evolution of the climatological habitable zone around a star with 1.3 $M_{\odot}$ at ZAMS. 39
4.7 Evolution of the climatological habitable zone around stars with ZAMS masses of 1.2 $M_{\odot}$, 1.3 $M_{\odot}$, 1.4 $M_{\odot}$, and 1.5 $M_{\odot}$ for their main-sequence phase. 40
4.8 DNA damage at the climatological habitable zone limits around F0 V, F2 V, F5 V, F8 V stars (1). 47
4.9 DNA damage at the climatological habitable zone limits around F0 V, F2 V, F5 V, F8 V stars (2). 48
4.10 DNA damage at the climatological habitable zone limits around F0 V, F2 V, F5 V, F8 V stars (3). 49
4.11 Change in DNA damage at the Earth-equivalent position around an F2 V star with varied attenuation parameter A. 52
4.12 Change in DNA damage at the climatological habitable zone limits around an F2 V star with varied attenuation parameter A. 53
4.13 Change in DNA damage with varied attenuation parameter B at the Earth-equivalent position around an F2 V star. 54
4.14 Change in DNA damage with varied attenuation parameter B at

the climatological habitable zone limits around an F2 V star. 55
4.15 Change in DNA damage with varied attenuation parameter C at the Earth-equivalent position around an F2 V star. 56
4.16 Change in DNA damage with varied attenuation parameter C at the climatological habitable zone limits around an F2 V star. 57
4.17 Development of DNA damage at the climatological habitable zone limits around stars with ZAMS masses of 1.2 $M_\odot$, 1.3 $M_\odot$, 1.4 $M_\odot$, and 1.5 $M_\odot$ for their main-sequence phase (1). 59
4.18 Development of DNA damage at the climatological habitable zone limits around stars with ZAMS masses of 1.2 $M_\odot$, 1.3 $M_\odot$, 1.4 $M_\odot$, and 1.5 $M_\odot$ for their main-sequence phase (2). 61
4.19 Development of DNA damage at the average Earth-equivalent positions around stars with ZAMS masses of 1.2 $M_\odot$, 1.3 $M_\odot$, 1.4 $M_\odot$, and 1.5 $M_\odot$ for their main-sequence phase. 65
5.1 The six selected F-type stars known to host planets. 77
5.2 The distances of climatological habitable zones around the F-type stars. 78
5.3 DNA damage at the climatological habitable zone limits around the selected F-type stars (1) 79
5.4 DNA damage at the climatological habitable zone limits around the selected F-type stars (2) 80
5.5 DNA damage at the climatological habitable zone limits around each selected F-type star. 81

List of Tables

Table Page

2.1 The weighted biochemically effective irradiance in W m^{-2} for six cases of atmospheres at the boundaries of climatological habitable zones around K2 V, G2 V, and F2 V stars (Cockell, 1999) 10

3.1 Climatological habitable zone boundaries of M0 V, G2 V, and F0 V stars from Kasting et al. (1993) 18

3.2 Boundaries of the present Solar HZ from Selsis et al. (2007) 19

4.1 Properties of main-sequence F-type stars derived with PHOENIX code and motivated by previous work by Gray (2005) and Kurucz (private communication, 2012) 28

4.2 Evolutionary properties of F-type stars during main-sequence phase . 36

4.3 The effective temperature and mass of F0 V through G0 V stars derived with PHOENIX code 37

4.4 Climatological habitable zones including stellar main-sequence evolution — extreme positions 37

4.5 Climatological habitable zones including stellar main-sequence evolution — continuous domains 41

4.6 DNA Damage in case of no attenuation 43

4.7 DNA Damage in case of $A = 0.05$, $B = 300$, $C = 0.5$ 44

4.8 DNA Damage in case of atmospheric attenuation expressed by a higher order ATT function 45

4.9 Development of DNA Damage with time in the case of no atmospheric attenuation at the average Earth equivalent positions 58
4.10 Development of DNA Damage with time in the case of default atmospheric attenuation at the average Earth equivalent positions 62
5.1 Properties of F-type Planetary Systems 74
5.2 Properties of Planets in the F-type Planetary Systems 75

CHAPTER 1

Introduction

Since the first discovery of the exoplanets, PSR B1257+12 b and c, in 1992 (Wolszczan & Frail, 1992), the number of confirmed exoplanets has been growing exponentially as the detection technologies advance. The contribution of Kepler Space Telescope is especially significant, adding 961 planets within 5 years from its launch. The total of 1779 planets in 1102 systems are known as of March 2014 (Exoplanet TEAM, 2014). In the search for exoplanets, one of the biggest interests is whether those planets are habitable or not, and if habitable, whether there actually exists any life on them.

There are various factors involved in the determination of a planet's habitability. First of all, the planet must exist long enough in a relatively stable environment to harbor life on it. Very massive stars such as typical O and B-type stars (see Figure 1.1 for appearances of stars of different types) have main-sequence lifetimes shorter than a few million years, which is the time required for a planet to form and settle down. Around stars having more lifetimes, some planets form or move in a stable orbit and other planets collide with another object or are ejected into interstellar space in a fairly short period of time from the formation. If a planet is situated in a stable orbit, the planet is required to meet some criteria to be considered a habitable place. For any life forms, availability of liquid water, complex organic molecules building the bodies, and energy are essential to their existence. The habitability of a planet is determined by the properties of the host star, distance between the planet and star, planetary size, and planetary atmosphere. The size of planet must be about the same

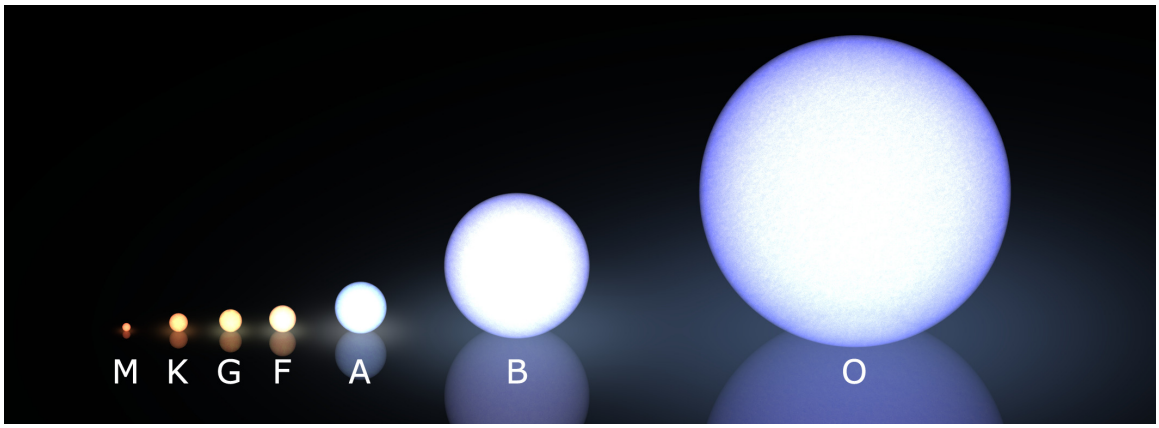

Figure 1.1. Typical size and color of a main-sequence star in each spectral type between O and M-type (LucasVB, 2006).

as that of Earth. If it is too large, the planet becomes gaseous like Jupiter. If it is as small as Mars, the planet cannot retain internal heat and loses plate tectonics, which plays an important role in climate regulation. Also, a small planet cannot trap atmospheres and water vapor on the surface because of weaker gravity and absence of a protective magnetosphere. Atmospheres keep water on the surface and have a partial role in controlling the planetary surface temperature and the amount of harmful stellar radiation, such as UV and X-rays, reaching the surface. The properties of the host star and distance between the planet and star mainly determine the energy input to the planet and consequently the temperature of planetary surface. Each star has a circumstellar region called "climatological habitable zone," in which an Earth-like planet with anoxic atmospheres can maintain surface liquid water. A planet closer to the star than the climatological habitable zone will dry out and one farther than the region will freeze. Figure 1.2 illustrates the climatological habitable zones around hot, intermediate (Sun-like), and cool stars. Generally, the more luminous and hotter the stars are, the broader and farther away the climatological habitable zones are located. Additionally, the properties of stars and orbital distance affect the amount

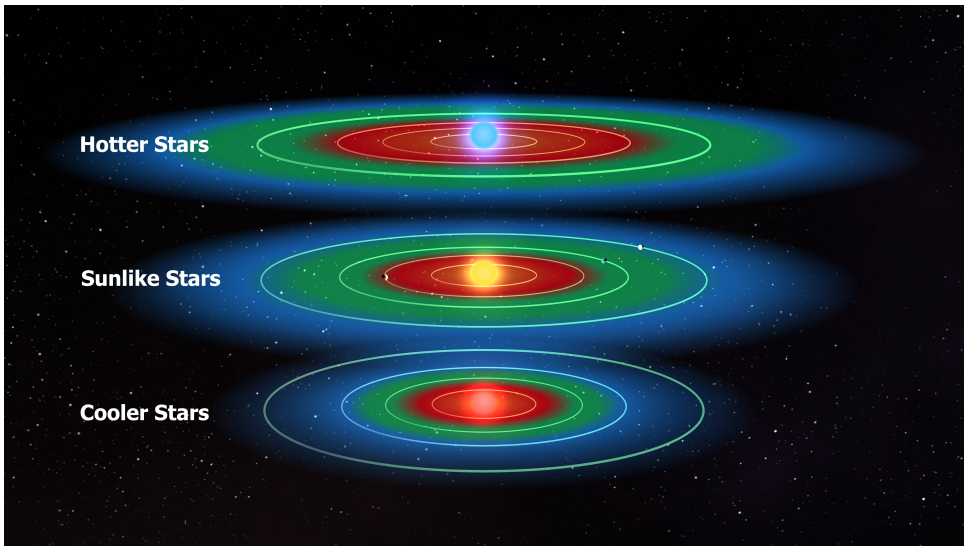

Figure 1.2. Illustration of the climatological habitable zones for a Sun-like star (middle) and stars hotter (top) and cooler (bottom) than the Sun. The circles around the stars are the orbits of Mercury, Venus, Earth, and Mars. The green areas show the climatological habitable zones. A planet inside the red areas would not be cool enough and inside the blue areas would not be warm enough to maintain surface liquid water (Berry, 2009).

of UV and shorter-wavelength radiation received by the planet (Kasting et al., 1993; Bennett & Shostak, 2006; Lammer et al., 2009).

UV and shorter-wavelength radiation have damaging or lethal impact on organisms on Earth. A few common and familiar examples of the damage caused by UV radiation are sunburns and skin cancers (Diffey, 1991). Also a disinfection method called ultraviolet germicidal irradiation uses UV rays to destroy the nucleic acids of microorganisms in food, water, and air. From the astrobiological point of view, I am only concerned with UV radiation at the wavelength between 200 and 400 nm. With the protection of ozone layers and atmospheres, UV radiation at wavelengths shorter than 290 nm does not reach the Earth's surface (Henderson, 1977). The Earth's atmosphere was anoxic at first, but still UV radiation shorter than 200 nm was unlikely to reach the Earth's surface because CO_2 absorbs it (Cockell, 2002). Visible light at

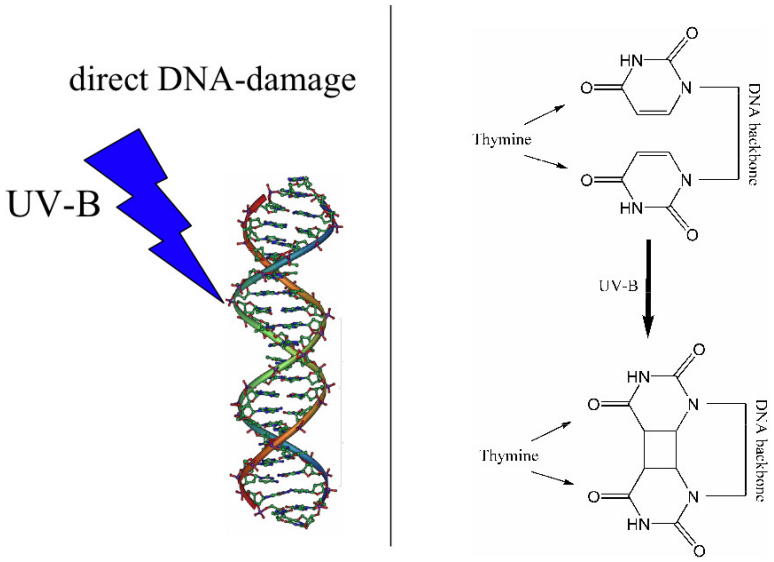

Figure 1.3. Formation of a pyrimidine dimer, an example of DNA damage caused by UV-B (Gerriet41, 2008).

longer wavelengths than 400 nm does not cause life-threatening damage in organisms. Within the wavelengths of interest, UV-B (320-290 nm) and UV-C (290-200 nm) are absorbed by DNA and protein and give direct damage to the molecules. For example, by absorbing UV-B, adjacent thymine base pairs in DNA bond together at originally double-bonded carbon atoms and form molecular lesions called pyrimidine dimers (see Figure 1.3). UV-A (400-320 nm) is mostly responsible for indirect DNA damage. Free radicals and reactive oxygen species produced by UV-A cause oxidative damage to DNA and proteins when they come into contact. Unrepaired DNA and protein damage will lead to various disorders in the body, including mutation, termination of cells, and cancer. The shorter the wavelength is, the more severe damage the light gives to organisms (Peak & Peak, 1991).

The relative biological responses to a spectrum of light can be represented by "action spectra" or "biological weighting functions." Integration of the product of action spectrum and the spectral irradiance over the wavelengths of interest gives

the relative biological effectiveness of the spectrum of light. This enables us to compare the biological damage in the environments of different stars. It is common to use DNA action spectra to compare the relative biological damage in circumstellar environments because DNA is a good proxy for carbon-based macromolecules. Even though there is no guarantee that there exists extraterrestrial life based on the same biochemistry as ours, hydrocarbons are considered as the best candidate for the main composition of extraterrestrial organisms (Cockell, 1999). I follow the same strategy to compare the habitability of different circumstellar UV environments. To include the atmospheric protection on the planetary surface, I compute the spectral irradiance, which is to be multiplied to the DNA action spectrum, by multiplying parameterized atmospheric attenuation functions to the raw spectral irradiance from the star at a particular distance.

As we live beside G2 V star, G-type stars are the main candidate for habitable planetary systems. K-type stars are also considered to provide environments suitable for existence and evolution of life. UV emission from the stars of these types are tolerable for organisms on Earth with a certain level of atmospheric protection. Since the spectrum shifts toward red as the stellar effective temperature decreases, or implicitly as the stellar mass decreases, the spectral energy distributions of late-type main-sequence stars are biochemically more gentle to organisms. M-type stars, however, occasionally emit flare with energy too excessive for life. Moreover, a planet would be tidally locked to the M-type star in the climatological habitable zone, and it would experience tidal heating and have a permanent day side and night side. A few advantages of M-type stars in terms of habitability include the large population in the Milky Way Galaxy and their slow stellar evolution. The main-sequence lifetimes of M-type stars exceed a hundred billion years. On the other hand, F-type main-sequence stars are relatively unpopular in the study of circumstellar habitabil-

ity compared to G, K, and M-type stars because of their severe UV environments and the rarity, compromising on a fraction as small as 2% of the total number of stars in the universe. However, F-type stars also have a potential to provide habitable environments. The lifetimes of F-type stars are shorter than later-type stars, but still sufficient for life to arise and evolve on planets. More importantly, F-type stars have larger climatological habitable zones than later-type stars. The climatological habitable zone of an F0 V star is 6-8 times broader than that of an M0 V star. Hence, an F-type star is more likely to have a planet in the climatological habitable zone than an M-type star (Kasting et al., 1993; Bennett & Shostak, 2006).

The habitability around F-type stars is previously investigated by some researchers including Cockell (1999), Segura et al. (2003), and Buccino et al. (2006). They conclude that the UV conditions around F-type stars are not necessarily an obstacle to the emergence of life with protection of certain types of atmospheres. Segura et al. (2003) argues F-type environments would result in even better protection from UV radiation if Earth with the atmospheres consisting of the present level of oxygen was orbiting the Earth-equivalent position because the F-type environments thicken the ozone layer. Buccino et al. (2006) also predicts that for some observed F-type stars, the climatological habitable zones and the regions that give the best UV condition for life, the "UV habitable zones," broadly overlap. They found the F-star system, υ And has a giant planet inside the overlapping region of the climatological and UV habitable zones. The result suggests that if the planet, υ And d, has an Earth-size moon, the moon could be habitable. Figure 1.4 is an artist's concept of a fictional habitable exomoon around the exoplanet, υ And d.

My study is motivated by these previous studies indicating that the stellar UV environment is one of the most decisive factors in determining the habitability of exoplanets and exomoons. I investigate the general habitability of F-type circumstel-

Figure 1.4. Artist's concept of fictional exomoons around the observed exoplanet, υ And d, in the climatological habitable zone of υ And (Lucianomendez, 2011).

lar environments by comparing DNA damage in the climatological habitable zones. The features of my study are parameterized atmospheric functions and development of UV environment with stellar age as a result of stellar evolution. By varying the parameters in the atmospheric functions, I observe the general effect of atmospheres on DNA damage.

I explain my study in this dissertation as follows. In Chapter 2, I introduce the previous results by Cockell (1999) and Buccino et al. (2006). Chapter 3 describes the theoretical approach. The key components of my research include (1) climatological habitable zones, (2) the DNA action spectrum, and (3) planetary atmospheric attenuation. In Chapter 4, I present the study of general F-type stars. The chapter gives background information of F-type stars such as their properties, stellar radiation, and stellar evolution. In the stellar case studies, I focus on (1) spectral types of the host stars, especially F0 V, F2 V, F5 V, and F8 V, (2) positions of planets in

the stellar habitable zones, including the general and conservative inner limits, the Earth-equivalent positions, and the general and conservative outer limits, (3) effects of planetary atmospheric attenuation approximated by the attenuation functions, and (4) the relative impact of UV-A, UV-B, and UV-C on DNA. Also, habitability in consideration of F-star evolution is investigated. I apply the method to six discovered F-type planetary systems (1) CoRoT-3, (2) WASP-14, (3) HD 197286, (4) HD 179949, (5) υ And, and (6) HD 86264. The information of the selected systems and results are found in Chapter 5. In Chapter 6, I summarize the main points of my study and give conclusions.

CHAPTER 2

Previous Results

2.1 Previous Results by Cockell (1999)

Cockell investigated DNA damage of UV radiation for K2 V, G2 V, and F2 V stars and for different partial pressures of CO_2 and N_2 in the planetary atmosphere and compared the results with the estimated DNA damage on Archean Earth. DNA damage was quantified by the integration of the UV irradiance reaching the planetary surface multiplied by DNA action spectra across UV range and was called the "weighted biochemically effective irradiance." Cockell calculated UV irradiance at the planetary surface for several atmospheric compositions by using Beer's law and Delta-Eddington approximation. The atmospheric models were anoxic and consisting of N_2 of 0.1 bar or 1 bar and CO_2 at partial pressures between 40 mb and 10 bar. The present atmosphere of Earth contains 800 mb of N_2 and it may be similar to the atmosphere on early Earth. The higher value, 1 bar, for N_2 was chosen as an approximation of actual Earth's atmosphere. 0.1 bar for N_2 was used to examine the effect of N_2 scattering on UV exposure. CO_2 partial pressures on Earth between 2.7 and 2.2 Gyr ago might be about 40 mb, which is suggested from Precambrian soil weathering profiles (Rye et al., 1995). 10 bar is the highest partial pressure of CO_2 suggested for early Earth by Walker (1985). Cockell calculated the weighted biochemically effective irradiance received at the boundaries and midpoints of the climatological habitable zones. The climatological habitable zone is the region where an Earth-type planet is considered to be able to sustain liquid water on its surface. The details of climatological habitable zone are discussed in the next chapter.

Table 2.1. The weighted biochemically effective irradiance in W m^{-2} for six cases of atmospheres at the boundaries of climatological habitable zones around K2 V, G2 V, and F2 V stars (Cockell, 1999)

	K2 V		**G2 V**		**F2 V**	
	0.4 AU	0.98 AU	0.84 AU	1.77 AU	1.5 AU	3.2 AU
0.1 bar N_2						
40 mb CO_2	47.9	8.3	324.6	73.1	2607	572.9
1 bar CO_2	19.7	3.4	137.1	30.1	981.9	215.7
10 bar CO_2	2.9	0.5	20.4	4.6	141.3	31
1 bar N_2						
40 mb CO_2	25.8	4.3	178.4	40.2	1302	286.1
1 bar CO_2	14.3	2.4	100.2	22.6	708.8	155.7
10 bar CO_2	0.4	0.3	19.3	4.3	133.8	19.2

The UV spectrum of a typical star for each stellar type of K2 V, G2 V, and F2 V was obtained from the IUE Low-Dispersion Spectra Reference Atlas. Those stars were HD 22049 (K2 V), HD 10307 (G2 V), and HD 40136 (F2 V). A part of the results are summarized in Table 2.1. The weighted biochemically effective irradiance for Archean Earth, Earth about 3 Gyr ago, was estimated as 96.1 W m^{-2} by assuming 40 mb CO_2 and 800 mb N_2 atmospheres and the 25% fainter Sun than present. The weighted irradiance for the present Earth was typically 0.07 W m^{-2} with an ozone shield.

The results show that the weighted biochemically effective irradiance received in the environment of F2 V star radiation was 6 and 27 times higher than on Earth 3 Gyr ago at the inner and outer boundaries of climatological habitable zone, respectively, for the case of most diffuse atmospheres. For the densest case of atmospheres, the values were 20% of Archean Earth at the inner boundary and 1.4 times at the outer boundary. On the other hand, the weighted biochemically effective irradiance for K2 V stars was from 8.6% to 50% of those on Earth 3 Gyr ago in the habitable zone

for the case of most diffuse atmospheres; and thus, it is considered that planets within the habitable zones of K-type stars have favorable UV environments for DNA-based organisms. However, Cockell argues that F-type stars cannot be ruled out as hosts of habitable places even with such a high UV level since oceans, rocks, and sands could provide adequate shields from strong UV rays.

2.2 UV Habitable Zone Based on Buccino et al. (2006)

Buccino's group investigated UV habitable zone, which is a region around a star where the amount of reaching stellar UV radiation is safe for life and enough for biogenesis. They set the limits of maximum UV damage tolerable to DNA-based organisms and of minimum UV energy required for the chemical synthesis of complex molecules in biogenesis process and computed the distances from stars corresponding to the conditions. The limits were determined by applying the "Principle of Mediocrity," that is, the conditions that have led to the origin and evolution of life on Earth are average compared to other worlds and are common in the universe.

In their study, the measure of DNA damage caused by UV radiation is expressed as

$$N^*_{\mathrm{DNA}}(d) = \int_{200\ \mathrm{nm}}^{315\ \mathrm{nm}} B(\lambda)\frac{\lambda}{hc}\frac{F(\lambda,t)}{d^2}\,d\lambda \tag{2.1}$$

where λ is the wavelength, h is the Planck constant, c is the speed of light, $B(\lambda)$ is the biological action spectrum, $F(\lambda)$ is the UV flux at 1 AU and d is the distance. In our research, we call the biological action spectrum the DNA action spectrum and assign S_λ. $B(\lambda)$ can be approximated by the following equation,

$$\log B(\lambda) \approx \frac{6.113}{1+\exp((\lambda[\mathrm{nm}]-310.9)/8.8)} - 4.6 \tag{2.2}$$

The equation was obtained semi-empirically from previous works including Setlow & Doyle (1954), Setlow (1974), Green & Miller (1975), Lindberg & Horneck (1991), and

Cockell (1998). The inner limit is the distance where $N^*_{DNA}(d)$ is twice the value of that at the top of the Earth's atmosphere 3.8 Gyr ago, $N^*_{\rm DNA}(1\ {\rm AU})|_{t=t^{\odot}_{\rm Arc}}$. The value for Archean Earth was calculated by using 75% the present value of $F(\lambda, t)$ for the Sun. The outer habitable zone is the distance where the amount of UV radiation reaching,

$$N^*_{\rm UV}(d) = \int_{200\ {\rm nm}}^{315\ {\rm nm}} \frac{\lambda}{hc} \frac{F(\lambda, t)}{d^2}\, d\lambda \tag{2.3}$$

is half the UV flux received by the top of the Earth's atmosphere 3.8 Gyr ago.

Instead of considering a variety of atmospheric conditions, they included the effect of atmospheric attenuation in the "mediocrity factor" along with other complex factors determining the UV conditions and life's durability to UV exposure. They estimated a constant attenuation factor, α, for each stellar type, which is the ratio between UV fluxes attenuated by the atmosphere with O_2 at 10^{-5} times the present concentration in the Earth's atmosphere and those without O_2 concentration, and then they found $\alpha = 0.84$ for K and G-type stars and 0.74 for F-type stars.

They simulated the evolution of climatological habitable zones and UV habitable zones from 1 to 10 Gyr from the formation of the system in 17 real planetary systems, assuming the luminosities of F, G and K-type stars evolve in a similar way as the Sun and that the UV radiation follows the same pattern. The spectra of the selected stars were obtained from the IUE public library.

The result for the Solar System is shown in Figure 2.1. The dashed lines represent the boundaries of climatological habitable zone and the solid lines represent the boundaries of UV habitable zone. The UV habitable zone for the present Sun is between 0.71 and 1.90 AU. The inner and outer boundaries of UV habitable zone are slightly closer to the Sun than the inner and outer boundaries of climatological habitable zone, respectively, but they are overlapping in a large area.

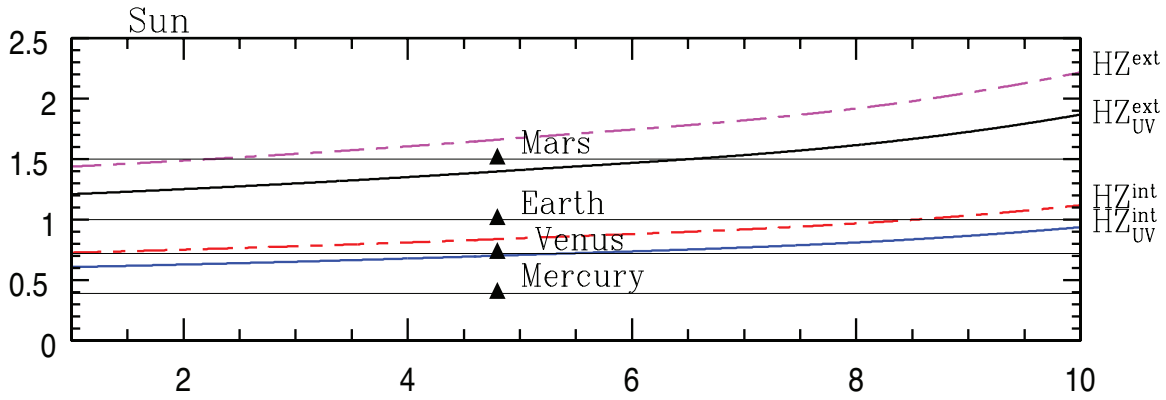

Figure 2.1. Evolution of UV habitable zone and climatological habitable zone around the Sun (Buccino et al., 2006).

Among the 17 simulated planetary systems, 7 of them have overlapping regions of climatological habitable zone and UV habitable zones. These stars are υ And (F8 V), HD 89744 (F7 V), HD 114762 (F9 V), ρ CrB (G0 Va), HD 147513 (G5 V), τ Boo (F6 IV), and ρ Ind (G2.5 IV). Only υ And is known to have a planet within the overlapping region. The climatological habitable zones of HD 114762 and τ Boo are completely within the UV habitable zones. υ And and HD 89744 also have mostly overlapping climatological and UV habitable zones. All the selected K-type stars, some G-type stars, and an F8 V star have UV habitable zones closer to the stars than climatological habitable zones. Therefore, they concluded that the UV level in the climatological habitable zones is inadequate for the origin and evolution of life around those stars.

CHAPTER 3

Theoretical Approach

3.1 Stellar Habitable Zones

The climatological habitable zone, sometimes generically refined to as "stellar habitable zone," is defined as the region around a star, in which the terrestrial objects can maintain moderate surface temperatures to sustain liquid water on their surfaces. Huang (1959) first introduced the term "habitable zone." Other early important contributions to this topic were made by several researchers, for example, Rasool & De Bergh (1970), Hart (1979), and Kasting et al. (1993). The notion of climatological habitable zone is based on the idea that liquid water is the most essential to emergence and survival of life. The liquid water requirement is one of the three criteria for habitable environments that are mentioned in *The NASA Astrobiology Roadmap* (Des Marais et al., 2008), which is the guide for NASA's research and technology development in astrobiology. These criteria are (1) extended regions of liquid water, (2) conditions favorable for the assembly of complex organic molecules, and (3) energy sources to sustain metabolism. Any organism on Earth needs liquid water during at least part of their life cycle. Liquid water works as the most essential solvent for biochemistry to take place. There have been arguments that other liquids such as liquid ammonia, methane, ethane, and nitrogen have the potential to be a solvent for extraterrestrial biology (Bains, 2004), but liquid water is considered to be among the best for its characteristics including a large dipole moment, the capability to form hydrogen bonds, to stabilize macromolecules, and to orient hydrophobic-hydrophilic molecules (Lammer et al., 2009). Also, water stays liquid

at a wide range of temperatures and pressures. Additionally, water is unique in the way that ice floats in liquid water. The flotation of water ice has a great advantage in long-term climate stability (Bennett & Shostak, 2006). Most other possible solvents are in the liquid state at lower temperatures (see Figure 3.1) and have higher or lower pH than water. Most of our intermediary metabolites are insoluble in cold liquid and many are unstable at high or low pH. Therefore, even if another liquid could be a solvent for extraterrestrial biology, the life depending on the liquid would not be carbon-based. Instead, silicon chemistry-based life might be possible in other liquids (Bains, 2004). Silicon, however, has some disadvantages as the core element in exotic biochemistry compared to carbon (Pace, 2001). For example, silicon does not form stable bonds with as many other elements as carbon. Moreover, silicon's double or triple bond are weaker than carbon's. Although silicon-based biochemistry is not completely implausible, it is considered that carbon-based and water-dependent biology has more possibility to arise in extraterrestrial worlds. Also, since I have no information about UV effectiveness in silicon chemistry-based life and such biology requires totally different analyses, I set it aside in my study.

Water molecules can be found everywhere in the universe (Cernicharo & Crovisier, 2005). However, to keep water on the surface of a terrestrial object in liquid state requires a temperature and atmospheric pressure in the appropriate ranges. The surface temperature of a planet mostly depends on the stellar radiative flux received by the planet. The radiative input is determined by the stellar luminosity, the shape of the photospheric spectrum as given by the temperature, distance between the planet and star, and coverage of cloud or albedo of the planet. Thermal emission from the planet also plays an important role in the maintenance of a moderate surface temperature. In the case of Earth, greenhouse gases such as water vapor, CO_2, CH_4, N_2O, and O_3 mainly control the thermal emission.

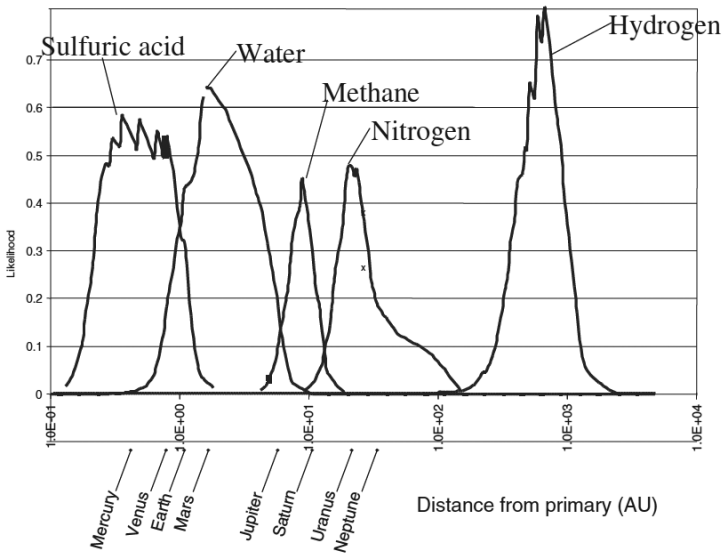

Figure 3.1. Probability distribution for occurrence of various kinds of surface and subsurface liquids as a function of distance from the Sun (Bains, 2004).

Kasting et al. (1993) estimated the distances of climatological habitable zone boundaries, which have been widely used as the first criterion for measuring habitability of discovered exoplanets. In their model, an Earth-type planet with a full terrestrial ocean of surface water (1.4×10^{21} cm^3) and N_2, CO_2, and H_2O atmospheres are assumed. No O_2 or O_3 is included. 1 bar of N_2 and 300 ppmv of CO_2 are used as the standard values. The effect of clouds can be included by assuming a high surface albedo, but the standard model is cloud-free. They calculated the net incident stellar flux, $F_{\rm S}$, and the net outgoing infrared flux, $F_{\rm IR}$, at the top of the atmosphere for given surface temperatures between 220 to 2000 K. The ratio of $F_{\rm IR}$ to $F_{\rm S}$ is called the effective stellar flux, $S_{\rm eff}$. The distance where the planet can maintain a specific surface temperature is derived from the stellar luminosity, L, in the unit of $L_\odot$, and the required effective stellar flux, $S_{\rm eff}$, in $S_0 = 1360$ W m^{-2};

$$d = 1 \text{ AU} \left(\frac{L}{S_{\text{eff}}} \right)^{0.5} \tag{3.1}$$

Therefore, the habitable zone boundaries can be computed by finding the limits of surface temperature that can maintain certain conditions required for a planet to keep liquid water on its surface, and the corresponding S_{eff}.

They investigated three inner and three outer boundaries of climatological habitable zones: water-loss, runaway-greenhouse, and recent-Venus inner habitable boundaries, and 1st condensation, maximum greenhouse, and early Mars outer boundaries. The distances of the boundaries are summerized in Table 3.1.

The water-loss inner boundary is the maximum distance where the atmosphere is warm enough to have a wet stratosphere. At the distance, water is gradually lost by photodissociation and hydrogen loss from the stratosphere. The runaway-greenhouse inner boundary is the maximum distance where water vapor enhances the greenhouse effect and eventually the water will be lost by the surface temperature of the planet reaching the critical point of water. The recent-Venus inner boundary for the solar system corresponds to the distance where the amount of reaching solar flux is the same as that on Venus 1 Gyr ago. Venus is believed to have had liquid water at first but then lost to outer space for at least 1 Gyr. The recent-Venus inner boundary for the solar system is 0.75 AU, according to Kasting et al. (1993) and the boundary distance for other types of stars is scaled by the effective stellar flux for water loss inner boundary.

The 1st condensation outer boundary is the minimum distance where CO_2 clouds start to form at the surface temperature of 273 K. The maximum greenhouse outer boundary is the maximum distance where a cloudless CO_2 atmosphere can maintain a surface temperature of 273 K. The Earth's climate is regulated by the negative feedback of CO_2 cycle, but the climate regulation would not function

Table 3.1. Climatological habitable zone boundaries of M0 V, G2 V, and F0 V stars from Kasting et al. (1993)

	M0 V		G2 V		F0 V	
Boundary	S_{eff}	d (AU)	S_{eff}	d (AU)	S_{eff}	d (AU)
Recent Venus	1.60	0.19	1.76	0.75	2.00	1.47
Runaway Greenhouse	1.05	0.24	1.41	0.84	1.9	1.50
Water Loss	1.00	0.25	1.10	0.95	1.25	1.85
1st Condensation	0.46	0.36	0.53	1.37	0.61	2.70
Max. Greenhouse	0.27	0.47	0.36	1.67	0.46	3.06
Early Mars	0.24	0.50	0.32	1.77	0.41	3.24

outside those boundaries. CO_2 clouds increase a planetary albedo by reflecting solar radiation. Also, condensation of CO_2 will cause reduction in the magnitude of the greenhouse effect since the released latent heat should decrease the lapse rate in the convective region of the atmosphere. The early Mars outer boundary is based on the idea that Mars was warm enough to keep standing bodies of liquid water in its early days. The early Mars outer boundary for the solar system is 1.77 AU, and the boundary distance for other types of stars is scaled by the effective stellar flux for maximum greenhouse outer boundary.

Water loss and 1st CO_2 condensation boundaries are also called the conservative inner and outer habitable zone limits, and they are denoted by iC and oC, respectively in this dissertation. In a similar way, runaway greenhouse and maximum greenhouse boundaries are also called the general inner and outer habitable zone limits, and they are denoted by iG and oG, respectively.

Various other distances for iG, iC, oC, and oG are suggested by more recent work with updated models of Kasting et al. (1993) or different models, including Williams & Kasting (1997), Forget & Pierrehumbert (1997), Mischna et al. (2000), Williams & Pollard (2002), Underwood et al. (2003), and Selsis et al. (2007). In

Table 3.2. Boundaries of the present Solar HZ from Selsis et al. (2007)

	Venus Crit.	Clouds 0%	Clouds 50%	Clouds 100%
$l_{\text{in}\odot}$ (AU)	0.72	0.84-0.95	0.68-0.76	0.46-0.51
	Mars Crit.	Clouds 0%	Clouds 50%	Clouds 100%
$l_{\text{out}\odot}$ (AU)	1.77	1.67	1.95	2.40

my research, I followed Selsis et al. (2007), which derived the equations to estimate the inner and outer boundaries for stars with any luminosity L and any effective temperature T_{eff} between 3700 K and 7200 K from the climatological habitable zone boundaries published in Kasting et al. (1993). When producing these equations, the authors made a correction in the solar effective temperature to 5777 K, which was as low as 5700 K in Kasting et al. (1993). In addition, they investigated the habitable boundaries of Earth-type planets partially or completely covered by clouds.

$$l_{\text{in}} = (l_{\text{in}\odot} - 2.7619 \times 10^{-5} T_{\star} - 3.8095 \times 10^{-9} T_{\star}^2) \left(\frac{L}{L_{\odot}}\right)^{\frac{1}{2}} \tag{3.2}$$

$$l_{\text{out}} = (l_{\text{out}\odot} - 1.3786 \times 10^{-4} T_{\star} - 1.4286 \times 10^{-9} T_{\star}^2) \left(\frac{L}{L_{\odot}}\right)^{\frac{1}{2}} \tag{3.3}$$

where l_{in} is the inner boundary and l_{out} is the outer boundary in AU for a star with the effective temperature T_{eff} in K and luminosity L. In the equations, $T_{\star} = T_{\text{eff}} - 5700$ and $L_{\odot}$ is the solar luminosity. $l_{\text{in}\odot}$ and $l_{\text{out}\odot}$ are the boundaries of Solar habitable zones, and the value for each case is shown in Table 3.2. The two values for l_{in} are the distances of runaway greenhouse and water-loss inner boundaries. l_{out} with 0%, 50%, and 100% clouds correspond to maximum greenhouse outer boundary.

In addition to climatological habitable zones, there are regions called continuously habitable zones, which are the regions in the climatological habitable zones over a certain period of time (Kasting et al., 1993). Since stellar luminosities increase with

time, the climatological habitable zones migrate outward with time. The continuously habitable zone of the Sun for 4.6 Gyr is from 0.95 to 1.15 AU. The time interval for which Earth can be in the climatological habitable zone is about 6 Gyr while the lifetime of the Sun is about 10 Gyr. More massive main sequence stars have regions that are continuously in the habitable zones for shorter periods. Especially, O and B-type stars evolve too fast and consequently end their lifetime earlier than the time taken for Earth-like planets to form and have a mild and stable climate in the climatological habitable zones. Looking at the history of life on Earth as the only sample we have, it is assumed that a planet needs to be in the climatological habitable zone continuously for at least 1 Gyr to harbor microbial life on it (Schopf, 1993), and thus existence of life is least expected around the stars more massive than late-A type. On the other hand, the continuously habitable zones of K and M-type stars for 10 Gyr are nearly equal to the climatological habitable zones at their zero age because they evolve very slowly. Additionally, K and M-type stars are more abundant than G-type stars, and therefore, the possibility of finding exoplanets within the climatological habitable zones is considered high around those stars. However, the climatological habitable zones exist so close to M-type host stars that the exoplanets inside the regions would be tidally locked. Also, the exoplanets in the climatological habitable zones of M-type stars are possibly exposed to high stellar UV radiation damaging to DNA. Moreover, the less luminous the star is, the narrower the climatological habitable zones are. Hence, an M-type star has less chance to have a planet inside the habitable zone compared to an earlier type star such as an F-type star (Bennett & Shostak, 2006).

3.2 The DNA Action Spectrum

A more extended assessment of circumstellar habitability requires the consideration of the UV energy flux. Stars emit light in a wide range of wavelength including UV and X-rays, which give a damaging effect on organisms. UV radiation damages DNA and causes mutation. Mutation can result in various disorders, but at the same time, it can promote evolution. Also, UV radiation is considered one of the most important energy sources on early Earth to synthesize many biochemical molecules (Toupance et al., 1977). In the case of Earth, ozone layer, clouds, and atmospheres filter out most UV and X-rays and keep a moderate level of UV radiation at the Earth's surface.

As described in the previous chapter, Cockell (1999) studied DNA damage of UV radiation at the climatological habitable zone boundaries in comparison with that on Archean Earth. Buccino et al. (2006) estimated UV habitable zone boundaries, which are the time-evolving maximum and minimum distances in favorable UV conditions for survival and emergence of life, and tested to see if real planetary systems have overlapping UV habitable zones and climatological habitable zones.

To incorporate the biological effectiveness of UV radiation into my calculations, I used DNA action spectrum. DNA action spectrum is a parameter that describes the relative effectiveness of energy at different wavelengths in causing DNA damage, which is shown in Figure 3.2. The spectrum was given in relative units normalized to unity for $\lambda = 300$ nm. DNA was taken as a proxy for carbon-based macromolecules since extraterrestrial biology is generally assumed to be most likely based on hydrocarbons. Consequently, the DNA action spectrum was utilized to represent the impact of stellar UV radiation.

The total effective dose of UV rays can be found by integrating UV irradiance multiplied by DNA action spectrum over the whole range of wavelengths of interest.

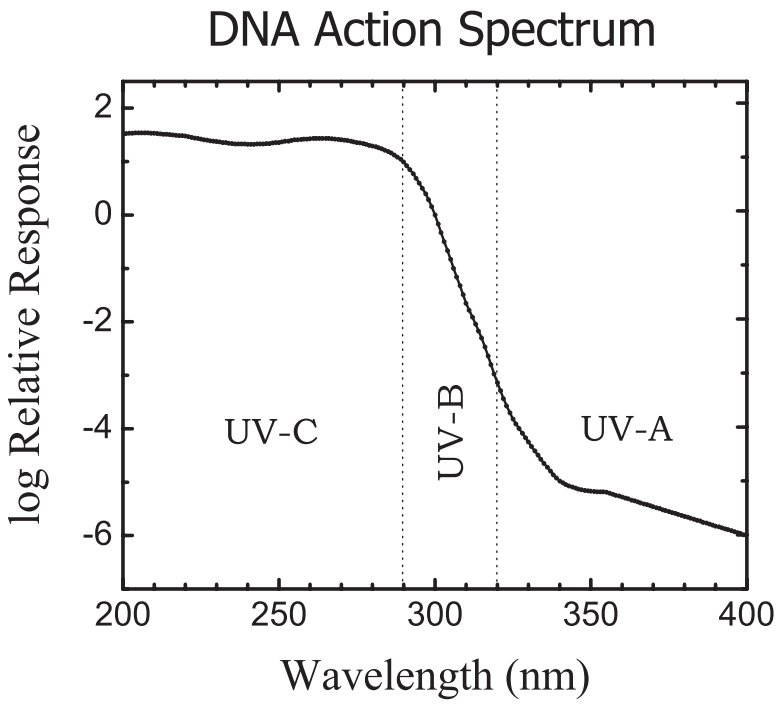

Figure 3.2. DNA action spectrum following Horneck (1995) and Cockell (1999).

The biologically effective irradiance of total stellar UV light at the ground, E_{eff}, is calculated with the following formula:

$$E_{\text{eff}} = \int_{\lambda_1}^{\lambda_2} E_\lambda(\lambda) S_\lambda(\lambda) \text{ATT}(\lambda)\, \text{d}\lambda \tag{3.4}$$

where λ is the wavelength, E_λ is the stellar irradiance of a specific wavelength, S_λ is the action spectrum, and ATT is the atmospheric attenuation coefficient. ATT is described in the next section. $E_\lambda(\lambda)$ is defined as

$$E_\lambda(\lambda) = F_\lambda(\lambda)\frac{R^2}{d^2} \tag{3.5}$$

where F_λ is the stellar radiative flux, R is the stellar radius, and d is the distance of the planet from the host star.

I use a DNA action spectrum following Horneck (1995) and Cockell (1999). Cockell (1999) provides information on the DNA action spectrum for the range from 200 and 290 nm and Horneck (1995) for the range from 285 to 400 nm.

The biological effectiveness of UV radiation varies with the wavelength. UV radiation can be divided into three regimes by the effectiveness at the planetary surface: UV-A, UV-B, and UV-C. UV-A is from 400 to 320 nm and not damaging to DNA. UV-B is from 320 to 290 nm. UV-B is harmful to DNA and a part of the incident UV-B rays passes through the ozone layer. UV-C is from 290 to 200 nm and more harmful but attenuated greatly by the atmospheres. The divisions within UV range are somewhat arbitrary and vary slightly depending on the discipline involved. I followed Diffey (1991) for the divisions. 290 nm was chosen for the division between UV-B and UV-C since UV radiation at shorter wavelength is usually only present at high altitude on Earth (Henderson, 1977). 320 nm was chosen for the division between UV-A and UV-B since UV radiation at shorter wavelength than 320 nm is more photobiologically damaging than longer wavelength.

3.3 Planetary Atmospheric Attenuation

Habitability of a planet or moon depends on its atmosphere as well as the star-related boundary conditions. The amount and composition of atmospheres affect the surface temperature of the planet by the greenhouse effect and the clouds raising the albedo. Also, a planet can keep water on its surface with the presence of atmospheres. Another important role of the atmosphere in habitability is the protection of the organisms against harmful UV radiations by absorption and scattering. In the case of Earth, the ozone layer at the stratosphere attenuates UV-C (<280 nm) from 7 W m^{-2} to 10^{-23} W m^{-2} and UV-B (280-315 nm) from 16 W m^{-2} to 1.3 W m^{-2} (Segura et al., 2003). The ozone molecules in the stratosphere are formed from the oxygen molecules

absorbing the UV rays shorter than 240 nm. The ozone molecules are also broken down by absorbing radiations between 240 and 310 nm. Additionally, CO_2 attenuates the radiations shorter than 200 nm.

In the Archean era (3.9-2.5 Gyr ago), it is supposed that the atmosphere on Earth did not contain much oxygen. Without oxygen in the air, Archean Earth lacked the protection from UV radiations by the ozone layer. Segura et al. (2003) predicts that if the amount of UV rays was the level of the present solar UV emissions and the O_2 concentration was 10^{-2} PAL (Present Atmospheric Levels), 7.1×10^{-4} W m^{-2} of UV-C and 3.452 W m^{-2} of UV-B would reach the surface. If the O_2 concentration was 10^{-5} PAL, 4.351 W m^{-2} of UV-C and 14.924 W m^{-2} of UV-B would reach the surface. As discussed in the previous section, the UV levels certainly affect the amount of damage to DNA. According to Cockell (2002), there are discussions in which a sulfur haze at high temperatures, a CH_4-generated hydrocarbon smog, and an organic aldehyde haze may have provided enough protection from the UV radiations in the early eras. UV flux is also reflected back and attenuated by clouds. In liquid water, even more UV flux is attenuated.

In an attempt to express the atmospheric attenuation for 200-400 nm with simple functions, the ATT data presented by Cockell (2002) were compared with

$$y = \frac{1}{2}C[1 + \tanh(A(x - B))] \tag{3.6}$$

for various combinations of (A, B, C) (see Figure 3.3). Parameter A represents the inclination, B shows the point where the half maximum ATT is located, and C is the maximum ATT. The function can represent the effect of various composition of atmospheres by changing the parameters, A, B, and C. The solid lines in Figure 3.3 show ATT for the Earth atmosphere of 3.5 Gyr ago for the case with 40 mb CO_2 and 0.8 N_2 atmosphere.

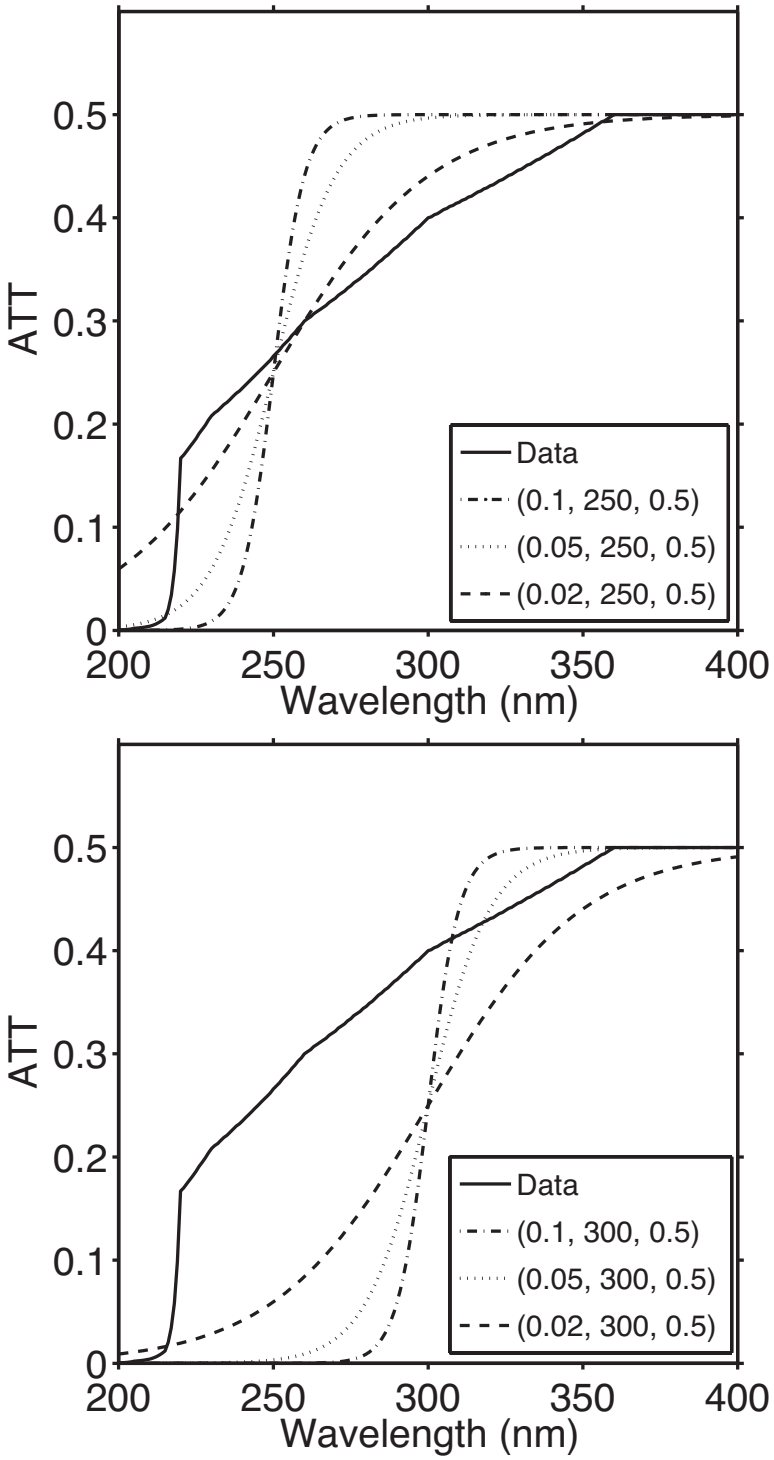

Figure 3.3. Plots of Equation (3.6) for six combinations of A, B, and C. In both figures, C is set to 0.5 and lines for $A = 0.1$, 0.05, and 0.02 are shown. $B = 250$ for top figure and $B = 300$ for bottom figure. Solid lines show the original data of attenuation.

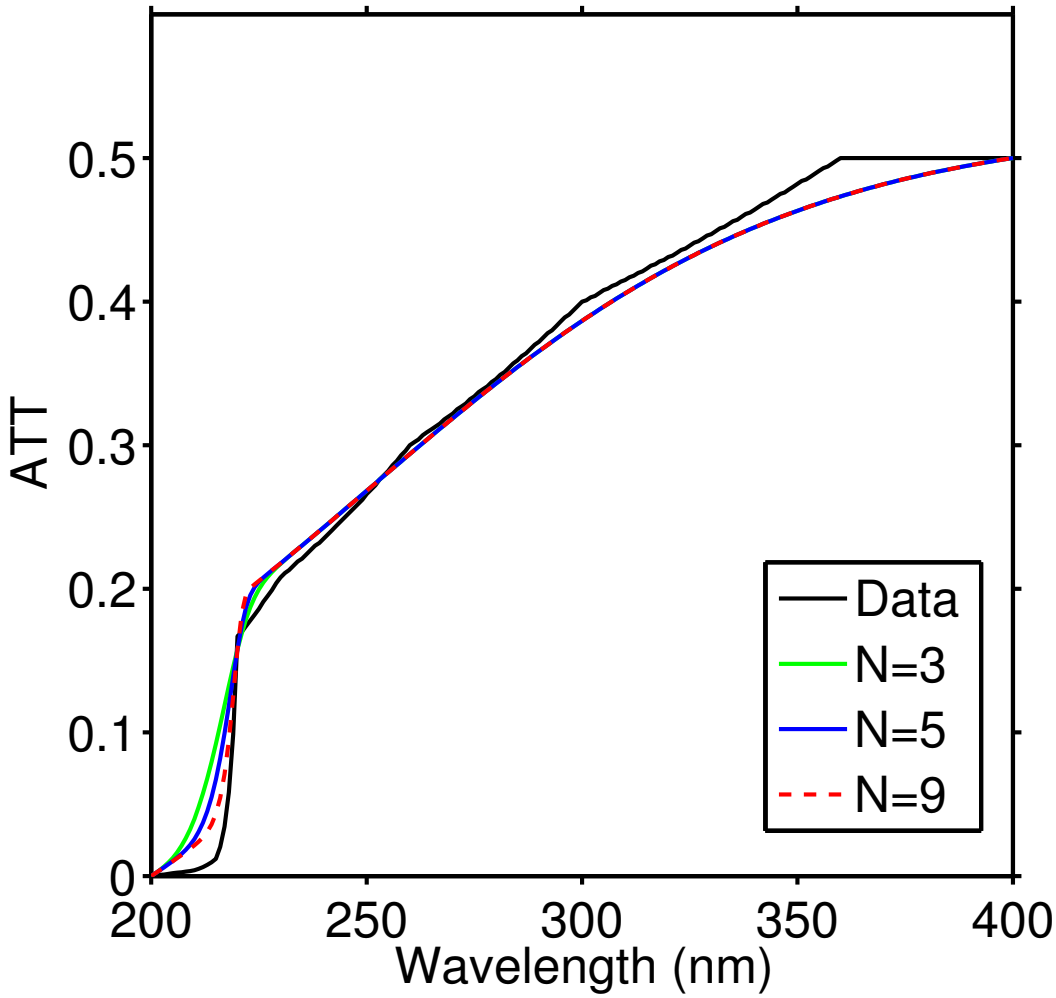

Figure 3.4. Plots of Equation (3.7) for $N = 3$, 5, and 9.

Additionally, better fitting functions to the original data were considered. These functions are compared in Figure 3.4. With this example, I tried to demonstrate that I can express ATT by combining tanh-terms when I need more complex atmospheric models.

$$\text{ATT} = 0.15 \tanh\left[0.05(x-200)\right]^N + 0.256 \tanh\left[0.01(x-250)\right] + 0.1183$$

$$\text{for } 200 \leq x \leq 400 \tag{3.7}$$

CHAPTER 4

Application to F-type Stars

4.1 Background Information of F-type Stars

4.1.1 Properties of F-type Main-sequence Stars

F-type main-sequence stars are hotter, more luminous, more massive and larger than the Sun, which is categorized as a G2 V star. Most F-type stars have a core, radiative zone, and a relatively thin convection zone. The spectra from F-type stars are characterized by the hydrogen lines weaker than A-type stars and the lines for ionized metals weaker than G-type stars. F-type stars show strong H and K lines for Ca II (Kroupa, 2002; Kutner, 2003). The properties of F-type stars are summarized in Table 4.1. Typically, the effective temperatures are between 6050 and 7200 K, radii are between 1.12 and 1.62 $R_{\odot}$, luminosities are between 1.51 and 6.33 $L_{\odot}$, and masses are between 1.05 and 1.60 $M_{\odot}$ (Gray 2005; Kurucz, private communication in 2012). Their apparent colors are white. Their fraction of all main-sequence stars is only about 2%. This fraction is much smaller, compared to later type stars, which are considered to have more favorable environments for organisms. G-type stars constitute 7%, K-type stars 15%, and M-type stars 75% (Bennett & Shostak, 2006). Therefore, the chance of finding planets in the climatological habitable zones for F-type stars is likely to be smaller than the late type stars. Also, the lifetime of F-type stars is shorter than 10-Gyr lifetime of Sun-like stars. Generally speaking, a more massive star has a shorter lifetime on main-sequence. According to the stellar evolutionary models that I used, the main-sequence lifetime of a star with $M = 1.2\ M_{\odot}$ is about 4.3 Gyr and that of a star with $M = 1.5\ M_{\odot}$ is about 2.7 Gyr.

Table 4.1. Properties of main-sequence F-type stars derived with PHOENIX code and motivated by previous work by Gray (2005) and Kurucz (private communication, 2012)

Spectral Type	$T_{\rm eff}$ (K)	R ($R_\odot$)	L ($L_\odot$)	M ($M_\odot$)
F0 V	7200	1.62	6.33	1.60
F2 V	6890	1.48	4.43	1.50
F5 V	6440	1.40	3.03	1.25
F8 V	6200	1.20	1.91	1.10
G0 V	6050	1.12	1.51	1.05

Although the number of the F-type stars is smaller and their lifetime is shorter than Sun-like stars, the climatological habitable zones of F-type stars are wider than those of later-type stars. Additionally, since their climatological habitable zones are farther away from the stars than M-type stars, no tidal locking occurs inside the climatological habitable zones unlike M-type planetary systems. Figure 4.1 shows the conservative (dark gray) and general (light gray) climatological habitable zones and Earth-equivalent positions (dashed line) for F0 V, F2 V, F5 V, F8 V, and G0 V stars. As is obvious from the figure, the climatological habitable zones are narrower and located closer to the stars for cooler stars.

4.1.2 Stellar Radiation from F-type Main-sequence Stars

I utilized the photospheric models computed by the PHOENIX code following Hauschildt (1992) to include in my derivations the necessary and accurate account of solar radiation such as its spectral energy distribution. Figure 4.2 shows the spectra for F0 V, F2 V, F5 V, F8 V, and G0 V stars generated by the PHOENIX code. I adopted the models for the effective temperature inputs of 7200 K for F0 V, 7000 K for F1 V, 6890 K for F2 V, 6700 K for F3 V, 6440 K for F5 V, 6200 K for F8 V, and 6050 K for G0 V (see Tables 4.1 and 4.3).

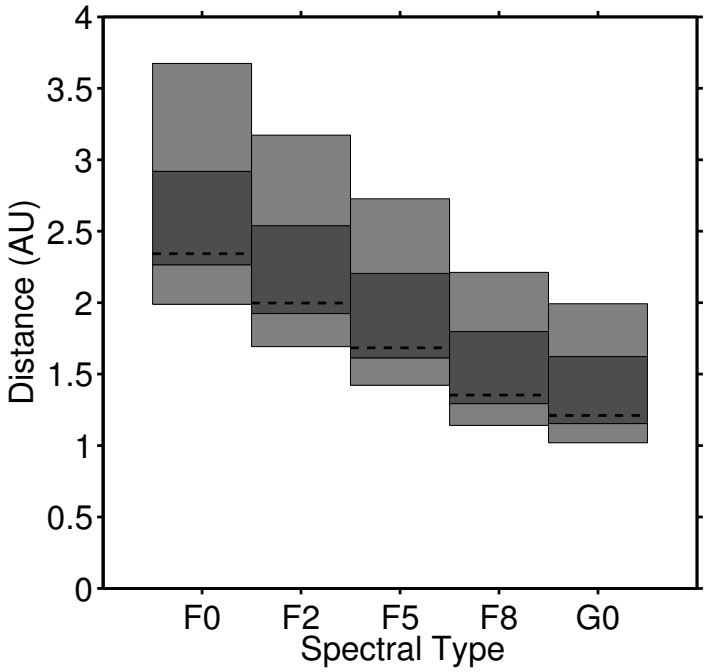

Figure 4.1. The climatological habitable zones around F0 V, F2 V, F5 V, F8 V, and G0 V stars. The dark gray areas indicate the conservative habitable zones. The light gray areas indicate the general habitable zones. The distances at the dashed lines are the Earth-equivalent positions.

The PHOENIX code is a general-purpose code that produces model atmospheres and synthetic spectra of a broad range of celestial objects including novae, super novae, dwarfs, brown dwarfs, giants, white dwarfs, and accretion disks in active galactic nuclei (Hauschildt, 1992; Hauschildt et al., 1999, 2003). The code uses nested iterations of atmospheric structure, equation of state, radiative transfer equation, and some other physical and mathematical equations required to derive the atmospheric models in radiative and hydrostatic equilibrium. The code solves the radiative transfer equation in 1-D spherically symmetric geometry for each of a large number of local thermodynamic equilibrium (LTE) and non-LTE (NLTE) background spectral lines without using simple approximations. Also, a set of physical variables such as temperatures, densities, population number of each atomic energy level and the ra-

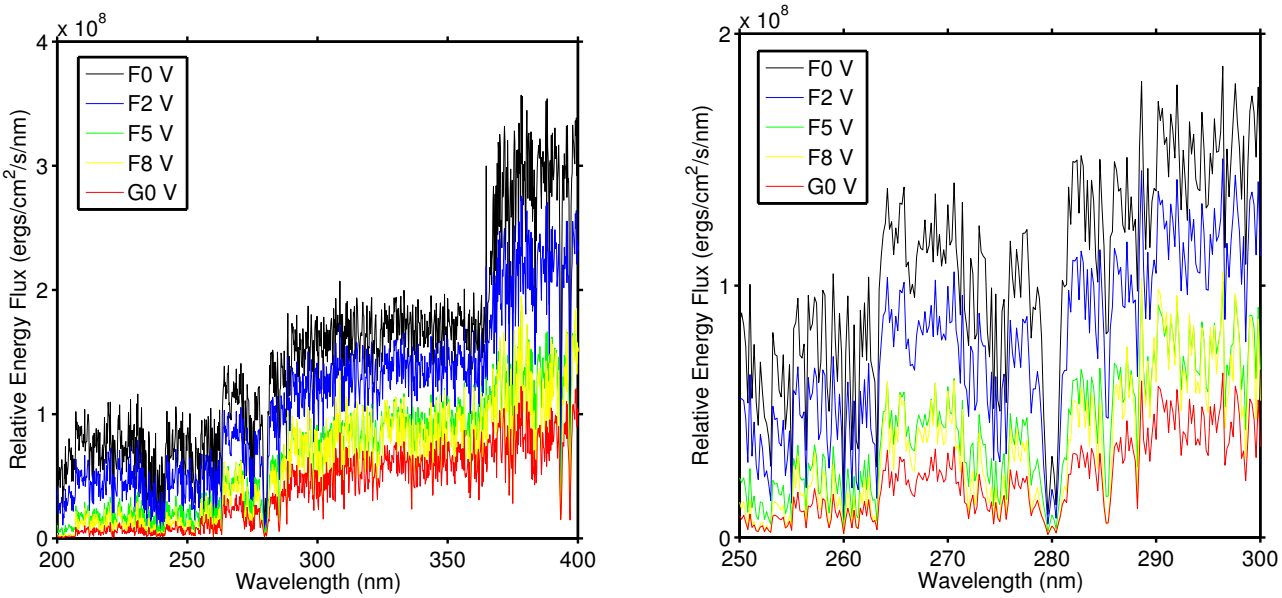

Figure 4.2. Stellar flux from F0 V, F2 V, F5 V, F8V, and G0 V stars. The spectra was calculated by the PHOENIX code given by Hauschildt (1992) and subsequent work. The left panel shows the spectra from 200 to 400 nm, which is the whole range used in my research. A part of the spectra is enlarged in the left panel to show the details.

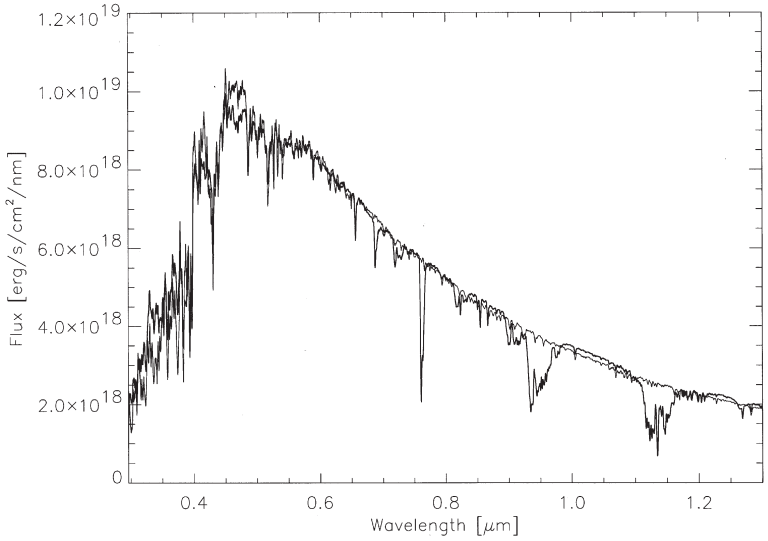

Figure 4.3. Comparison between the Kitt Peak Solar Atlas spectrum (thick curve) and the solar NLTE model (thin curve) between 0.3 and 1.3 μm. The resolution of the Kitt Peak Solar Atlas spectrum is reduced from $\Delta\lambda = 0.01$Å to 0.1 Å. The model's resolution is reduced from $\Delta\lambda \leq 0.05$Å to 0.1 Å(Hauschildt et al., 1999).

diation field, at each location in the atmosphere is calculated so that all constraint equations are simultaneously fulfilled, and the atmospheric model is constructed self-consistently from the input parameters including the effective temperature, stellar radius, surface gravity, and metallicity. The code includes several hundred species of atoms, ions, and molecules in the equation of state. Energy transport by convection is taken into account in the mixing length approximation with the mixing length set to unity. Also, the special relativistic effects in advection and aberration are incorporated in the calculations. Opacities are sampled dynamically over about 80 million lines from atomic transitions and billions of molecular lines, in addition to background opacities.

The spectra generated by the PHOENIX code are detailed and very realistic as can be seen in Figures 4.3, in which the Kitt Peak Solar Atlas spectrum observed at the National Solar Observatory (Kurucz et al., 1984) and the solar NLTE model generated by the PHOENIX code are compared (Hauschildt et al., 1999). For the computation, $T_{\rm eff} = 5770$ K, $\log g = 4.44$, and solar abundances were used. Also, the model includes the effects of multilevel NLTE on the equation of state, the radiative transfer, and the structure of the atmosphere. Although no attempts were made to fine-tune the model, the synthetic spectrum matches Kitt Peak Solar Atlas very well. The troughs of the Kitt Peak Solar Atlas spectrum at about 0.75, 0.95, and 1.12 μm are terrestrial features. The authors insist that a fine-tuned model matches the real spectrum even better. They explain the differences from the real spectrum resulted from the slightly different abundances, different methods for treating the line blanketing, different molecular line lists, and different treatment of scattering and b-f and f-f opacities.

As part of my study, the spectra emergent from a stellar model atmosphere were calculated with a high resolution of $\Delta\lambda = 0.01$Å, for a highly complete inclusion of

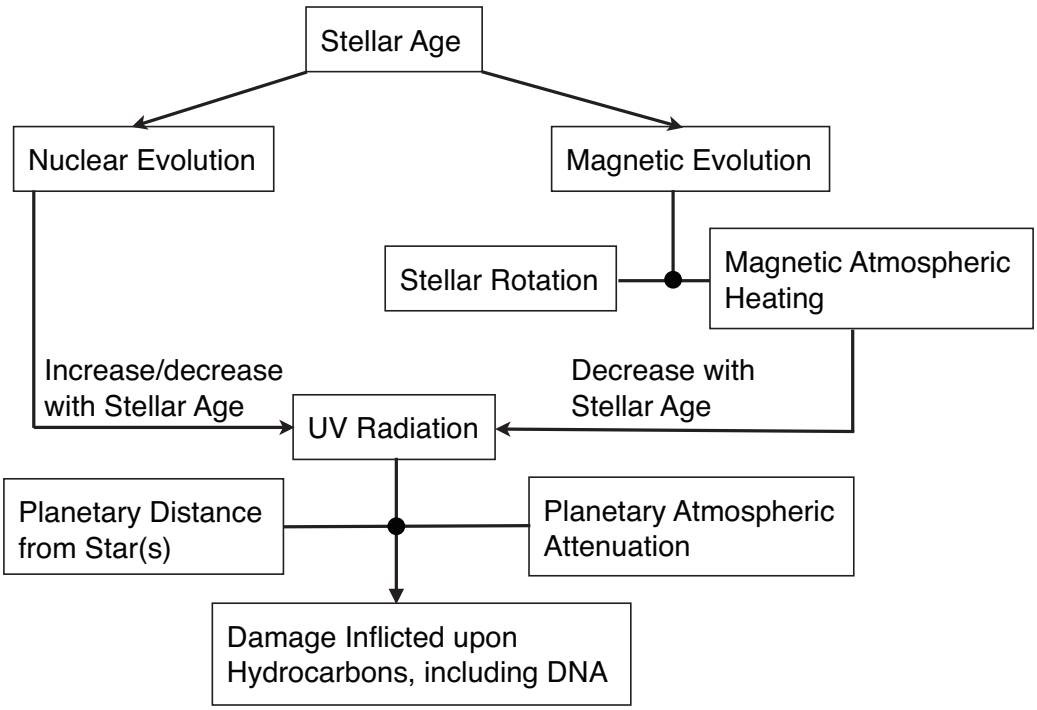

Figure 4.4. Overview of the studies in biological damage caused by stellar UV radiation.

the lines, and then I lowered the resolution to a more practical level for my subsequent astrobiological analyses.

4.1.3 Evolution of F-type Main-sequence Stars

In the calculations of the damage inflicted upon hydrocarbons, three factors are involved directly: the amount of stellar UV radiation, planetary distance from the host star, and planetary atmospheric attenuation. The amount of stellar UV radiation depends on the stellar age since stars experience nuclear and magnetic evolutions. In the process of nuclear evolution, the photosphere becomes more luminous and hotter, and emits more UV radiation. Magnetic evolution is related to the variation

in chromospheric UV radiation. As a star ages, it rotates slower, which causes a decrease in radiation emitted from the chromosphere. The emitted energy reduces by d^2 and is absorbed by the atmospheres before reaching the planetary surface. In this research, the effects of stellar types, ages, and atmospheric attenuation on the amount of UV radiation were integrated to investigate DNA damage on planets orbiting at the distances of climatological habitable zone boundaries. Figure 4.4 shows the overview of my study. For the case of F-type stars, magnetic evolution was ignored, since it is insignificant.

The evolutionary tracks for F-type stars were derived by using the advanced version of the Eggleton code (Eggleton, 1971; Eggleton et al., 1973; Eggleton, 1973; Pols et al., 1995, 1998). One of the main features of this code is a self-adapting non-Lagrangian mesh. The code follows a model smoothly through many phases of stellar evolution with no need for a redistribution of mesh points. In the code, both the stellar structure equations and the diffusion equations for the chemical composition are solved simultaneously, and that enables the code to accurately model phases where the composition changes rapidly and can affect rapid structural changes. Another feature is that the code treats convective mixing and semiconvection as diffusion processes. Since stars with $T_{\rm eff} \leq 6500$ K have deep outer convection zones, and very massive stars have convective cores during their core hydrogen burning phase, the representation of the convection greatly affects the results for these stars. A free parameter of overshooting, $\delta_{\rm ov}$, is introduced in the code in order to avoid inaccuracy caused by an adjustable parameter required in the mixing length theory, $l_{\rm ov}$, the distance of "overshooting" of convective elements into non-convective layers. Instead of $l_{\rm ov}$, the code defines the region satisfying $\nabla_{\rm rad} > \nabla_{\rm ad} - \delta(\delta_{\rm ov})$ as the mixing region. $\nabla_{\rm rad}$ is a radiative gradient and $\nabla_{\rm ad}$ is an adiabatic gradient. In this advanced version of the Eggleton code, improvements have been made in the equation of state (Pols et al.,

1995, 1998). Also, the opacity tables, nuclear reaction rates, and neutrino loss rates have been updated. The stellar models generated with the Eggleton code have been thoroughly tested, and proved to represent various types of stars, including giants and supergiants with well-known masses (Schröder et al., 1997; Pols et al., 1998). At the same time, the two parameters α, which is the ratio of typical mixing length to the local pressure scale height, and $\delta_{\rm ov}$ were calibrated by matching accurately the physical properties of those stars.

I computed the effective temperatures, luminosities, and masses at different points of time for Zero Age Main-Sequence (ZAMS) masses of $M = 1.0$, 1.2, 1.3, 1.4, and 1.5 $M_{\odot}$ with the code. For the abundance of heavy elements, which decisively affects the opacities, I used $Z = 0.02$. This value is slightly higher than the Solar value, $Z = 0.0188$ (Schröder & Connon Smith, 2008). During the main-sequence phase, no mass variation was found in the models. Table 4.2 summarizes the evolution of $T_{\rm eff}$ and L for the star of each mass. Figure 4.5 shows the evolutionary tracks of the stars for only the main-sequence part.

As stars evolve, the climatological habitable zones migrate outward during their main-sequence phase. Figure 4.6 shows the migration of the climatological habitable zones for a star of 1.3 $M_{\odot}$ including the red giant phase. The dark gray area is the conservative habitable zone, and the light gray area is the general habitable zone. Stars of 1.3 $M_{\odot}$ stay in the main-sequence phase for about 3.3 Gyr. The main-sequence phase ends at the age when the climatological habitable zones suddenly move outward rapidly in the figure. The migration of climatological habitable zones for $M = 1.2$, 1.3, 1.4, and 1.5 $M_{\odot}$ is depicted in Figure 4.7. The distances of the extreme positions (most inward positions for inner boundaries and most outward positions for outer boundaries) are picked up in Table 4.4. Also, Table 4.5 presents the distances of the limits that are continuously inside the climatological habitable

zones during the main-sequence lifetime. The boundary positions of the continuous domains are also shown in Figure 4.7 as the horizontal lines in red for iG and oG and in blue for iC and oC. Additionally, the dashed line represents the Earth-equivalent position.

Table 4.2. Evolutionary properties of F-type stars during main-sequence phase

	$M = 1.2\ M_\odot$			$M = 1.3\ M_\odot$			$M = 1.4\ M_\odot$			$M = 1.5\ M_\odot$		
Age (Gyr)	$T_{\rm eff}$ (K)	L ($L_\odot$)	Spectral Type	$T_{\rm eff}$ (K)	L ($L_\odot$)	Spectral Type	$T_{\rm eff}$ (K)	L ($L_\odot$)	Spectral Type	$T_{\rm eff}$ (K)	L ($L_\odot$)	Spectral Type
0.5	6178	1.770	F8 −22 K	6444	2.644	F5	6720	3.780	F3 +20 K	7084	5.228	F1 +84 K
1.0	6195	1.878	F8	6447	2.839	F5	6682	4.077	F3 −18 K	6983	5.728	F1 −17 K
1.5	6205	1.996	F8	6432	3.036	F5	6589	4.361	F4 +59 K	6775	6.247	F3 +75 K
2.0	6211	2.121	F8 +11 K	6386	3.224	F6 +26 K	6428	4.591	F5 −12 K	6482	6.753	F5 +42 K
2.5	6204	2.247	F8	6303	3.383	F7 +23 K	6218	4.755	F8 +18 K	6117	7.047	F9
3.0	6178	2.366	F8 −22 K	6174	3.493	F8 −26 K	...	...	...	...	...	...
3.5	6130	2.468	F9	...	...	...	...	...	...	...	...	...
4.0	6058	2.555	G0	...	...	...	...	...	...	...	...	...

The spectral type corresponding to each $T_{\rm eff}$ is shown with the difference from $T_{\rm eff}$ of the model F-type stars. See Table 4.3.

Table 4.3. The effective temperature and mass of F0 V through G0 V stars derived with PHOENIX code

Type	$T_{\rm eff}(K)$	M $(M_{\odot})$
F0	7200	1.60
F1	7000	1.55
F2	6890	1.50
F3	6700	1.35
F4	6530	1.30
F5	6440	1.25
F6	6360	1.20
F7	6280	1.15
F8	6200	1.10
F9	6125	1.08
G0	6050	1.05

Table 4.4. Climatological habitable zones including stellar main-sequence evolution — extreme positions

$M(M_{\odot})$	$t_{\rm ms}$(Gyr)	iG (AU)	iC (AU)	oC (AU)	oG (AU)
1.2	4.255	1.066	1.208	2.174	2.668
1.3	3.291	1.283	1.455	2.511	3.085
1.4	2.605	1.510	1.716	2.888	3.555
1.5	2.706	1.735	1.975	3.581	4.388

4.1.4 Beyond F-type Stars: Effects of Nuclear and Magnetic Evolution in Other Types of Main-sequence Stars

Nuclear and magnetic evolution are responsible for the variation in the amount of UV radiation with stellar age. As hydrogen in the core is converted to helium, the increase of the core density leads the rise in core temperature and pressure. As a result, the luminosity and radius of a star increase over time. The effective temper-

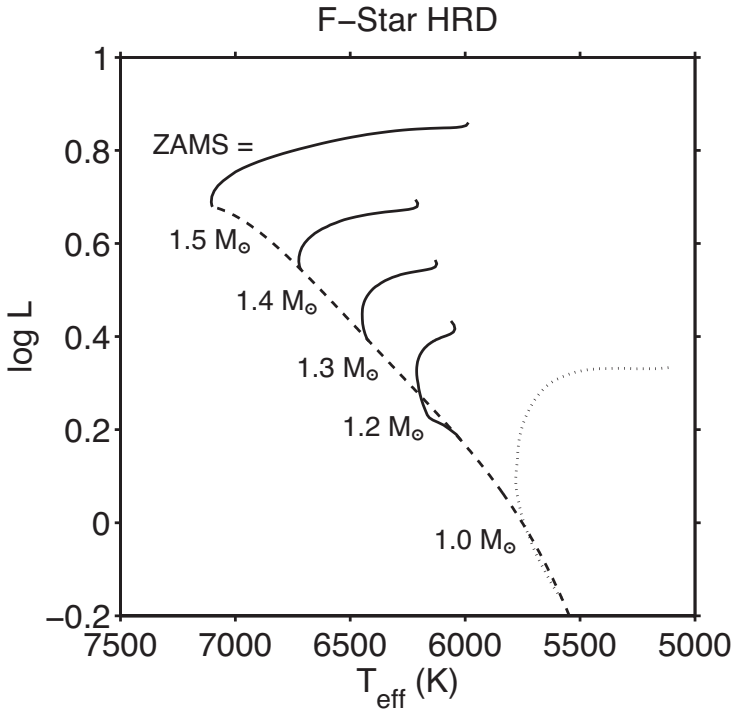

Figure 4.5. Evolutionary tracks of stars having ZAMS masses of 1.0 $M_{\odot}$, 1.2 $M_{\odot}$, 1.3 $M_{\odot}$, 1.4 $M_{\odot}$, and 1.5 $M_{\odot}$. Only the main-sequence phase is shown. The dashed line represents the points at ZAMS.

ature changes according to the development of luminosity and radius. UV radiation from photosphere varies accordingly as well. This is called nuclear evolution. On the other hand, in the process of magnetic evolution, UV radiation from chromosphere decreases with stellar age (Skumanich, 1972; Noyes et al., 1984; Cuntz et al., 1999; Guinan & Ribas, 2002; Cardini & Cassatella, 2007; Güdel & Kasting, 2011). Chromospheric emission is produced by two different mechanisms: acoustic heating and magnetic heating (Ulmschneider, 1990). Acoustic heating is the mechanism in which acoustic waves produced by the turbulence in the convection zone heat the chromosphere. UV radiation caused by acoustic heating is considered as the basal flux and is almost steady throughout the stellar lifetime. Magnetic heating is one of the expressions of stellar magnetic activity and declines with time. Stars have magnetic fields

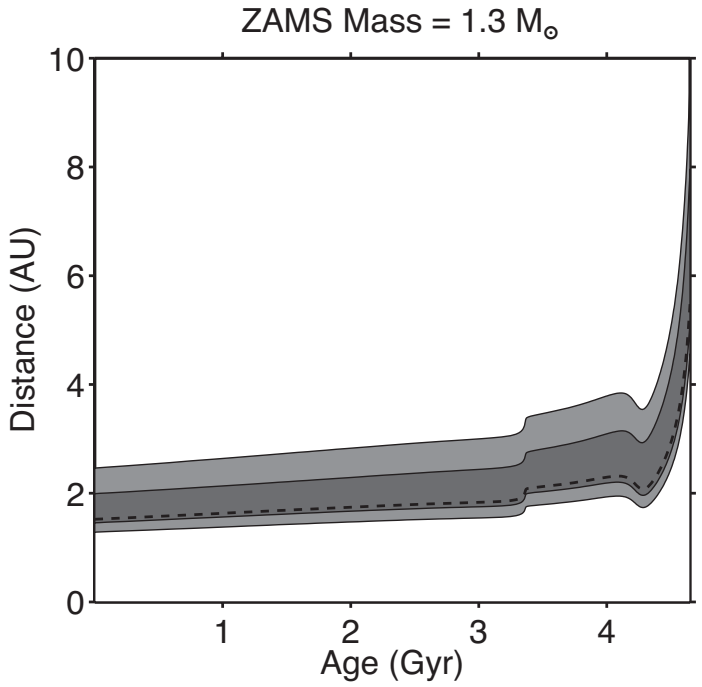

Figure 4.6. Evolution of the climatological habitable zone around a star with 1.3 $M_{\odot}$ at ZAMS. Dark gray area is the conservative habitable zone and light gray area is the general habitable zone. The dashed line represents the Earth-equivalent position.

generated by the motion of plasma due to convection and radial differential rotation in the convection zones. The magnetic activity is observed in various kinds of forms such as flare, coronal loop, starspots, photospheric faculae and chromospheric plage. It is known that young late-type stars show vigorous magnetic activity as well as fast rotation speed, but the activity subsides as the rotation speed slows down.The reason of spinning down is that magnetic wind takes away stellar angular momentum. Decline in the rotation speed causes weakening of its dynamo, which leads to less magnetic activity. The surface coverage by photospheric magnetic flux tubes can be expressed with the following equation resulted from a statistical analysis (Rüedi et al., 1997; Cuntz et al., 1999).

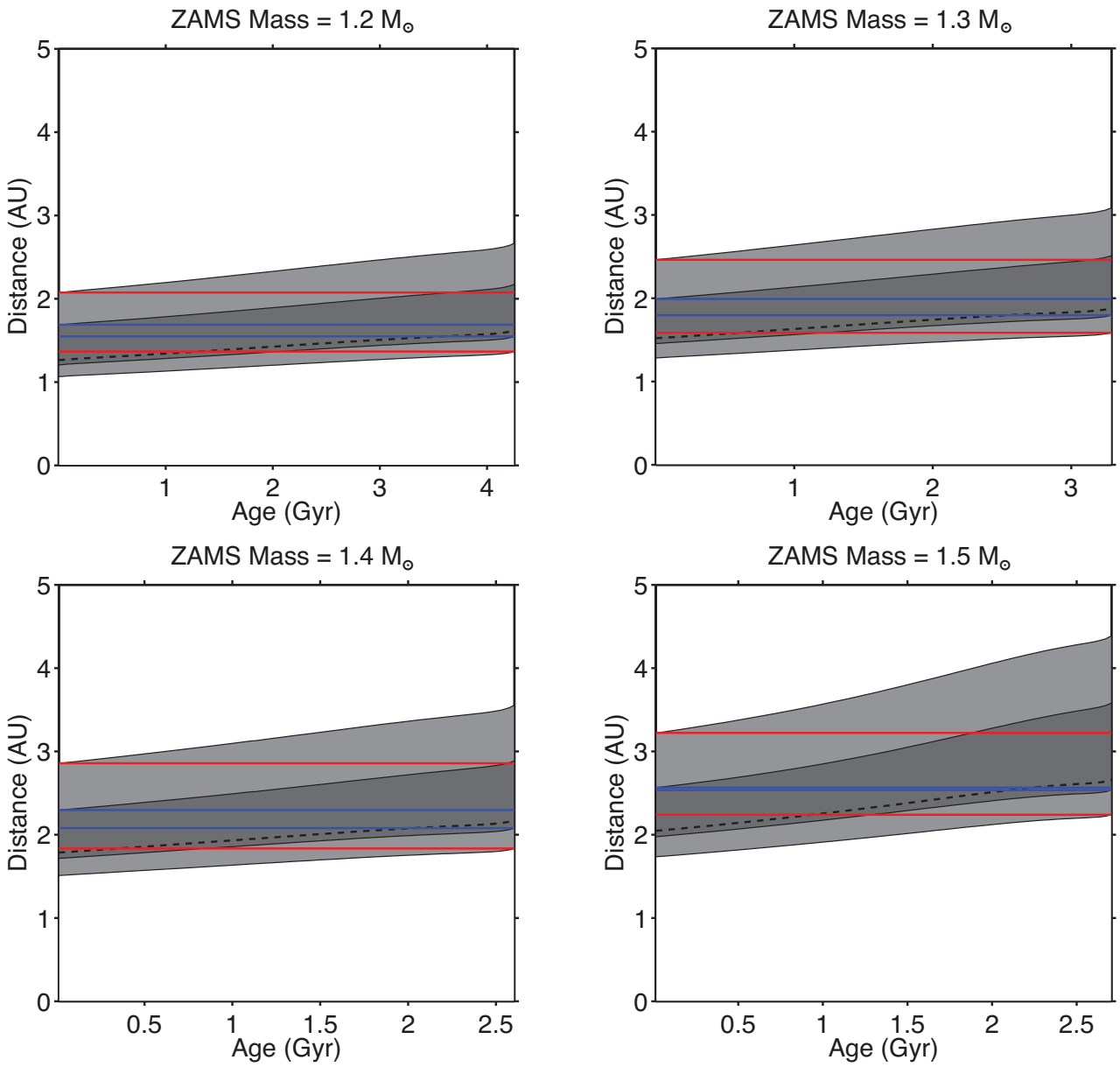

Figure 4.7. Evolution of the climatological habitable zone around stars with ZAMS masses of 1.2 $M_{\odot}$, 1.3 $M_{\odot}$, 1.4 $M_{\odot}$, and 1.5 $M_{\odot}$ for their main-sequence phase. Dark gray areas are the conservative habitable zones and light gray areas are the general habitable zones. The dashed lines represent the Earth-equivalent positions. The areas between blue lines and between red lines are always inside the conservative and general habitable zones, respectively, throughout the main-sequence phase.

Table 4.5. Climatological habitable zones including stellar main-sequence evolution — continuous domains

$M(M_\odot)$	$t_{\rm ms}$ (Gyr)	iG (AU)	iC (AU)	oC (AU)	oG (AU)
1.2	4.255	1.366	1.548	1.688	2.075
1.3	3.291	1.585	1.796	1.991	2.461
1.4	2.605	1.834	2.079	2.296	2.857
1.5	2.706	2.239	2.535	2.566	3.222

$$\Phi_{\rm mag} = B_0 f_0 = 238 - 5.51 P_{\rm rot} \tag{4.1}$$

for 10 days $\leq P_{\rm rot} \leq$ 50 days where B_0 is photospheric magnetic field strength in G, f_0 is photospheric magnetic filling factor and $P_{\rm rot}$ is rotational period in days. Also, the rotational period varies as

$$P_{\rm rot}(t, M) = (25.6 \pm 2.5) t^{0.45 \pm 0.06} (1.4 - M/M_\odot) \tag{4.2}$$

where t is stellar age in Gyr (Cardini & Cassatella, 2007). In addition to the rotation speed, the depth of convection zone relative to the stellar radius determines the strength of magnetic activity as well. If there were stars with the same rotational period and different stellar types, later-type stars, which have deeper convection zones, would show stronger magnetic activity than earlier-type stars.

In summary, the stellar UV fluxes, $F_{\rm UV}$, are emitted from the photosphere ($F^{\rm UV}_{\rm photo}$) and chromosphere ($F^{\rm UV}_{\rm chrom}$).

$$F_{\rm UV} = F^{\rm UV}_{\rm photo} + F^{\rm UV}_{\rm chrom} \tag{4.3}$$

The fluxes coming from the chromosphere consist of the fluxes generated by the waves ($F_{\rm wave}$), including acoustic and magnetic waves, and flares ($F_{\rm flare}$).

$$F^{\rm UV}_{\rm chrom} = F_{\rm wave} + F_{\rm flare} \tag{4.4}$$

$$F_{\rm wave} = F_{\rm ac}(T_{\rm eff}) + F_{\rm mag}(T_{\rm eff}, P_{\rm rot}) \tag{4.5}$$

where $F_{\rm ac}$ and $F_{\rm mag}$ indicate the fluxes of acoustic and magnetic wave origin, respectively. Both components depend on $T_{\rm eff}$. $F_{\rm mag}$ depends also on the rotational period $P_{\rm rot}$, which varies over time. $F_{\rm ac}$ is almost constant over time compared to $F_{\rm mag}$ even though $T_{\rm eff}$ shows small variation with time.

Any main-sequence stars experience the nuclear and magnetic evolutions, but the significance of them is different among stellar types. For F-type stars, $F^{\rm UV}_{\rm photo}$ is dominant over $F^{\rm UV}_{\rm chrom}$, and therefore $F_{\rm UV}$ is almost constant. On the other hand, $F^{\rm UV}_{\rm chrom}$ is dominant for G, K, and M-type stars (Noyes et al. 1984). Especially, M-type stars almost do not show nuclear evolution over several billions of years because they evolve very slowly. $F_{\rm UV}$ of G, K, and M-type stars is age dependent because of $F_{\rm mag}(T_{\rm eff}, P_{\rm rot})$.

4.2 Habitability around General F-type Main-sequence Stars

4.2.1 Stellar Case Studies

I investigated the biological damage of DNA due to stellar UV radiations around main-sequence F-type stars in terms of $E_{\rm eff}$, the ratio of the effective flux on a planet around the stars to that on a planet orbiting around the Sun at 1 AU with no consideration of atmospheric attenuation. In this study, I focused on the following aspects: (1) spectral types of the host stars, especially F0 V, F2 V, F5 V, and F8 V, (2) positions of planets in the climatological habitable zones, including the general and conservative inner limits, the Earth-equivalent positions, and the general and conservative outer limits, (3) effects of planetary atmospheric attenuation approximated by the attenuation functions, and (4) the relative impact of UV-A, UV-B, and UV-C on DNA.

Table 4.6. DNA Damage in case of no attenuation

Stellar Type	Distance (AU)		UV-A	UV-B	UV-C	Total
F0 V	iG	1.988	2.46e-5	0.386	9.41	9.80
	iC	2.265	1.90e-5	0.298	7.25	7.55
	E eqv	2.343	1.77e-5	0.278	6.77	7.05
	oC	2.919	1.14e-5	0.179	4.36	4.54
	oG	3.674	7.21e-6	0.113	2.75	2.87
F2 V	iG	1.692	2.26e-5	0.346	6.93	7.27
	iC	1.924	1.75e-5	0.268	5.36	5.62
	E eqv	1.997	1.62e-5	0.248	4.97	5.22
	oC	2.539	1.00e-5	0.154	3.08	3.23
	oG	3.172	6.43e-6	0.099	1.97	2.07
F5 V	iG	1.422	1.90e-5	0.280	3.94	4.22
	iC	1.614	1.47e-5	0.217	3.06	3.28
	E eqv	1.684	1.35e-5	0.200	2.81	3.01
	oC	2.205	7.88e-6	0.117	1.64	1.76
	oG	2.727	5.15e-6	0.076	1.07	1.15
F8 V	iG	1.141	1.98e-5	0.310	3.26	3.57
	iC	1.293	1.54e-5	0.241	2.54	2.78
	E eqv	1.353	1.41e-5	0.221	2.32	2.54
	oC	1.798	7.96e-6	0.125	1.31	1.44
	oG	2.212	5.26e-6	0.083	0.87	0.95
G2 V	Earth	1.000	8.37e-6	0.115	0.89	1.00

DNA damage without atmospheric attenuation in the climatological habitable zones around F0 V, F2 V, F5 V, and F8 V stars is depicted in Figure 4.8. Each panel in the figure shows the damage at five distances, which are the general inner (iG), conservative inner (iC), conservative outer (oC), and general outer (oG) habitable zone limits plus the Earth-equivalent (E eqv) position. The contributions of three UV regimes are shown in different colors. Also, the E_{eff} values for those F-type stars are listed in Table 4.6 along with the values for 1 AU from a G2 V or solar-like star. DNA damage on Earth without an atmosphere is $E_{\text{eff}} = 1$. In general, DNA damage around

Table 4.7. DNA Damage in case of $A = 0.05$, $B = 300$, $C = 0.5$

Stellar Type	Distance (AU)		UV-A	UV-B	UV-C	Total
F0 V	iG	1.988	1.13e-5	0.0684	0.159	0.228
	iC	2.265	8.74e-6	0.0527	0.123	0.175
	E eqv	2.343	8.17e-6	0.0492	0.115	0.164
	oC	2.919	5.26e-6	0.0317	0.074	0.106
	oG	3.674	3.32e-6	0.0200	0.047	0.067
F2 V	iG	1.692	1.04e-5	0.0612	0.131	0.192
	iC	1.924	8.05e-6	0.0473	0.101	0.148
	E eqv	1.997	7.47e-6	0.0439	0.094	0.138
	oC	2.539	4.62e-6	0.0272	0.058	0.085
	oG	3.172	2.96e-6	0.0174	0.037	0.055
F5 V	iG	1.422	8.74e-6	0.0494	0.091	0.140
	iC	1.614	6.78e-6	0.0383	0.070	0.109
	E eqv	1.684	6.23e-6	0.0352	0.065	0.100
	oC	2.205	3.63e-6	0.0205	0.038	0.058
	oG	2.727	2.38e-6	0.0134	0.025	0.038
F8 V	iG	1.141	9.11e-6	0.0541	0.085	0.139
	iC	1.293	7.09e-6	0.0421	0.066	0.108
	E eqv	1.353	6.48e-6	0.0385	0.060	0.099
	oC	1.798	3.67e-6	0.0218	0.034	0.056
	oG	2.212	2.42e-6	0.0144	0.023	0.037
G2 V	Earth	1.000	3.86e-6	0.0201	0.029	0.049

F-type stars is more significant than the case of Earth without an atmosphere if the planetary atmospheric attenuation is not considered. Only exception is the outer limit of general habitable zone around an F8 V star. E_{eff} is 0.95 at this position. However, atmospheres effectively reduce the damage to DNA. In this research, I used $A = 0.05$, $B = 300$, and $C = 0.5$ for the attenuation function as the default combination of parameters. The results are summarized in Figure 4.9 and Table 4.7. After the UV spectra are attenuated by the hypothetical atmosphere, the damage to DNA decreases to 23% at most at any positions in the climatological habitable zones

Table 4.8. DNA Damage in case of atmospheric attenuation expressed by a higher order ATT function

Stellar Type	Distance (AU)		UV-A	UV-B	UV-C	Total
F0 V	iG	1.988	1.07e-5	0.144	1.99	2.14
	iC	2.265	8.24e-6	0.111	1.53	1.64
	E eqv	2.343	7.70e-6	0.104	1.43	1.54
	oC	2.919	4.96e-6	0.067	0.92	0.99
	oG	3.674	3.13e-6	0.042	0.58	0.63
F2 V	iG	1.692	9.81e-6	0.129	1.53	1.66
	iC	1.924	7.58e-6	0.100	1.18	1.28
	E eqv	1.997	7.04e-6	0.093	1.10	1.19
	oC	2.539	4.36e-6	0.057	0.68	0.74
	oG	3.172	2.79e-6	0.037	0.44	0.47
F5 V	iG	1.422	8.23e-6	0.105	0.95	1.05
	iC	1.614	6.39e-6	0.081	0.73	0.82
	E eqv	1.684	5.87e-6	0.075	0.68	0.75
	oC	2.205	3.42e-6	0.044	0.39	0.44
	oG	2.727	2.24e-6	0.028	0.26	0.29
F8 V	iG	1.141	8.57e-6	0.116	0.82	0.93
	iC	1.293	6.68e-6	0.090	0.64	0.73
	E eqv	1.353	6.10e-6	0.082	0.58	0.66
	oC	1.798	3.45e-6	0.047	0.33	0.38
	oG	2.212	2.28e-6	0.031	0.22	0.25
G2 V	Earth	1.000	3.63e-6	0.043	0.25	0.29

around those stars, compared to the case of Earth without an atmosphere. Also, E_{eff} for F0 V, F2 V, F5 V, and F8 V stars reduces to 2.3%, 2.6%, 3.3%, and 3.9% of that before attenuation by the atmosphere. The reduction rates do not depend on the distance from the host star. At the inner limits of general habitable zones, E_{eff} for F0 V, F2 V, F5 V, and F8 V stars is 9.8, 7.3, 4.2, and 3.6 without planetary atmospheric attenuation, and decreases to 0.23, 0.19, 0.14, and 0.14 after attenuation by the atmosphere, respectively. At the Earth-equivalent positions, E_{eff} for those F-type stars is 7.1, 5.2, 3.0, and 2.5 without planetary atmospheric attenuation,

and 0.16, 0.14, 0.10, 0.10 with planetary atmospheric attenuation, respectively. At the outer limits of general habitable zones, E_{eff} is 2.9, 2.1, 1.1, and 0.95 without planetary atmospheric attenuation, and 0.067, 0.055, 0.038, and 0.037 with planetary atmospheric attenuation, respectively.

In all cases, DNA damage due to UV-A is unrecognizable in the figures. E_{eff} from UV-A at the inner limit of general habitable zone around an F0 V star is 2.46e-5 without the effect of atmosphere, which is the maximum value in the all tested cases. The value is reduced to 1.13e-5 if the planetary atmospheric attenuation is included. In the three regimes of UV light, the most affected by the planetary atmospheric attenuation is UV-C. For F0 V, F2 V, F5 V, and F8 V, DNA damage due to UV-C are 96%, 95%, 93%, and 91% of the total effect of all UV regimes, respectively. If the planetary atmospheric attenuation is included, DNA damage due to UV-C is reduced to 1.7%, 1.9%, 2.3%, and 2.6% of damage due to UV-C without planetary atmospheric attenuation, and occupies 70%, 68%, 65%, and 61% of the total effect for each attenuated case, respectively. The damage due to UV-C decreases with the stellar types from F0 V to F8 V, while the damage due to UV-A and UV-B decreases with the stellar types from F0 V to F5 V and then slightly increases for F8 V.

Additionally, a higher order ATT function, Equation (3.7) at $N = 3$, was applied to the same UV spectra of F-type stars. This function resembles the attenuation through the atmosphere with 40 mb CO_2 and 0.8 bar N_2 on Archean Earth calculated by Cockell (2002). The summary of the results can be found in Figure 4.10 and Table 4.8. Note that G2 V case in the table is for the present Sun, which is brighter than in Archean era. The damage to DNA is between 25% and 214% at any positions in the climatological habitable zones around F-type stars, compared to the case of present Earth without an atmosphere. E_{eff} for F0 V, F2 V, F5 V, and F8 V stars reduces to 22%, 23%, 25%, and 26% of those before attenuation by the atmosphere.

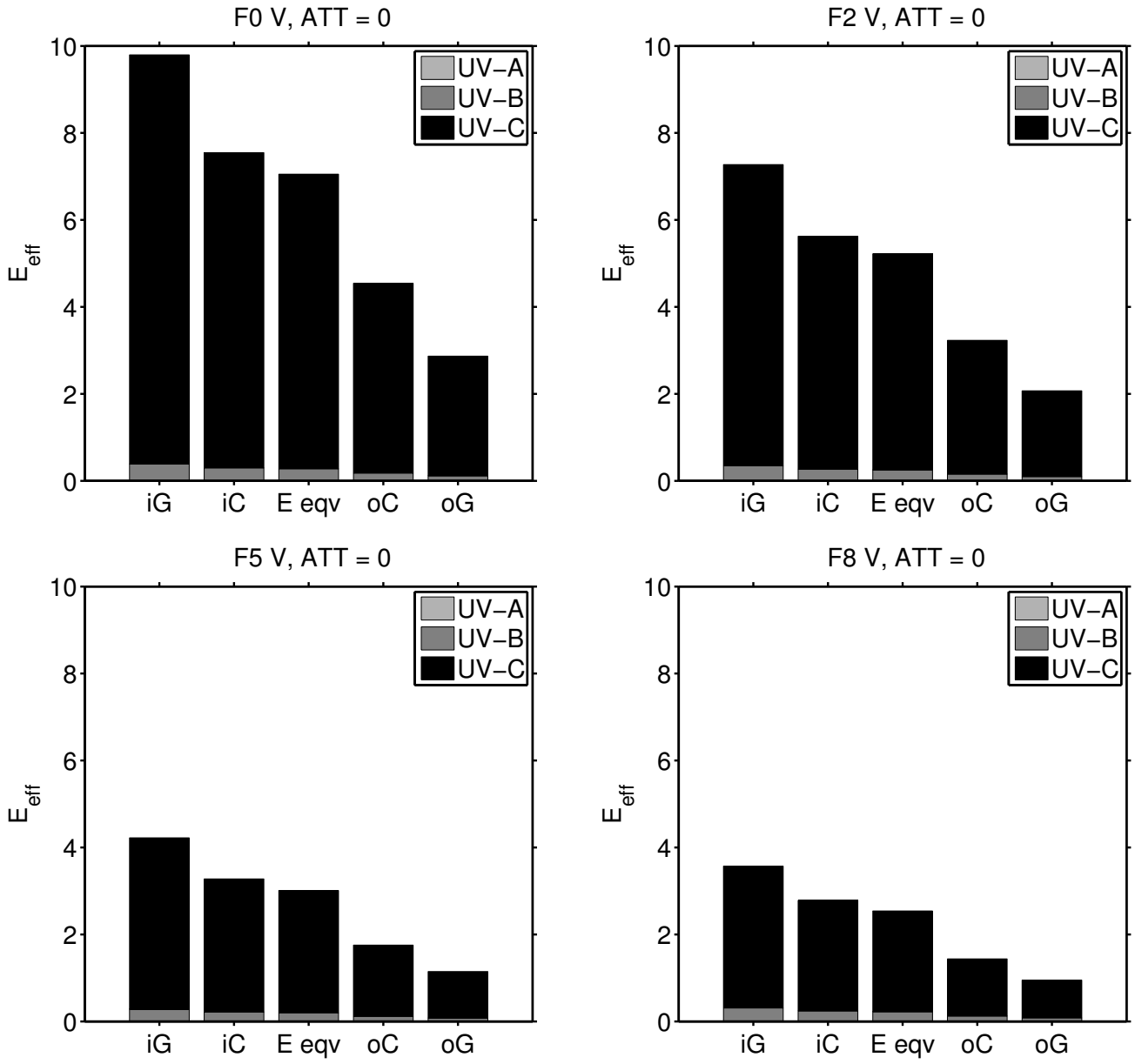

Figure 4.8. DNA damage at the climatological habitable zone limits around F0 V, F2 V, F5 V, F8 V stars (1). No atmospheric attenuation is assumed. Damage caused by UV-A is unrecognizable in the figure.

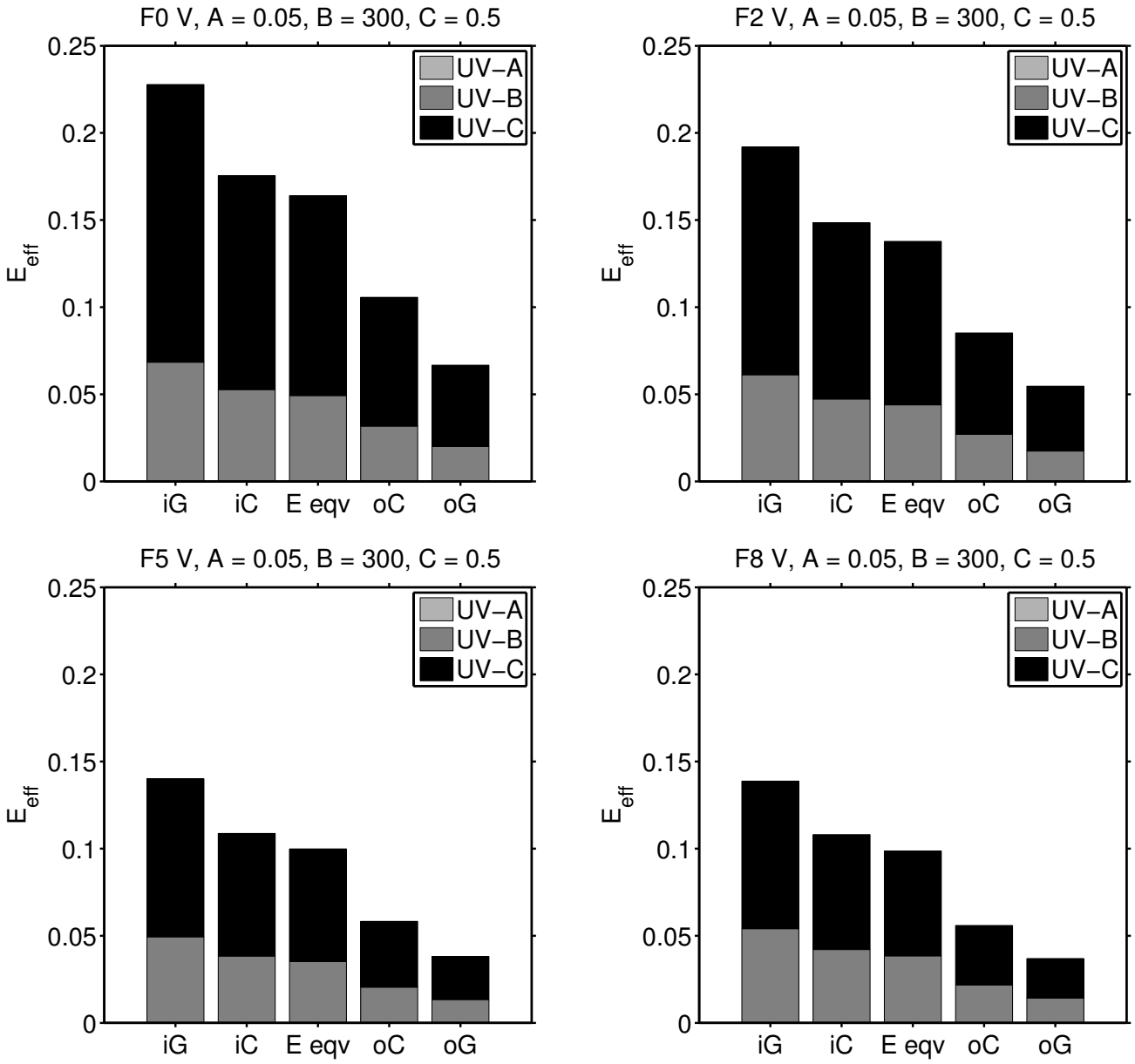

Figure 4.9. DNA damage at the climatological habitable zone limits around F0 V, F2 V, F5 V, F8 V stars (2). The effect of atmospheric attenuation with the parameters $(A, B, C) = (0.05, 300, 0.5)$ is included. Damage caused by UV-A is unrecognizable in the figure.

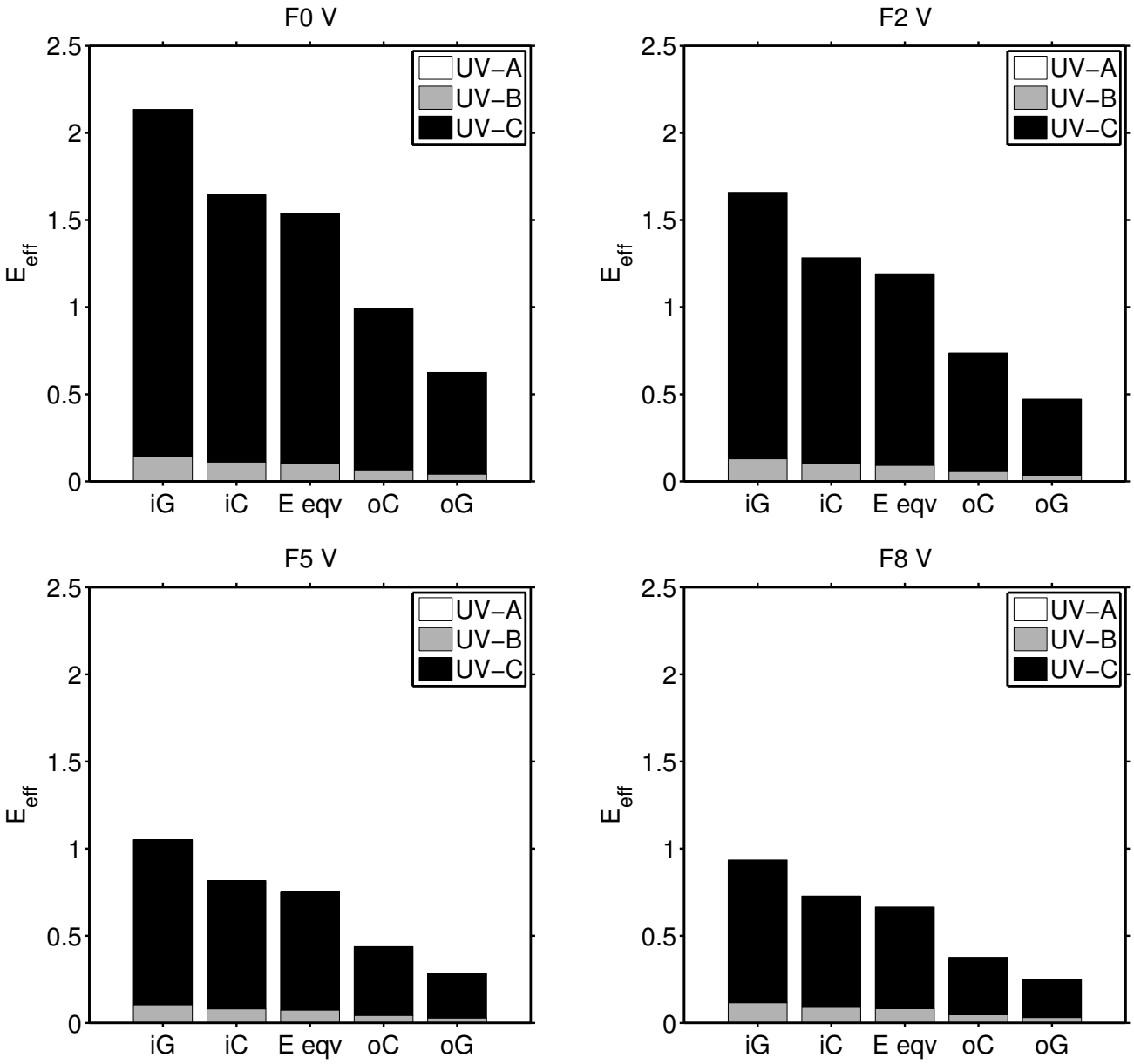

Figure 4.10. DNA damage at the climatological habitable zone limits around F0 V, F2 V, F5 V, F8 V stars (3). The effect of atmospheric attenuation expressed by a higher order ATT function is included. The ATT function is Equation (3.7) with $N = 3$. Damage caused by UV-A is unrecognizable in the figure.

At the inner limits of general habitable zones, E_{eff} for F0 V, F2 V, F5 V, and F8 V stars is 2.14, 1.66, 1.05, and 0.93 after attenuation by the atmosphere, respectively. At the Earth-equivalent positions, E_{eff} for those F-type stars is 1.54, 1.19, 0.75, and 0.66 and at the outer limits of general habitable zones, E_{eff} is as low as 0.63, 0.47, 0.29, and 0.25 with planetary atmospheric attenuation estimated for Archean Earth, respectively.

The results are broadly consistent with the results by Cockell (1999). According to the Cockell's results, the weighted biochemically effective irradiance at 1 AU around G2 V star is 132.7 W m^{-2} after attenuation by the atmosphere consisting of 40 mb CO_2 and 0.8 bar N_2. Since the weighted biochemically effective irradiance around an F2 V star is 1302 W m^{-2} at 1.5 AU and 286.1 W m^{-2} at 3.2 AU for the atmosphere consisting of 40 mb CO_2 and 1 bar N_2, the ratio of the weighted biochemically effective irradiance around an F2 V star to that of a planet with Archean atmosphere orbiting a G2 V star is 9.81 at 1.5 AU and 2.16 at 3.2 AU. My results show that the ratio of E_{eff} for an F2 V star to that of a planet orbiting a G2 V star at 1 AU is 7.24 at 1.5 AU and 1.60 at 3.2 AU, assuming the atmosphere consisting of 40 mb CO_2 and 0.8 bar N_2 for both G2 V and F2 V stars. The differences in results probably came from the different UV spectra, DNA action spectra, and atmospheric attenuation functions involved in his and my studies.

I also studied the effect of parameter choices for the attenuation functions. I applied the attenuation functions to an F2 V star, varying one of the parameters, A, B, or C at a time. Figure 4.11 and Figure 4.12 depict the change in E_{eff} when parameter A is varied from 0.01 to 1.0 and the other two parameters are fixed. Figure 4.11 shows the relative impact of UV-A, UV-B, and UV-C on DNA at the Earth-equivalent position. The impact of UV-A is, however, unrecognizable in the graphs. Figure 4.12 shows DNA damage at five positions in the climatological habitable zones of an F2

V star: inner limits of general and conservative habitable zones, Earth-equivalent position, and outer limits of conservative and general habitable zones. The dotted lines represent the limits of general habitable zone and the dashed lines represent the limits of conservative habitable zone. Since DNA damage is larger for a shorter distance from the star, the top two lines represent the inner limits and bottom two lines are the outer limits of the climatological habitable zones.

Parameter A determines the rate of change in ATT with increasing wavelength. As shown in Figure 4.11, the slope of ATT is mild with a small A value. Therefore, more light of long wavelengths and less light of short wavelengths compared to the center wavelength (the value of B) are attenuated by the atmosphere when a small A is used than when a large A is used. Parameter B determines the center wavelength and changes the response of each regime to varying A. Because of that, the appearance of E_{eff} vs. attenuation variable A heavily depends on the fixed value of parameter B.

If $B = 300$ is used, DNA damage due to UV-A increases, while that due to UV-B and UV-C decreases as parameter A increases. E_{eff} decreases from 0.73 to 0.0074 at the Earth-equivalent position with increasing A. The most change is occurred between $A = 0.01$ and 0.08, where E_{eff} due to UV-C declines dramatically. In this region, UV-C is responsible for the most of the DNA damage. At $A = 0.08$, E_{eff} due to UV-B and UV-C is about the same, and E_{eff} due to UV-B is greater than UV-C for larger A values.

If $B = 280$ is used, both E_{eff} from UV-A and UV-B regimes become increasing functions of variable A. E_{eff} from UV-C and whole UV regimes decreases from $A = 0.01$ until $A = 0.29$ and 0.28, respectively, and then show very slight increase for larger A. E_{eff} from UV-A, UV-B, and UV-C approaches to 8.1e-6, 0.12, and 0.29, respectively, at the Earth-equivalent position as variable A increases.

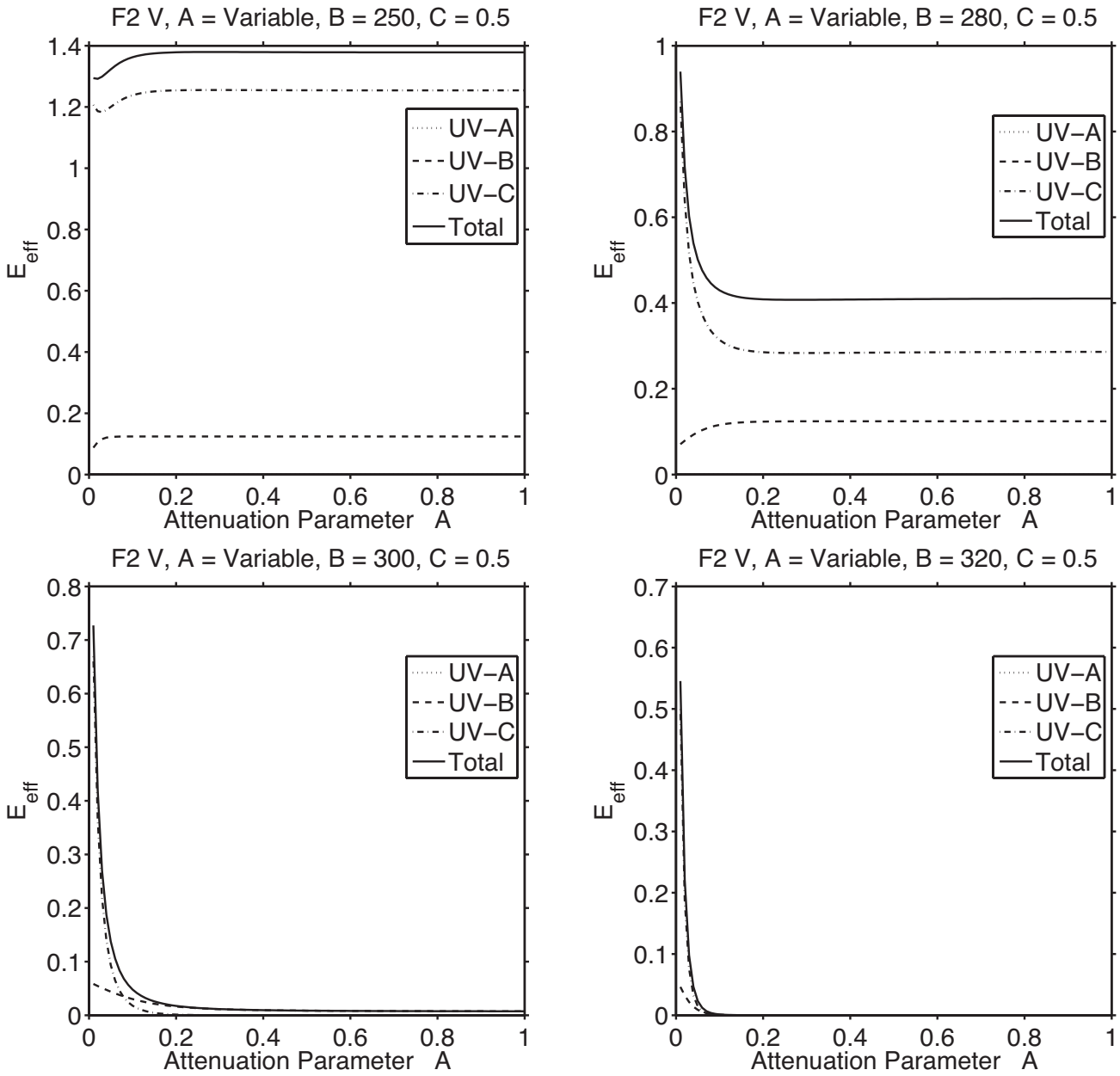

Figure 4.11. Change in DNA damage at the Earth-equivalent position around an F2 V star with varied attenuation parameter A. Parameters B and C are fixed while A is varied. The cases for $B = 250$, 280, 300, and 320 are shown. $C = 0.5$ in all cases in this figure.

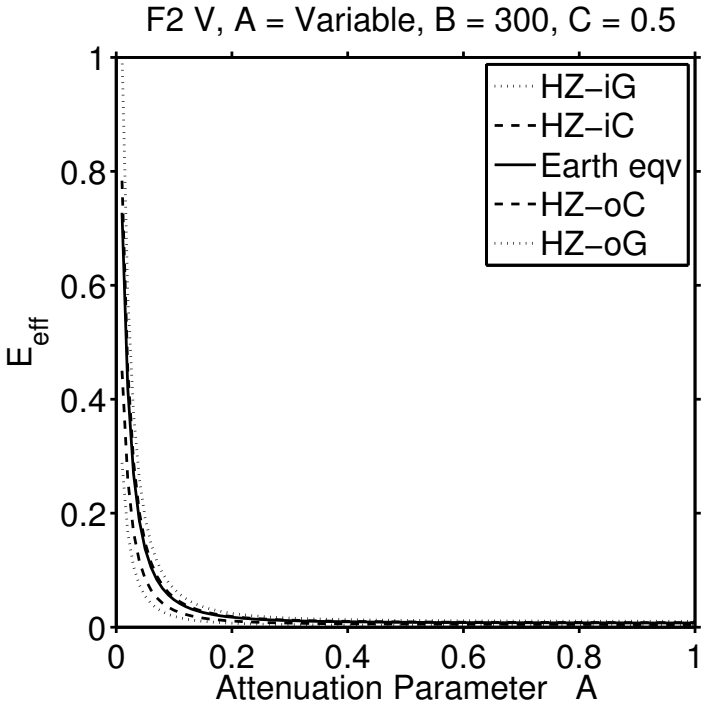

Figure 4.12. Change in DNA damage at the climatological habitable zone limits around an F2 V star with varied attenuation parameter A.

If $B = 250$ is used, DNA damage due to each regime is in most part constant. At $A = 0.01$, E_{eff} from UV-A, UV-B, and UV-C is 6.7e-6, 0.088, and 1.206, respectively. E_{eff} keeps increasing for UV-A and UV-B with increasing A, but for UV-C, E_{eff} shows small fluctuations for relatively small A. E_{eff} of UV-C has the minimum of 1.183 at $A = 0.03$. E_{eff} from UV-A, UV-B, and UV-C approaches to 8.1e-6, 0.12, and 1.25, respectively, at the Earth-equivalent position as variable A increases.

If $B = 320$ is used, the appearance of E_{eff} is similar to the case of $B = 300$. DNA damage is, however, generally smaller. E_{eff} of UV-A, UV-B, and UV-C starts at 4.4e-6, 0.046, and 0.499, respectively, at the Earth-equivalent position. E_{eff} of UV-A increases to 7.5e-6 by $A = 1.0$. E_{eff} of UV-B and UV-C quickly reduces to 0.0035 and 0.0031, respectively, at $A = 0.07$, and this is the point where E_{eff} from UV-B starts to exceed that of UV-C.

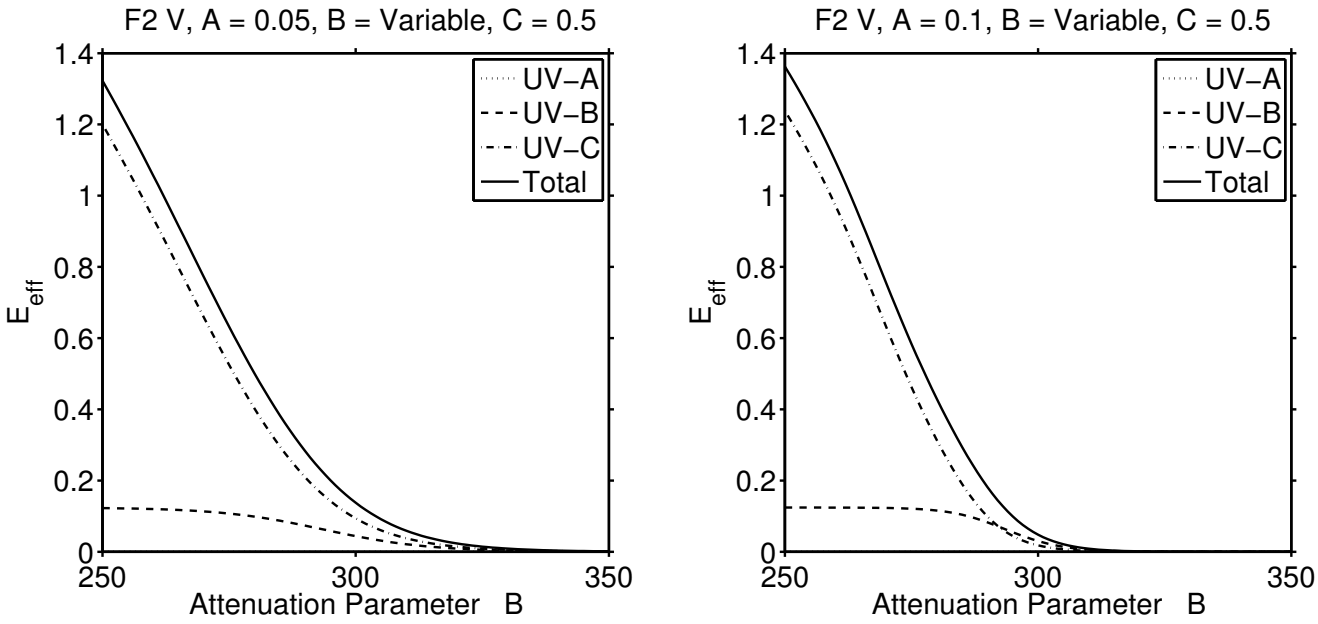

Figure 4.13. Change in DNA damage with varied attenuation parameter B at the Earth-equivalent position around an F2 V star.

Next, I varied parameter B from 250 to 350 while fixing the values of parameters A and C. The results are shown in Figure 4.13 and Figure 4.14. E_{eff} is a decreasing function for variable B. Since parameter B determines the center of the attenuation function, the effect of UV radiation diminishes from the lowest wavelengths as B is increased. In other words, UV-C is affected the most by varying B. If $A = 0.05$ and $C = 0.5$ are used, E_{eff} decreases from 1.32 at $B = 250$ to 0.14 at $B = 300$ and to 0.0012 at $B = 350$ at the Earth-equivalent position. If $A = 0.1$ and $C = 0.5$ are used, the appearance of each line is similar to the case with $A = 0.05$, but E_{eff} of UV-B exceeds that of UV-C at $B = 293$. The line for UV-C is steeper with $A = 0.1$ than with $A = 0.05$. The total E_{eff} decreases from 1.36 at $B = 250$ to 0.048 at $B = 300$ and to 3.9e-6 at $B = 350$ at the Earth-equivalent position.

When parameters A and B are fixed and parameter C is increased from 0 to 1.0, E_{eff} increases linearly from 0. The results are shown in Figure 4.15 and Figure 4.16.

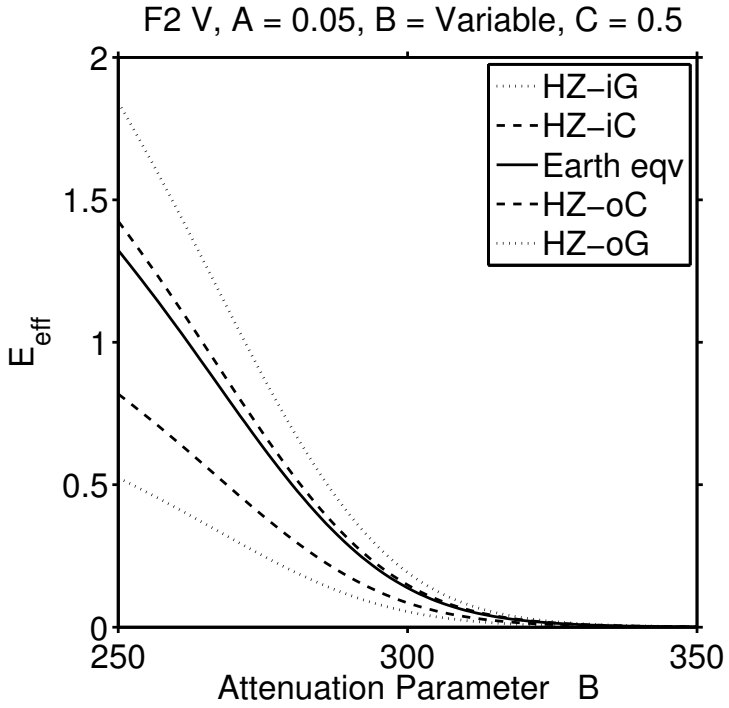

Figure 4.14. Change in DNA damage with varied attenuation parameter B at the climatological habitable zone limits around an F2 V star.

As is obvious from the function, parameter C does not affect the relative impact of different wavelengths on DNA. If $A = 0.05$ and $B = 300$ are used, the total E_{eff} is 0.28 at $C = 1.0$ at the Earth-equivalent position. Also, DNA damage is 0.0052% from UV-A, 32% from UV-B, and 68% from UV-C for the same case.

DNA damage is inversely proportional to the square of distance between a planet and the host star, and thus, the ratio of DNA damage at one position to another does not vary with the combinations of parameters. Because of that, if E_{eff}, the ratio of DNA damage at a position to the reference value, at different positions are compared, the differences are smaller for more effective combination of parameters. For example, DNA damage at the inner limits of general and conservative habitable zones and the outer limits of conservative and general habitable zones is 139%, 108%, 62%, and 40% of DNA damage at the Earth-equivalent position around an F2 V

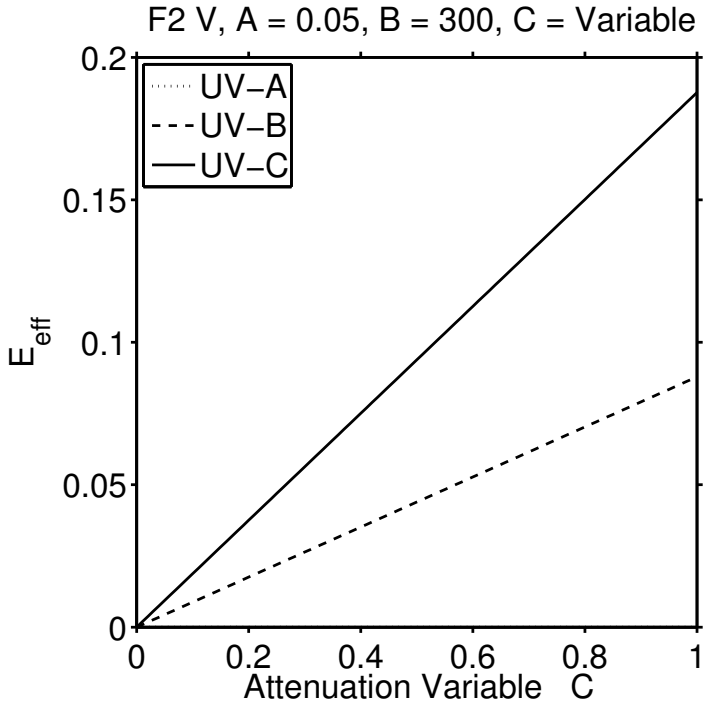

Figure 4.15. Change in DNA damage with varied attenuation parameter C at the Earth-equivalent position around an F2 V star.

star, respectively. If the parameters are (A, B, C) = (0.01, 300, 0.5), E_{eff} is 1.01, 0.78, 0.73, 0.45, and 0.29 at the inner limits of general and conservative habitable zones, the Earth-equivalent position, and the outer limits of conservative and general habitable zones, respectively. If the parameters are (A, B, C) = (0.5, 300, 0.5), E_{eff} is 0.0119, 0.0092, 0.0086, 0.0053 and 0.0034, respectively. As a result, there is 0.72 difference between E_{eff} at the inner and outer limits of general habitable zone for (A, B, C) = (0.01, 300, 0.5), while there is only 0.0085 difference between E_{eff} at the same limits for (A, B, C) = (0.5, 300, 0.5). This is depicted in Figure 4.12. The same can be said for Figure 4.14, in which parameter B is varied and for Figure 4.16, in which parameter C is varied. If the parameters are (A, B, C) = (0.05, 250, 0.5), E_{eff} is 1.84, 1.43, 1.32, 0.82, and 0.52 at the inner limits of general and conservative habitable zones, the Earth-equivalent position, and the outer limits of conservative

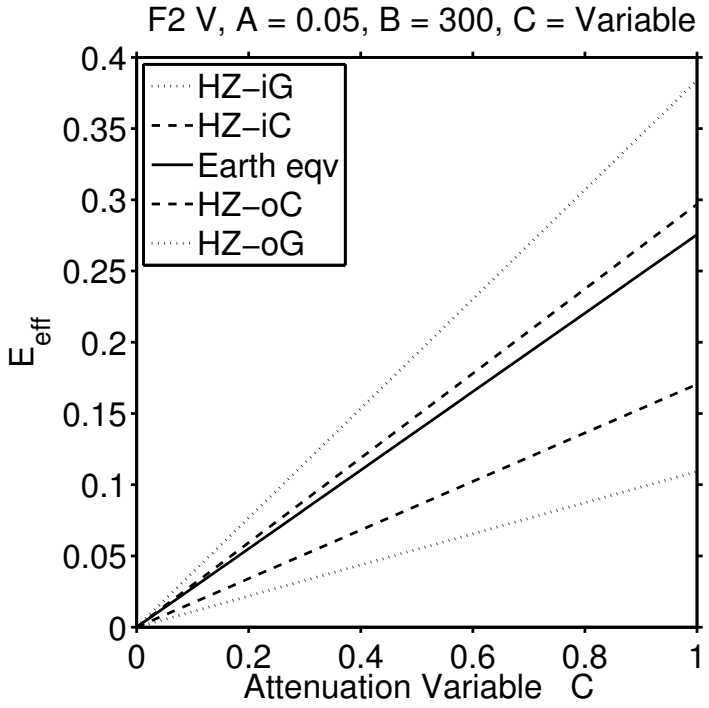

Figure 4.16. Change in DNA damage with varied attenuation parameter C at the climatological habitable zone limits around an F2 V star.

and general habitable zones, respectively. If the parameters are (A, B, C) = (0.05, 300, 0.5), E_{eff} is 0.19, 0.15, 0.14, 0.09 and 0.05, respectively. There is 1.32 difference between E_{eff} at the inner and outer limits of general habitable zone for (A, B, C) = (0.05, 250, 0.5), while there is only 0.14 difference between E_{eff} at the same limits for $(A, B, C) = (0.05, 300, 0.5)$.

4.2.2 Habitability in Consideration of F-star Evolution

I studied the effect of stellar evolution on DNA damage. I simulated the change of E_{eff} at the specific positions in the climatological habitable zones around the stars having masses of 1.2 $M_{\odot}$, 1.3 $M_{\odot}$, 1.4 $M_{\odot}$, and 1.5 $M_{\odot}$. The selected positions are the general outer limit at ZAMS (bottom dotted line in Figures 4.17 and 4.18), the conservative outer limit at ZAMS (bottom dashed line), the general inner limit at the

Table 4.9. Development of DNA Damage with time in the case of no atmospheric attenuation at the average Earth equivalent positions

Age (Gyr)	1.2 $M_\odot$	1.3 $M_\odot$	1.4 $M_\odot$	1.5 $M_\odot$
0.5	1.75	2.61	3.46	4.88
1.0	1.87	2.63	3.21	3.98
1.5	1.93	2.53	2.70	2.65
2.0	1.96	2.28	1.88	1.47
2.5	1.92	1.86	1.10	0.52
3.0	1.75	1.28	-	-
3.5	1.44	-	-	-
4.0	1.02	-	-	-

end of main-sequence (top dotted line), the conservative inner limit at the end of main-sequence (top dashed line), the Earth-equivalent positions at ZAMS (minimum, top solid line) and the end of main-sequence (maximum, bottom solid line). The distance of each position from the host star is found in Figure 4.7. Additionally, I considered the average Earth-equivalent positions (blue line), which were derived by interpolating the inner and outer limits, continuously staying inside the conservative habitable zones. The Earth-equivalent positions are weighted averages between the inner and outer limits of the conservative habitable zones in general. The inner limit, Earth-equivalent position, and outer limit can be approximated as $0.95\sqrt{L}$, $\sqrt{L}$, and $1.37\sqrt{L}$ with L in $L_\odot$, respectively, and I used the same weight to obtain the average Earth-equivalent positions from the conservative inner limit at the end of main-sequence and the conservative outer limit at ZAMS. Development of E_{eff} at the Earth-equivalent positions is summarized in Table 4.9 for the case of no atmospheric attenuation and Table 4.10 for the case of my default atmospheric attenuation. Additionally, the damage at the evolutionary Earth-equivalent positions (red line) was also investigated.

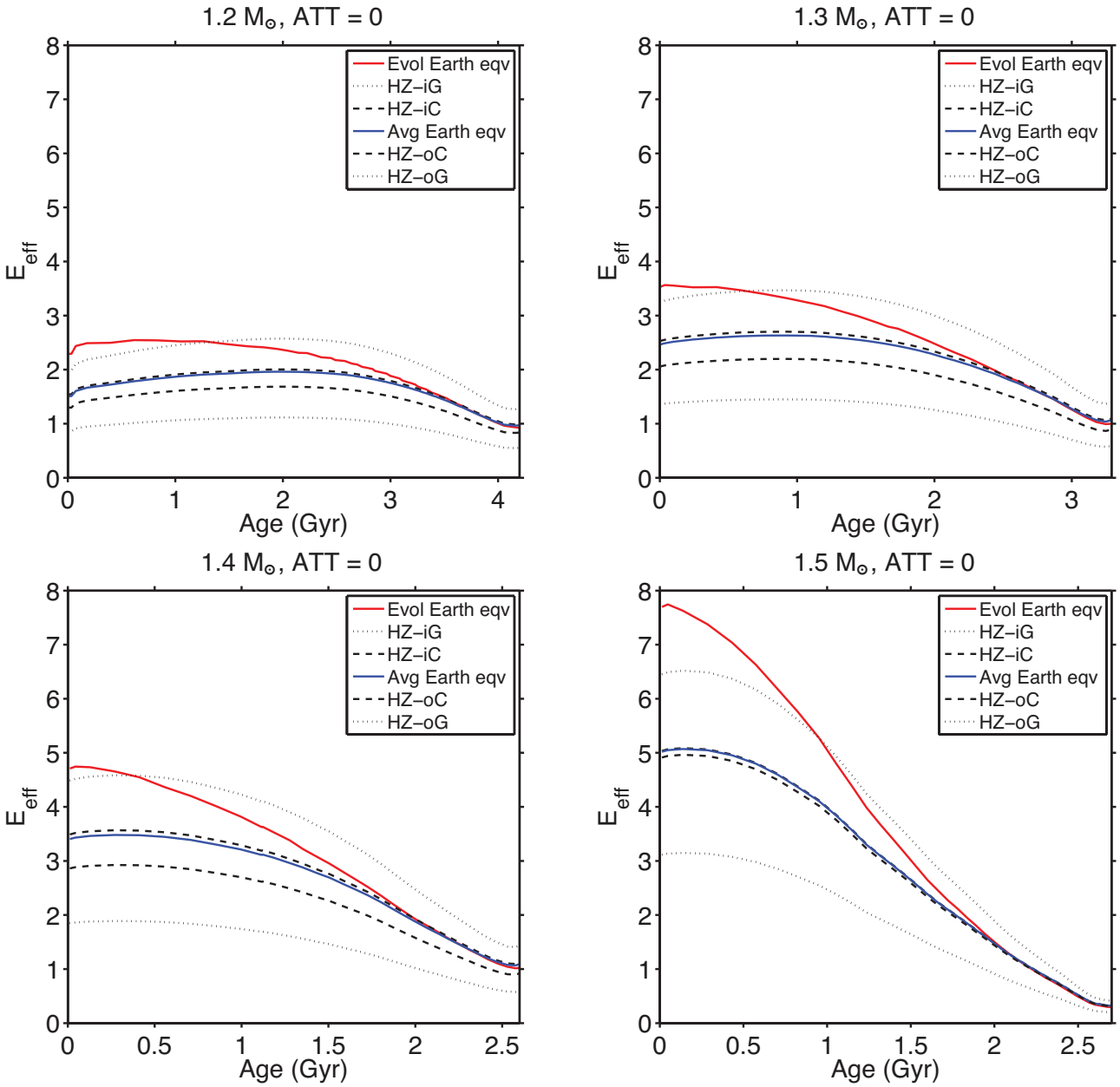

Figure 4.17. Development of DNA damage at the climatological habitable zone limits around stars with ZAMS masses of 1.2 $M_{\odot}$, 1.3 $M_{\odot}$, 1.4 $M_{\odot}$, and 1.5 $M_{\odot}$ for their main-sequence phase (1). No atmospheric attenuation is assumed. Note that the ZAMS point of the Earth-equivalent position for 1.2 $M_{\odot}$ looks contradicting with the text, which states $E_{\rm eff} = 0.91$, but the ZAMS point is only not clearly shown in the figure because $E_{\rm eff}$ increases to 1.51 within 0.03 Gyr. The same can be said of the plots within the initial ∼0.03 Gyr for other positions.

The damage of DNA at each position within the climatological habitable zones at ZAMS increases as the stellar mass increases. In all cases, the damage becomes slightly higher with time at first, but starts decreasing at some point, while the luminosity keeps increasing and the climatological habitable zones migrate outward all the time. The points where the damage starts decreasing are earlier for more massive stars. Those points for 1.2 $M_{\odot}$, 1.3 $M_{\odot}$, 1.4 $M_{\odot}$, and 1.5 $M_{\odot}$ occur at the age of 1.95 Gyr, 0.93 Gyr, 0.27 Gyr, and 0.14 Gyr, respectively. Also, the rate of decrease becomes greater as the stellar mass increases. If no planetary atmospheric attenuation is taken into account, ZAMS E_{eff} at the average Earth-equivalent positions for stars of 1.2 $M_{\odot}$, 1.3$M_{\odot}$, 1.4 $M_{\odot}$, and 1.5 $M_{\odot}$ is 0.91, 2.46, 3.41, and 5.02, respectively. The maximum E_{eff} at the same positions is 1.96, 2.63, 3.48, and 5.07. E_{eff} at the same positions at the end of the main-sequence phase is 0.96, 1.04, 1.07, and 0.32, respectively.

If the attenuation function with parameters (A, B, C) = (0.05, 300, 0.5) is assumed, the damage is reduced by up to 96%, 97%, 97%, and 98% for 1.2 $M_{\odot}$, 1.3 $M_{\odot}$, 1.4 $M_{\odot}$, and 1.5 $M_{\odot}$, respectively. The reduction rate depends on the effective temperature, and the maximum reduction rate occurs when the effective temperature and the damage are the highest. This is because the color shifts toward lower wavelength if the temperature becomes higher and UV-C is more affected by the attenuation functions than UV-B or UV-A. After the UV flux is attenuated, ZAMS E_{eff} at the average Earth-equivalent positions for stars of 1.2 $M_{\odot}$, 1.3$M_{\odot}$, 1.4 $M_{\odot}$, and 1.5 $M_{\odot}$ becomes 0.038, 0.082, 0.098, and 0.121, respectively. The maximum E_{eff} at the same positions is 0.075, 0.087, 0.099, and 0.122. E_{eff} at the same positions at the end of the main-sequence phase is 0.040, 0.041, 0.041, and 0.014, respectively.

For a specific age interval, E_{eff} changes in different ways around the stars having different masses. I was interested in the variation of E_{eff} between 0.5 Gyr and 2.5 Gyr.

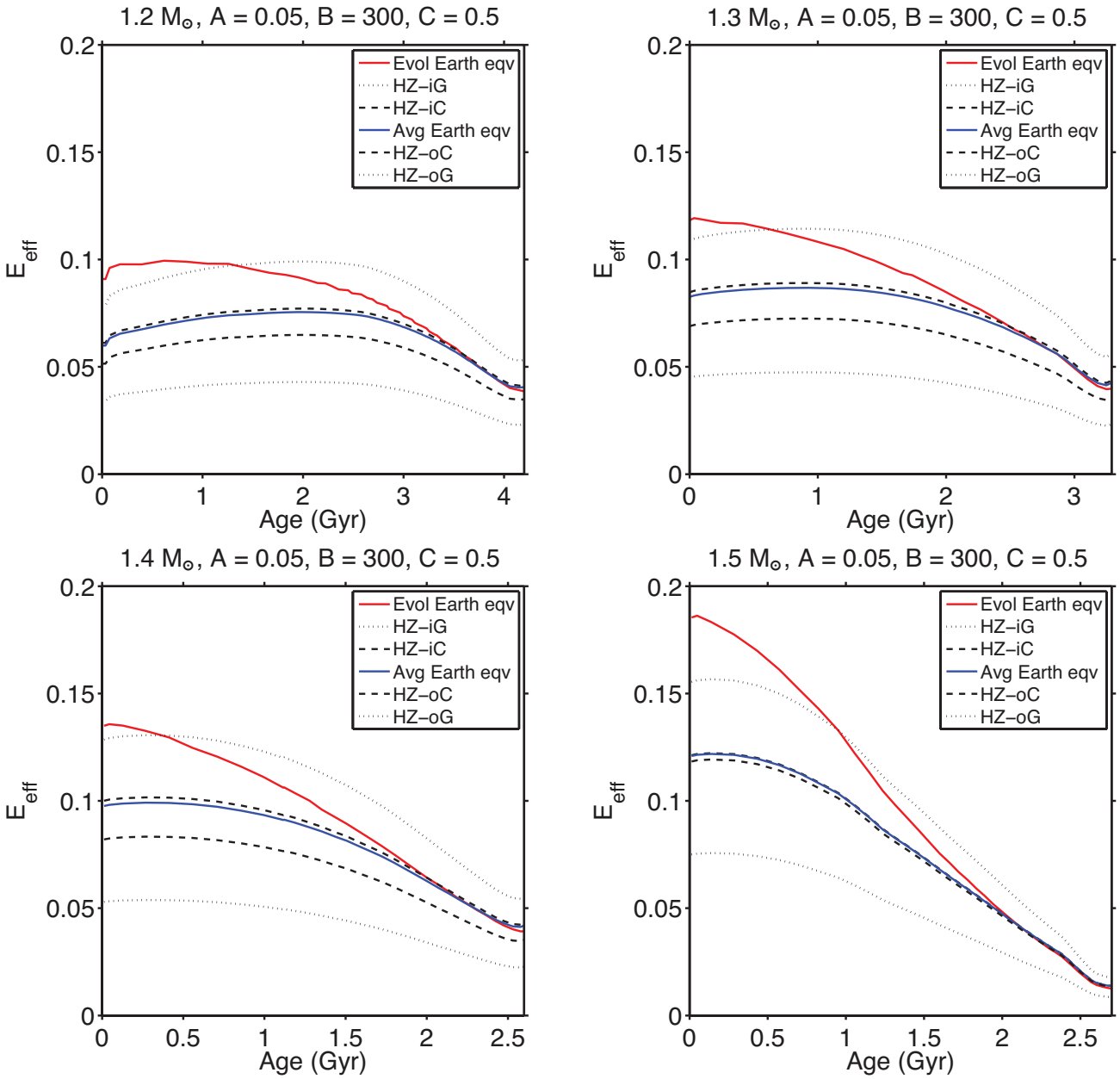

Figure 4.18. Development of DNA damage at the climatological habitable zone limits around stars with ZAMS masses of 1.2 $M_\odot$, 1.3 $M_\odot$, 1.4 $M_\odot$, and 1.5 $M_\odot$ for their main-sequence phase (2). The effect of atmospheric attenuation is included. Note that the ZAMS point of the Earth-equivalent position for 1.2 $M_\odot$ look contradicting with the text, which states $E_{\text{eff}} = 0.038$, but the ZAMS point is only not clearly shown in the figure because E_{eff} increases to 0.60 within 0.03 Gyr. The same can be said of the plots within the initial ∼0.03 Gyr for other positions for 1.2 $M_\odot$.

Table 4.10. Development of DNA Damage with time in the case of default atmospheric attenuation at the average Earth equivalent positions

Age (Gyr)	1.2 $M_{\odot}$	1.3 $M_{\odot}$	1.4 $M_{\odot}$	1.5 $M_{\odot}$
0.5	0.0685	0.0862	0.0987	0.1182
1.0	0.0727	0.0867	0.0933	0.1007
1.5	0.0746	0.0844	0.0816	0.0733
2.0	0.0755	0.0778	0.0626	0.0473
2.5	0.0743	0.0668	0.0423	0.0207
3.0	0.0684	0.0499	-	-
3.5	0.0574	-	-	-
4.0	0.0424	-	-	-

The earliest carbon isotope evidence dates to 0.77 Gyr from the birth of Earth, and thus the surface environments of Earh at about 0.5 Gyr of age is considered to be important for the emergence of life. Oxygen started to build up in the atmosphere at about 2.2 Gyr from the Earth's formation, and the oldest eularyotic fossils date to about 2.5 Gyr (Bennett & Shostak, 2006). For a star with a mass of 1.2 $M_{\odot}$, E_{eff} increases from 1.75 to 1.96 until 1.95 Gyr, and then decreases to 1.92 at the Earth-equivalent position and without planetary atmospheric attenuation. For a star with a mass of 1.3 $M_{\odot}$ in the same conditions, E_{eff} increases from 2.61 to 2.63 until 0.93 Gyr, and then decreases to 1.86. For a star with a mass of 1.4 $M_{\odot}$ in the same conditions, E_{eff} decreases from 3.46 to 1.10. For a star with a mass of 1.5 $M_{\odot}$ in the same conditions, E_{eff} decreases from 4.88 to 0.52. A planet in the climatological habitable zones of a star with a mass of 1.2 $M_{\odot}$ experiences the least change in the amount of DNA damage.

If there is the effect of planetary atmospheric attenuation, the climatological habitable zones around those stars can maintain a relatively mild environment throughout the same 2-Gyr period. For a star with a mass of 1.2 $M_{\odot}$, E_{eff} increases

from 0.069 to 0.075 until 1.95 Gyr, and then decreases to 0.074 at the Earth-equivalent position and with the planetary atmospheric attenuation. For a star with a mass of 1.3 $M_{\odot}$ in the same conditions, E_{eff} increases from 0.086 to 0.087 until 0.93 Gyr, and then decreases to 0.067. For a star with a mass of 1.4 $M_{\odot}$ in the same conditions, E_{eff} decreases from 0.099 to 0.042. For a star with a mass of 1.5 $M_{\odot}$ in the same conditions, E_{eff} decreases from 0.118 to 0.021.

In addition to DNA damage at the climatological habitable zone limits and average Earth-equivalent positions, I computed DNA damage at the evolutionary Earth-equivalent positions. The evolutionary Earth-equivalent positions are shown in dashed lines in Figure 4.7. For all cases from 1.2 $M_{\odot}$ to 1.5 $M_{\odot}$, the Earth-equivalent positions at ZAMS are located closer to the stars than the outer limits of general habitable zones at the end of main-sequence. In other words, the Earth-equivalent positions at ZAMS are not in the continuously habitable zones of the entire main-sequence phase. As the stars age, the Earth-equivalent positions migrate outward with the climatological habitable zones. With masses from 1.2 $M_{\odot}$ to 1.4 $M_{\odot}$, the Earth-equivalent positions at the end of main-sequence phase are located in the areas that remain in the conservative habitable zones throughout the main-sequence phase. With a mass of 1.5 $M_{\odot}$, the Earth-equivalent position passes across the area that is continuously in the conservative habitable zone, but remains in the area that is continuously in the general habitable zones until the end of main-sequence. Since DNA damage is proportional to the square of distance from the star, the results reflect the behavior of Earth-equivalent positions. The maximum DNA damage at the evolutionary Earth-equivalent positions without atmospheric attenuation around the stars of 1.2, 1.3, 1.4, and 1.5 $M_{\odot}$ is 2.55, 3.56, 4.74, and 7.74, respectively, which occurs at the very early time of the stellar life, and the minimum DNA damage is 0.92, 0.99, 1.01, and 0.29, respectively, which occurs at the end of main-sequence. DNA

damage is reduced by the atmosphere and the maximum damage becomes 0.099, 0.119, 0.136, and 0.186, respectively, with planetary atmospheric attenuation taken into consideration. The minimum damage reduces to 0.038, 0.040, 0.039, and 0.012, respectively.

The variation of $E_{\rm eff}$ in response to different cases of ATT was also investigated. Figure 4.19 shows development of DNA damage at the average Earth-equivalent positions for the cases of no attenuation (solid red line), $(A, B, C) = (0.05, 300, 0.5)$ (dashed black line), (0.02, 300, 0.5) (black dash-dot line), (0.05, 250, 0.5) (solid black line), and (0.02, 250, 0.5) (dotted black line).

If there are atmospheres on the planet, the change in DNA damage of UV radiation with stellar evolution is slow and small, compared to the case without an atmosphere. Less responses to stellar evolution are found as the planetary atmospheric attenuation becomes more efficient. In the four cases of ATT, my default case (0.05, 300, 0.5) is the most efficient and (0.05, 250, 0.5) is the least efficient. For the ZAMS mass of 1.5 $M_{\odot}$, the maximum and minimum $E_{\rm eff}$ are 5.02 and 0.32 without an atmosphere, respectively. Both values reduce to 1.22 and 0.11 for the least efficient case and 0.12 and 0.014 for the most efficient case, respectively. For the ZAMS mass of 1.2 $M_{\odot}$, the maximum and minimum $E_{\rm eff}$ are 1.96 and 0.91 without an atmosphere, respectively. Both values reduce to 0.61 and 0.30 for the least efficient case and 0.075 and 0.038 for the most efficient case, respectively.

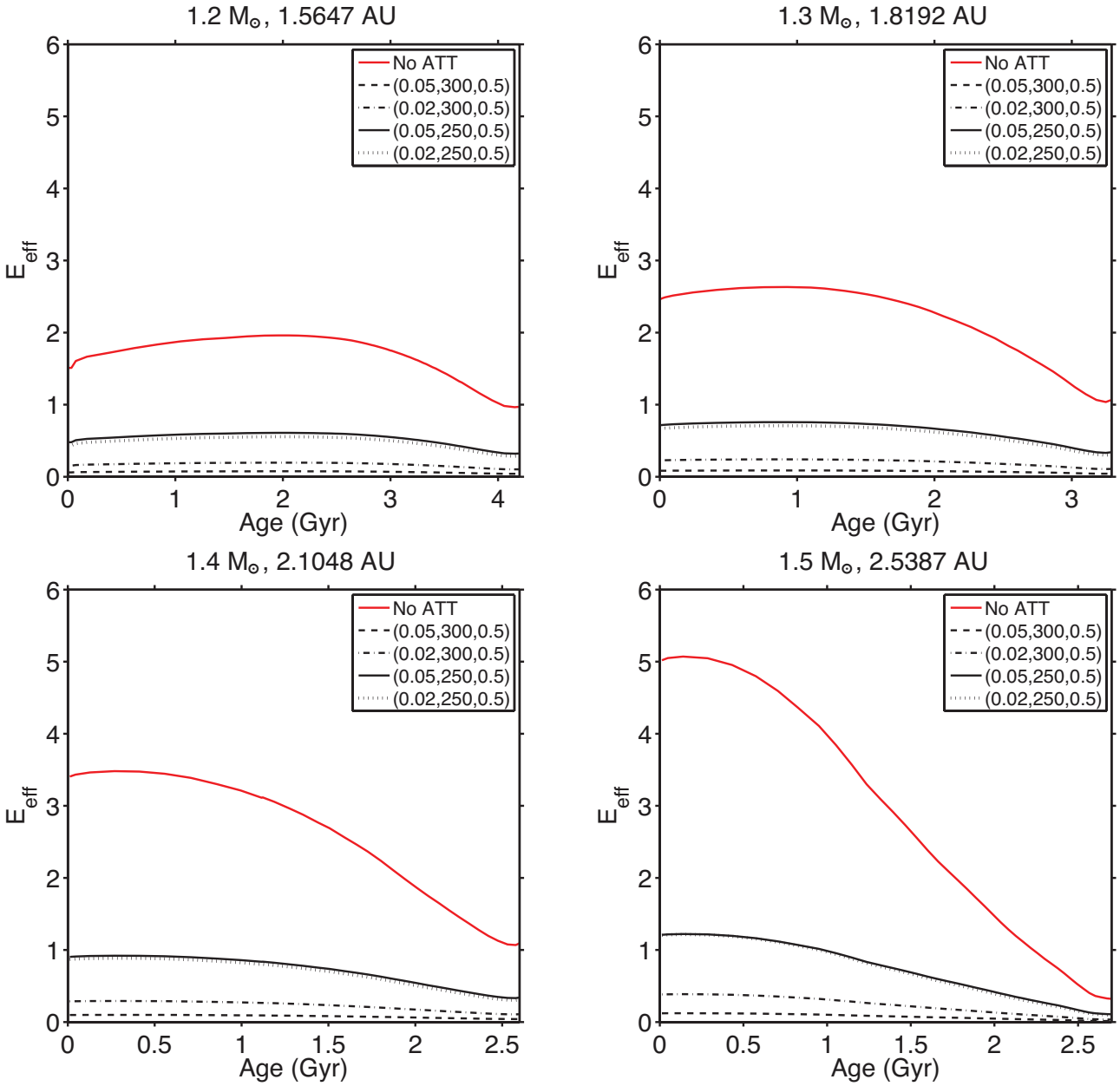

Figure 4.19. Development of DNA damage at the average Earth-equivalent positions around stars with ZAMS masses of 1.2 $M_{\odot}$, 1.3 $M_{\odot}$, 1.4 $M_{\odot}$, and 1.5 $M_{\odot}$ for their main-sequence phase. No attenuation case and 4 cases of atmospheric attenuation are shown.

CHAPTER 5

Application to Known F-type Planetary Systems

5.1 Selection of F-type Planetary Systems

Among 813 planetary systems known to date (information retrieved on February 16, 2014), 103 of their host stars are classified into F-type main-sequence and non-main-sequence stars (Exoplanet TEAM, 2014). I applied the same method used to investigate DNA damage around the model F-type main-sequence stars to known F-type planetary systems. I selected six F-type main-sequence stars with different effective temperatures ranging from 6740 to 6210 K: (1) CoRoT-3, (2) WASP-14, (3) HD 197286, (4) HD 179949, (5) υ And, and (6) HD 86264. The order of the systems is from the highest temperature to the lowest temperature. In the selection, only υ And and HD 86264 have exoplanets in their general habitable zones. These exoplanets are supposedly gas giants at least 7 times larger than Jupiter, and thus they are obviously not habitable. However, the exomoons, if existing, around these exoplanets could be habitable (Williams et al., 1997; Scharf, 2006; Heller & Barnes, 2013). The other stars have Jupiter-size planets very close to them. Even if the hot Jupiters have exomoons, they are very unlikely to be habitable. However, since there is a high possibility for the planetary systems to contain multiple planets, a few or all of them might have undiscovered Earth-type planets or exomoons in the climatological habitable zones. The properties of the systems are summarized in Table 5.1. The luminosities and effective temperatures of the stars are compared in Figure 5.1. In the figure, their masses provided in Table 5.1, which are obtained from the database of *The Extrasolar Planets Encyclopaedia*, disagree with the evolutionary tracks. One possible reason is

because estimated stellar masses vary with the mass determination methods and the values are highly uncertain.

5.1.1 Example (1): CoRoT-3 Planetary System

CoRoT-3 is an F3 V star with $T_{\rm eff} = 6740 \pm 140$ K. The star is located at $\alpha = 19^{\rm h}\ 28^{\rm m}\ 13.265^{\rm s}, \delta = +00^\circ\ 07'\ 18.62''$ and 680 ± 160 pc away from the Sun in the constellation of Aquila. Deleuil et al. (2008) performed spectral analysis and found the overall metallicity to be [M/H]$= -0.02 \pm 0.06$, which is the mean abundance of the elements including Ca, Ti, Cr, Fe and Ni. By using $T_{\rm eff}$ and [M/H] as well as $M^{1/3}R^{-1}$ obtained from the light curve analysis, they determined the stellar mass to be $M = 1.37 \pm 0.09\ M_\odot$ and the stellar radius to be $R = 1.56 \pm 0.09\ R_\odot$. These values were derived by using STAREVOL (Siess, 2006) stellar evolution models mainly and agree with CESAM (Morel & Lebreton, 2007) evolution models. Additionally, the age was estimated as a range between 1.6 and 2.8 Gyr. The metallicity [Fe/H] is -0.02 ± 0.06. They found no evidence for the star being chemically peculiar from the spectral analysis. The spectra does not show Ca II H and K lines. Also, the light curve lacks photometric variation. These facts indicate that CoRoT-3 is a non-active star.

A massive exoplanet, CoRoT-3b, was discovered in 2008 by the CoRoT space mission. CoRoT space mission is observing light curves of stars in the direction close to the Galaxy center and detects exoplanets transiting the stars. Discovery of the planet was also confirmed by ground-observations: high-precision radial-velocity measurements (RV), on-off photometry, and high signal-to-noise spectroscopic observations. The combined analyses provided accurate information on the properties of CoRoT-3b. The planet orbits CoRoT-3 synchronously at $a = 0.057 \pm 0.003$ AU with the period of 4.25680 days. No significant eccentricity was detected. The mass of the

planet is $m_{\rm p} = 21.66 \pm 1.0\ M_{\rm J}$, which is considered to be in the range of low-mass brown dwarfs. The traditional definition describes a brown dwarf an object heavier than 13 $M_{\rm J}$ and capable of fusing deuterium. However, there are schools of thought that insist a brown dwarf is defined by its formation process. According to some models, "superplanets" with masses up to 25 $M_{\rm J}$ can form via core accretion (Mordasini et al., 2008). Since the formation process of CoRoT-3b is unknown, it is debatable if the planet is a "superplanet" or a low-mass brown dwarf. The planet's radius is $R_{\rm p} = 1.01 \pm 0.07\ M_{\rm J}$, the density is $\rho = 26.4 \pm 5.6$ g cm^{-3} and the surface gravity is $\log g = 4.72 \pm 0.07$.

5.1.2 Example (2): WASP-14

WASP-14 is an F5 V star located at $\alpha = 14^{\rm h}\ 33^{\rm m}\ 06.356^{\rm s}, \delta = +21^\circ\ 53'\ 40.99''$ and 160 ± 20 pc away from the Sun in the constellation of Boötes. The star has a hot Jupiter more than 7 times as massive as Jupiter. The planet was discovered in 2008 in the SuperWASP survey, which detects transition of exoplanets in front of stars with a ground based instrument. After the discovery, photometric and spectroscopic follow-ups by other ground based observations were performed. Along with the report of discovery, Joshi et al. (2009) provide the parameters of WASP-14 determined through the observations. The effective temperature of the star was estimated as $T_{\rm eff} = 6475 \pm 100$ K by using the infrared flux method (Blackwell & Shallis, 1977). Also, the stellar radius was found to be $R = 1.306^{+0.066}_{-0.073}\ R_\odot$. They used the stellar evolutionary tracks given by Girardi et al. (2000) and showed that the star with such an effective temperature and a radius has a mass of $1.211^{+0.127}_{-0.122}$ and age between 0.5 and 1.0 Gyr. The star's lithium abundance as high as $\log N({\rm Li}) = 2.84 \pm 0.05$ and rotational speed as fast as $v \sin(i) = 4.9 \pm 1.0$ km s^{-1} also indicate that the star is young since F-type stars with the effective temperature should have depleted Li, being close to

the Li gap (Boesgaard & Tripicco, 1986; Böhm-Vitense, 2004; Balachandran, 1990). Additionally, the metallicity is [M/H]$= 0.0 \pm 0.2$.

WASP-14b is the only discovered planet around the star, whose parameters are $m_{\rm p} = 7.341^{+0.508}_{-0.496}\ M_{\rm J}$, $R_{\rm p} = 1.281^{+0.075}_{-0.082}\ R_{\rm J}$, $\rho = 3.501^{+0.636}_{-0.495}\ \rho_{\rm J}$, and $\log g = 4.010^{+0.049}_{-0.042}$. This planet orbits the star as close as $a = 0.036 \pm 0.001$ AU at the rate of a period every 2.243 days with the orbital eccentricity of $e = 0.087 \pm 0.002$ (Blecic et al., 2013). At this distance, the planetary orbit is expected to have been completely circularized by strong tidal energy dissipation by the estimated stellar age (Matsumura et al., 2008). Joshi et al. (2009) discusses the possible reasons for the high eccentricity of a planet orbiting at such a close distance from the star would be either that the system age is comparable to the tidal circularization time scale or there is another planet perturbing the first planet's orbit. However, there are considerable uncertainties in the estimation of tidal dissipation parameters. Also, the RV measurements by Joshi et al. (2009) and Husnoo et al. (2011) do not show evidence for the presence of any third body in the system.

5.1.3 Example (3): HD 197286

HD 197286 or WASP-7 is an F5 V star located at $\alpha = 20^{\rm h}\ 44^{\rm m}\ 10.2190^{\rm s}, \delta = +39^\circ\ 13'\ 30.894''$ and 140 ± 15 pc away from the Sun in the constellation of Microscopium. A planet slightly smaller than Jupiter has been found around the star through the WASP-South survey. The effective temperature of the star is $T_{\rm eff} = 6400 \pm 100$ K, which comes from an analysis of the Hα line obtained using CORALIE spectrograph (Hellier et al., 2009). The metallicity is [Fe/H]$= 0.0 \pm 0$. Ca H+K or $\rm Li_I$ 6708 Å lines are not detected for the star. The star with the above effective temperature falls in the Li gap (Böhm-Vitense, 2004), and thus the Li line does not provide an age constraint. Southworth et al. (2011) performed a follow-up

photometric observation and model fitting of the stellar parameters. They used five models, Claret (Claret, 2004), Y^2 (Demarque et al., 2004), Teramo (Pietrinferni et al., 2004), VRSS (VandenBerg et al., 2006), and DSEP (Dotter et al., 2008) models, and took the unweighted mean of the five sets of results to determine the parameters. They found the mass is $M = 1.276 \pm 0.061\ M_\odot$, the radius is $R = 1.432 \pm 0.092\ R_\odot$, and the age is $2.4^{+0.8}_{-1.0}$ Gyr.

The model fitting also provides the parameters of WASP-7b. The planet orbits the star at $a = 0.0617 \pm 0.0010$ AU with the period of 4.95 days. The mass is $m_{\rm p} = 0.96\ M_{\rm J}$ and the radius is $R_{\rm p} = 1.330 \pm 0.093\ R_{\rm J}$, which makes the density $\rho = 0.41 \pm 0.10\ \rho_{\rm J}$ and surface gravity $g = 13.4 \pm 2.6$ m s^{-1}. The planet is definitely a hot Jupiter with the equilibrium temperature at 1487 ± 48 K, excluding the energy redistribution factor. The precise eccentricity is unknown, but Hellier et al. (2009) found $e < 0.17$, and they adopted $e = 0$ for their calculations.

5.1.4 Example (4): HD 179949

HD 179949 is an F7 V star located at $\alpha = 19^{\rm h}\ 15^{\rm m}\ 33.23^{\rm s}, \delta = -24^\circ\ 10'\ 45.67''$ and 27.05 ± 0.59 pc away from the Sun (Butler et al., 2006) in the constellation of Sagittarius. The effective temperature of the star is $T_{\rm eff} = 6260 \pm 43$ K, the mass is $M = 1.28\ M_\odot$ (Santos et al., 2004), the radius is $R = 1.19\ R_\odot$ (Fischer & Valenti, 2005). This metal rich star has the metallicity of [Fe/H]$= 0.22 \pm 0.05$ (Santos et al., 2004). Saffe et al. (2005) estimates the stellar age as 2.05 Gyr from the Ca II H+K lines, which represent the chromospheric activity, using the calibration method presented by Donahue (1993).

A hot Jupiter around HD 179949 was discovered by the RV measurement in the Anglo-Australian Planet Search in 2000 (Tinney et al., 2001). HD 179949 b orbits the star at the distance of $a = 0.045 \pm 0.001$ AU with the period of 3.09 days.

The minimum mass is $m_{\rm p} \sin i = 0.95 \pm 0.04\ M_{\rm J}$. The eccentricity was found to be $e = 0.022 \pm 0.014$. These planetary parameters were derived by Wittenmyer et al. (2007) using Keplarian orbital fits. Wittenmyer et al. (2007) also discuss no indication of another planet from their analysis. Since the transit of the planet has not been detected, its radius or inclination is unknown (Tinney et al., 2001).

It is observed that the chromospheric emission of HD 179949 was enhanced by ∼4% when the planet was in front of the star (Shkolnik et al., 2003). The Ca II emission of the star was significantly enhanced compared to other stars. The X-ray flux was also twice as much as that of other single F8-9 V stars, and ∼ 10 times that of the Sun. The best-fit spot model to the observation requires a bright spot to appear at a latitude of 30° and a stellar inclination angle to be $i = 87°$. However, if the stellar inclination angle was at 83°-97°, the transit of the planet would be visible from Earth, assuming that the orbital and stellar inclination angles are similar. Additionally, the period of chromospheric enhancement shows the star is not tidally synchronized with the planet's orbit.

5.1.5 Example (5): υ And

υ And is a binary star located at $\alpha = 01^{\rm h}\ 36^{\rm m}\ 47.84216^{\rm s}, \delta = +41°\ 24'\ 19.6443''$ and 13.47 ± 0.13 pc away from the Sun (Fuhrmann et al., 1998) in the constellation of Andromeda. The primary star, υ And A, is an F8 V and the secondary star, υ And B, is an M4.5 V star having a mass of 0.2 $M_\odot$ (Lowrance et al., 2002). The projected separation between the stars is ∼750 AU. The system has 4 discovered planets around υ And A. The effective temperature of υ And A is $T_{\rm eff} = 6212 \pm 64$ K (Santos et al., 2004), the metallicity is [Fe/H]= 0.09 ± 0.06, the mass is $M = 1.27 \pm 0.06\ M_\odot$ (Fuhrmann et al., 1998), and the radius is $R = 1.631 \pm 0.014\ R_\odot$ (Baines et al., 2008). Fuhrmann et al. (1998) estimated the mass and age from evolutionary tracks that

make use of the model atmospheres as upper boundary condition, which is described in Bernkopf (1998), and include helium diffusion. The age was found to be 3.8 ± 1.0 Gyr.

The innermost planet, υ And b was discovered at a distance of $a = 0.059 \pm 0.001$ AU by RV measurements in 1996. The orbital period is 4.62 days. The minimum mass is $m_{\rm p} \sin i = 0.62 \pm 0.09\ M_{\rm J}$ and the eccentricity is $e = 0.013 \pm 0.016$. It was observed that the chromospheric emission from υ And was enhanced once per orbit of υ And b, which suggests that the planet has magnetic interaction with the star and enhances the chromospheric activity (Shkolnik et al., 2005).

The existence of the 2nd and 3rd planets, υ And c and d, was detected from the significant remaining residuals in the RV measurements in 1999. The semi-major axes are $a = 0.861$ and 2.55 AU, respectively. They have high eccentricities of $e = 0.24$ and 0.274 (McArthur et al., 2010; Barnes et al., 2011). A large part of the orbit of υ And d is in the climatological habitable zones. The periastron of the planet is 1.88 AU and the apastron is 3.19 AU. The general habitable zone for the star is between 1.56 and 3.02 AU and the conservative habitable zone is between 1.76 and 2.45 AU. According to Buccino et al. (2006), the UV level at $a = 2.55$ AU is 0.9 times as severe as the condition on the Earth's surface 3.8 Gyr ago. The minimum masses of υ And c and d are $m_{\rm p} \sin i = 1.8 \pm 0.26$ and $3.75 \pm 0.54\ M_{\rm J}$, respectively (Ligi et al., 2012). Their orbital periods are 237.7 days and 3.50 years, respectively.

The 4th planet, υ And e, was found in a 3:1 resonance orbit with υ And d in 2010. The planet shares some similar features with Jupiter. The minimum mass is $m_{\rm p} \sin i = 1.059 \pm 0.028\ M_{\rm J}$ and the semi-major axis is $a = 5.2456 \pm 0.00067$ AU. However, the true mass might be larger since the inclination i is not known. The orbital period is 10.5 years. The eccentricity is $e = 0.00536 \pm 0.00044$ (Curiel et al., 2010).

5.1.6 Example (6): HD 86264

HD 86264 is an F8 V star located at $\alpha = 09^{\rm h}\ 56^{\rm m}\ 57.839^{\rm s}, \delta = -15^\circ\ 53'\ 42.43''$ and 72.6 pc away from the Sun (Fischer et al., 2009) in the constellation of Hydra. The effective temperature of the star is $T_{\rm eff} = 6210 \pm 44$ K, the mass is $M = 1.42 \pm 0.05\ M_\odot$, the radius is $R = 1.88 \pm 0.12\ R_\odot$. The star is metal rich and the metallicity is [Fe/H]= 0.202 ± 0.04. Fischer et al. (2009) derived $T_{\rm eff}$ by using spectral synthesis modeling and iterating until surface gravity matched the value predicted from interpolation of the Y^2 isochrones. They also found that the chromospheric activity index is $S_{\rm HK} = 0.20$ and the chromosphere emission ratio is $\log R'_{\rm HK} = -4.73$, and therefore, the star is moderately active. The age was estimated as 2.24 Gyr.

A planet, HD 86264 b, was discovered in 2009 from the Doppler data obtained at Lick Observatory. The planet orbits HD 86264 in a highly eccentric orbit at the semi-major axis of $a = 2.86 \pm 0.07$ AU. The eccentricity is estimated as $e = 0.7 \pm 0.2$. However, the standard deviation is so large that χ^2_ν fits for $e = 0.4$ are only worse by 5% than those for $e = 0.7$. The distance of the semi-major axis is between the distances of conservative and general outer habitable boundaries, 2.82 AU and 3.47 AU, respectively, but the planet does not stay in the general habitable zone for the entire orbit because of the high eccentricity. The periastron is 0.86 AU, which is closer to the star than the general inner habitable boundary at 1.79 AU, and the apastron is 4.86 AU, which is outside of the general outer habitable boundary, if $e = 0.7$. The orbital period is 4.04 years. The planet's minimum mass is $m_{\rm p} \sin i = 7.0 \pm 1.6\ M_{\rm J}$ (Fischer et al., 2009).

Table 5.1. Properties of F-type Planetary Systems

	Planetary Systems	Spectral Type	T_{eff} (K)	$L(L_{\odot})$	$R(R_{\odot})$	$M(M_{\odot})$	Apparent Magnitude	Age (Gyr)	Metallicity	Distance (pc)
(1)	CoRoT-3	F3 V +40 K	6740	4.51	1.56	1.37	13.3	2	-0.02	680
(2)	WASP-14	F5 V +35 K	6475	2.69	1.306	1.211	9.75	0.75	0	160
(3)	HD 197286	F5 V -40 K	6400	3.09	1.432	1.276	9.51	2.4	0	140
(4)	HD 179949	F7 V -20 K	6260	1.95	1.19	1.28	6.25	2.05	0.22	27
(5)	υ And	F8 V +12 K	6212	3.56	1.631	1.27	4.09	3.8	0.09	13.47
(6)	HD 86264	F8 V +10 K	6210	4.72	1.88	1.42	7.42	2.24	0.202	72.6

T_{eff}, R, and M are obtained from *The Extrasolar Planets Encyclopaedia* (http://exoplanet.eu). Spectral types are derived by using the effective temperatures, and there are discrepancies with the spectral types found at *The Extrasolar Planets Encyclopaedia* for a few cases.

Table 5.2. Properties of Planets in the F-type Planetary Systems

Exoplanets	$m_{\rm p}$ ($M_{\rm J}$)	$R_{\rm p}$ ($R_{\rm J}$)	Period (days)	a (AU)	e	i (degree)	Discovery Year	Detection Method	Inside of HZ
CoRoT-3 b	21.77	1.01	4.26	0.057	0	85.9	2008	Transit	No
WASP-14 b	7.34	1.28	2.24	0.036	0.087	84.79	2008	Transit	No
HD 197286 b	0.96	1.33	4.95	0.0617	0	87.03	2008	Transit	No
HD 179949 b	0.95	N/A	3.09	0.045	0.022	N/A	2000	RV	No
υ And b	0.62	N/A	4.62	0.059	0.013	30	1996	RV	No
υ And c	1.8	N/A	237.7	0.861	0.24	8	1999	RV	No
υ And d	10.19	N/A	1302.61	2.55	0.274	24	1999	RV	b/w oC & oG
υ And e	1.059	N/A	3848.86	5.2456	0.00536	N/A	2010	RV	No
HD 86264 b	7	N/A	1475	2.86	0.7	N/A	2009	RV	b/w oC & oG

The values are obtained from *The Extrasolar Planets Encyclopaedia* (http://exoplanet.eu).

5.2 Habitability around the Planetary Systems

First of all, I derived the general and conservative habitable zones and Earth-equivalent position for each star. As shown in Figure 5.2, the distances of climatological habitable zones depend on the stellar luminosities rather than the spectral types, or effective temperatures. The numbers in the figure correspond to those given to the stars in the previous section. The luminosities for the spectral types are not necessarily consistent with the typical ones listed in Table 4.1; hence, the results differ from the distances and widths of climatological habitable zones that appear in Figure 4.1. Each of υ And and HD 86264 has an exoplanet between its conservative and general habitable limits.

Next, I investigated DNA damage at the inner and outer limits of conservative and general habitable zones as well as the Earth-equivalent positions. The results are presented in Figures 5.3, 5.4, and 5.5 for the both cases with and without atmospheric attenuation. In spite of little correlation between the distance of climatological habitable zone and effective temperature, DNA damage in the climatological habitable zones is highly correlated to the effective temperature. At the general inner habitable limits, $E_{\rm eff}$ is (1) 6.22, (2) 4.48, (3) 4.13, (4) 3.76, (5) 3.61, and (6) 3.61, which is the highest value for the climatological habitable zone of each system. At the Earth-equivalent positions, $E_{\rm eff}$ is (1) 4.46, (2) 3.20, (3) 2.94, (4) 2.67, (5) 2.57, and (6) 2.56. At the general outer habitable limits, $E_{\rm eff}$ is (1) 1.74, (2) 1.22, (3) 1.12, (4) 1.00, (5) 0.96, and (6) 0.96, and therefore, DNA damage at the general habitable limits of HD 179949, υ And, and HD 86264 is about the same as the condition of Earth without an atmosphere.

If the UV flux is attenuated by the default hypothetical atmosphere, $E_{\rm eff}$ is reduced to almost the same level for all the cases except CoRoT-3. At the general inner habitable limits, $E_{\rm eff}$ is (1) 0.176, (2) 0.145, (3) 0.140, (4) 0.139, (5) 0.139, and

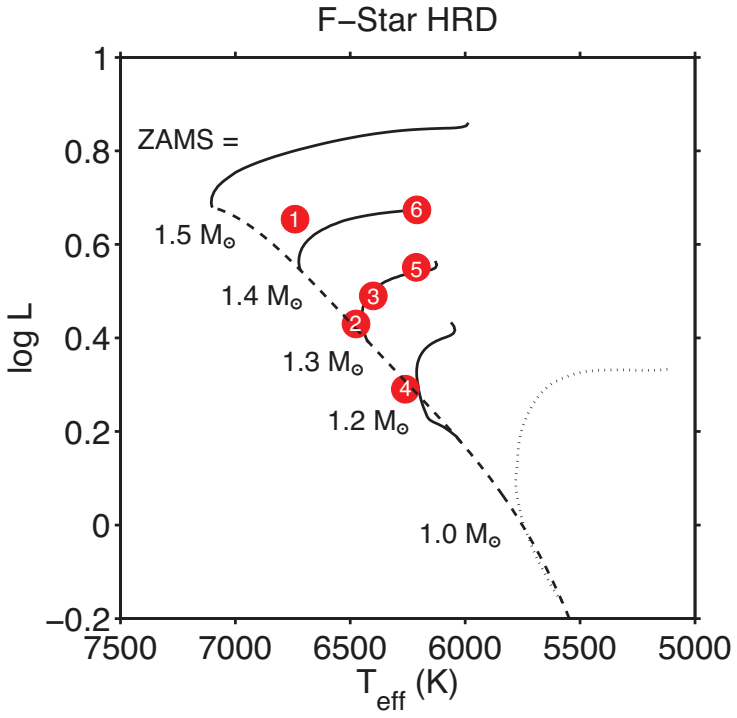

Figure 5.1. The six selected F-type stars known to host planets. The numbers in the figure correspond to those given to the stars in the text. Refer to Figure 4.5 for additional details of the figure.

(6) 0.139. At the Earth-equivalent positions, E_{eff} is (1) 0.126, (2) 0.103, (3) 0.100, (4) 0.099, (5) 0.099, and (6) 0.099. At the general outer habitable limits, E_{eff} is (1) 0.049, (2) 0.040, (3) 0.038, (4) 0.037, (5) 0.037, and (6) 0.037.

In Figures 5.4 and 5.5, five cases of atmospheric attenuation are compared: no attenuation case and four cases with different parameter combinations (A, B, C), (i) (0.05, 300, 0.5), (ii) (0.02, 300, 0.5), (iii) (0.05, 250, 0.5), and (iv) (0.02, 250, 0.5). As shown in the study of the effect of parameter variation in Section 4.2.1, DNA damage is reduced more with higher B. In this case, the attenuation function with $B = 300$ reduces DNA damage more effectively than with $B = 250$. When $B = 250$, the attenuation function with $A = 0.02$ shows slightly more effectiveness in reduction of DNA damage than with $A = 0.05$. On the other hand, When $B = 300$ is used, the

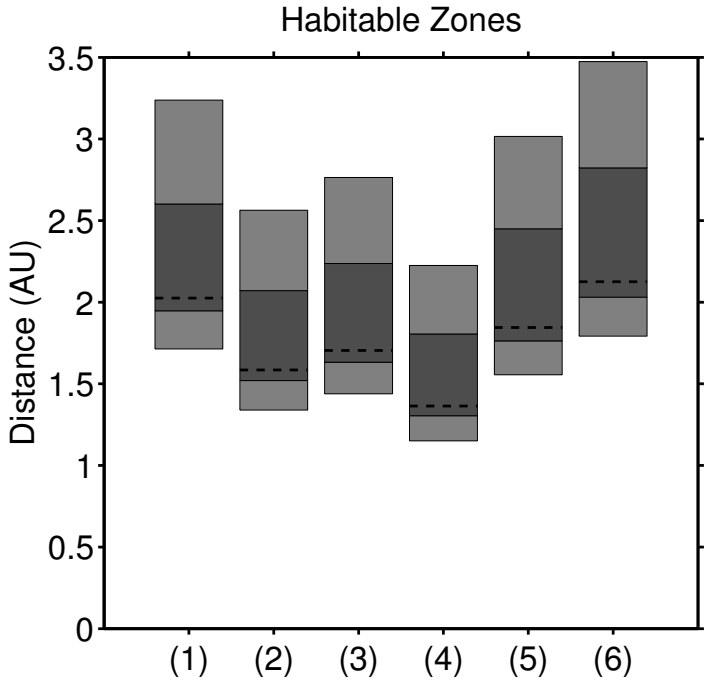

Figure 5.2. The distances of climatological habitable zones around the F-type stars. The dark gray areas indicate conservative habitable zones. The light gray areas indicate general habitable zones. The dashed lines are Earth-equivalent positions.

attenuation function with $A = 0.05$ reduces DNA damage more effectively than with $A = 0.02$.

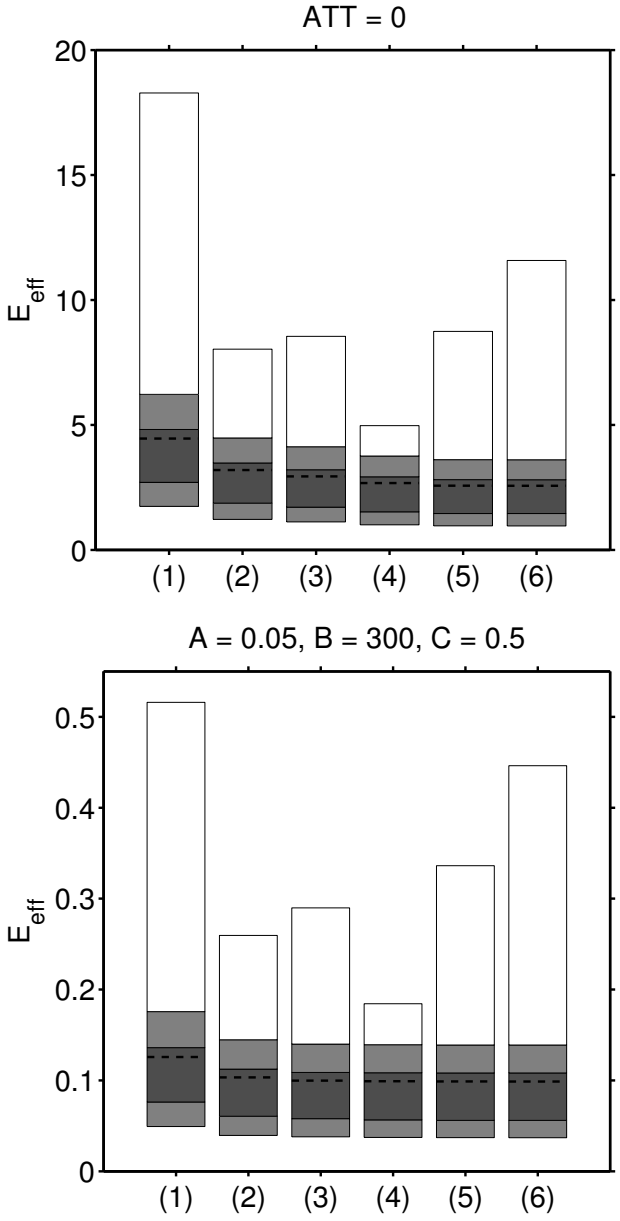

Figure 5.3. DNA damage at the climatological habitable zone limits around the selected F-type stars (1). Top: No atmospheric attenuation is assumed. Bottom: The effect of atmospheric attenuation is included. The dark gray areas indicate conservative habitable zones. The light gray areas indicate general habitable zones. The dashed lines are Earth-equivalent positions. The top lines of the white areas indicate DNA damage at 1 AU.

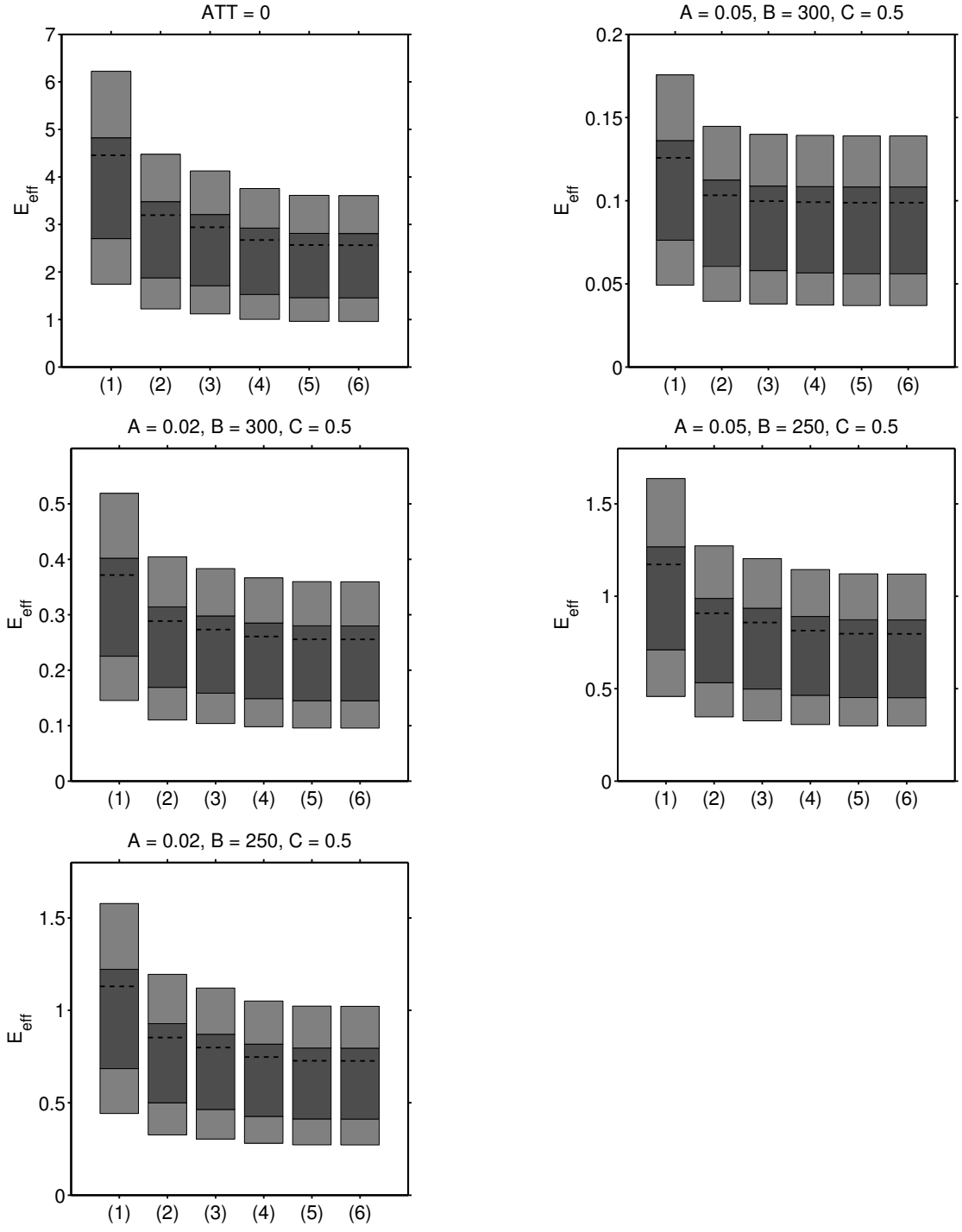

Figure 5.4. DNA damage at the climatological habitable zone limits around the selected F-type stars (2). Five cases of atmospheric attenuation are shown. The color indications are the same as Figure 5.3.

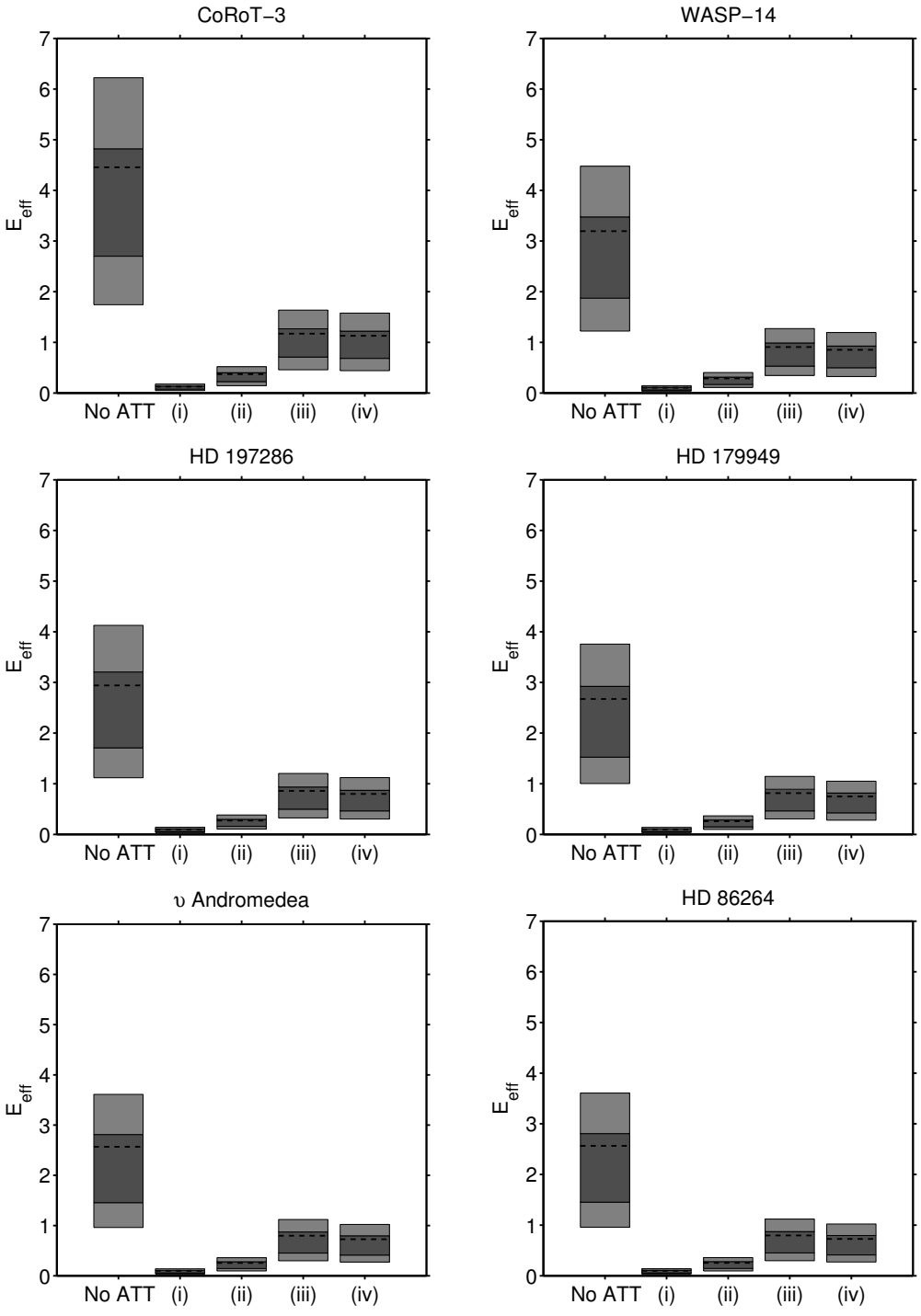

Figure 5.5. DNA damage at the climatological habitable zone limits around each selected F-type star. Five cases of atmospheric attenuation are shown: no planetary attenuation, (i) $(A, B, C) = (0.05, 300, 0.5)$, (ii) $(A, B, C) = (0.02, 300, 0.5)$, (iii) $(A, B, C) = (0.05, 250, 0.5)$, and (iv) $(A, B, C) = (0.02, 250, 0.5)$. The color indications are the same as Figure 5.3.

CHAPTER 6

Summary and Conclusions

I explored the general astrobiological significance of F-type main-sequence stars. F-type stars are hotter, more luminous, more massive and larger than the Sun. They have a larger radiative zone than the Sun and relatively thin convective zone. F-type stars stay in the main-sequence phase for about 2.7-4.3 Gyr, while the main-sequence lifetime for the Sun is about 10 Gyr. In this study, DNA was taken as a proxy for carbon-based macromolecules since extraterrestrial biology is generally assumed to be most likely based on hydrocarbons. Consequently, the DNA action spectrum was utilized to represent the impact of stellar UV radiation. Planetary atmospheric attenuation was approximated based on parameterized attenuation functions, ATT, informed by previous terrestrial analyses. DNA damage at various positions in the climatological habitable zones around F-type stars with different $T_{\rm eff}$ or ZAMS masses was compared in terms of $E_{\rm eff}$, the ratio of damage for a set of given conditions for a planet or moon to the damage for an object without an atmosphere at 1 AU from a solar-like star. Therefore, if an Earth-size planet with Earth-like atmospheres exists at a point within a habitable zone and where $E_{\rm eff}$ is 1, the planet is considered to be habitable. The important aspects of this study were the role of stellar main-sequence evolution, the distance between the host stars and planets or moons in the climatological habitable zones, and the general impact of planetary atmospheric attenuation. The method was applied to observed planetary systems such as CoRoT-3, WASP-14, HD 197286, HD 179949, υ And, and HD 86264.

In the present study, the following results were obtained:

- DNA damage was assessed at distinct positions inside both the general and conservative habitable zones. The definitions of the climatological habitable zones followed Kasting et al. (1993), and the positions of the boundaries were computed with the formulas provided by Selsis et al. (2007). The general habitable zone is defined as the region between the runaway greenhouse inner limit and maximum greenhouse outer limit. The conservative habitable zone is the region between the water-loss inner limit and 1st CO_2 condensation outer limit. In addition, DNA damage at Earth-equivalent positions, which was derived by interpolation between the inner and outer boundaries of conservative habitable zone, was investigated. My derivation confirmed that the climatological habitable zones and Earth-equivalent positions are located farther away from an F-type star than a Solar-like star, and that as a star evolves, the habitable zones as well as Earth-equivalent positions migrate outward.
- Inside the general habitable zones, E_{eff} for an F0 V star is between 2.87 and 9.80 and E_{eff} for an F8 V star is between 0.95 and 3.97 without planetary atmospheric attenuation. I found the atmospheres effectively reduce the damage on DNA. If the parameters of ATT are chosen as $(A, B, C) = (0.05, 300, 0.5)$, those E_{eff} values decrease to the ranges between 0.067 and 0.288 for an F0 V star and between 0.037 and 0.139 for an F8 V star. This choice of parameter set can be considered as the case of atmospheres associated with ozone layers (Segura et al., 2003). A higher order ATT resembling the atmospheric attenuation of Archean Earth is less efficient in reducing the damage, but still greatly lowers E_{eff} to the ranges between 0.63 and 2.14 for an F0 V star and between 0.25 and 0.93 for an F8 V star.
- UV spectrum can be divided into three regimes: UV-A(400-320 nm), UV-B(320-290 nm), and UV-C(290-200 nm). The limits are set according to the amount

reaching the Earth's surface and biological effectiveness. UV radiation shorter than 290 nm does not reach the Earth's surface. As the wavelength decreases, biological responses to UV radiation greatly increases around 320 nm. Contribution of UV-A to DNA damage is negligible even without planetary atmospheric attenuation as previously known. UV-C is the most harmful to organisms, but at the same time, the regime is blocked the most by the atmosphere. Without an atmosphere, $E_{\rm eff}$ due to UV-C is more than 90% of total $E_{\rm eff}$ for all the cases. My default ATT reduces $E_{\rm eff}$ due to UV-C by more than 97%.

- The effectiveness of ATT function in reduction of each regime and accordingly the whole regime depends on the choice of parameter A, B, and C. The parameter B, which determines the position of the center of a tanh-function, has relatively more impact on the results than A for the same C. Parameter A has an effect in the ratio of attenuation between the ranges of shorter and longer wavelength than B. Parameter C controls the maximum of ATT.
- As a star evolves, the climatological habitable zones always migrate outward throughout the main-sequence phase. In other words, the temperature of an object at a certain distance from the host star increases with stellar evolution. On the other hand, DNA damage on the object declines for a large part of the lifetime of F-type stars. The peaks of DNA damage occur at 1.95 Gyr for 1.2 $M_{\odot}$, 0.93 Gyr for 1.3 $M_{\odot}$, and within 0.5 Gyr from the birth for 1.4 and 1.5 $M_{\odot}$.
- DNA damage at a position in the climatological habitable zones is less severe and more stable for a less massive star. UV environment in the climatological habitable zone of a star with 1.2 $M_{\odot}$ is more favorable for long-term habitability than a star with 1.5 $M_{\odot}$. Without the effect of atmosphere, $E_{\rm eff}$ around a star of 1.2 $M_{\odot}$ changes between 1.96 and 0.96 at the average Earth-equivalent position

during its lifetime of 4.3 Gyr, while $E_{\rm eff}$ around a star of 1.5 $M_{\odot}$ changes between 5.07 and 0.32 at the same position during its lifetime of 2.7 Gyr. If planetary atmospheric attenuation is taken into account, $E_{\rm eff}$ around a star of 1.2 $M_{\odot}$ decreases to between 0.075 and 0.040, while $E_{\rm eff}$ around a star of 1.5 $M_{\odot}$ reduces to between 0.122 and 0.014.

- Planetary atmospheric attenuation of four different parameter sets are applied to stars of 1.2-1.5 $M_{\odot}$ and it is found that ATT with $(A, B, C) = (0.05, 300, 0.5)$ reduces DNA damage more effectively than with (0.05, 250, 0.5) as predicted in the study of parameter dependency of ATT. Also, the results show a more efficient ATT provides a more stable UV environment around an F-type star through its stellar evolution.
- In the six selected planetary systems, DNA damage is more severe in the climatological habitable zones of hotter stars. DNA damage at 1 AU from the stars is not correlated to the effective temperature or the spectral type. Without an atmosphere, $E_{\rm eff}$ at the outer limit of general habitable zone is 1.00 for HD 179949 and 0.96 for υ And and HD 86264, which means those planetary systems have regions in similar UV environments to present Earth. The result for υ And agrees with the study by Buccino et al. (2006), who investigated the locations of UV habitable zones (see Section 2.2 for the detail). Since υ And and HD 86264 have a giant planet in each general habitable zone, exomoons around the planets, if existing, could be habitable.
- If the effect of my default ATT is included, $E_{\rm eff}$ for all six systems becomes about the same level in the habitable zones. For CoRoT-3, the star having the most severe UV environment, $E_{\rm eff}$ in the general habitable zone is between 1.74 and 6.22 without an atmosphere, while $E_{\rm eff}$ attenuated by the default ATT is between 0.049 and 0.176. $E_{\rm eff}$ in the general habitable zones of υ And and

HD 86264, which provide the mildest UV environments, is between 0.96 and 3.61 without planetary atmospheric attenuation. Their $E_{\rm eff}$ reduces to the amount between 0.037 and 0.139.

- The goal of this study was to improve and augment the previous work on habitability of F-type main-sequence stars, espescially by Cockell (1999). Improvement was made in the following six points. (1) The DNA action spectrum including UV-A regime was used. (2) DNA damage of UV radiation was analyzed at more positions in the climatological habitable zones than the previous work. (3) Atmospheres based on analytic attenuation function was considered in order to investigate a broader range of effects by the atmosphere. (4) UV environments of a larger range of F-type spectral type were investigated. (5) Effects of stellar evolution were taken into account. (6) More sophisticated photospheric spectra computed by PHOENIX code were used. Because of the improvement, direct comparison between the previous results and my results may not be very meaningful, but they are broadly consistent. DNA damage at 1.5 AU and 3.2 AU from an F2 V star was 9.81 and 2.16, respectively, from Cockell (1999) and 7.24 and 1.60, respectively, from this study for similar atmospheric attenuation functions.

Although F-type stars are much more rare and emit stronger UV radiation compared to cooler and less massive G, K, and M-type stars, it is worth investigating the habitability around F-type stars. F-type stars have broader climatological habitable zones than cooler stars, and thus there is more chance of a planet forming or moving in the climatological habitable zones. DNA damage due to UV radiation is higher in most parts of F-type climatological habitable zones than the damage on Earth at the top of atmosphere, but at least the outer part of late F-type stars have similar UV conditions to Earth. Planetary atmospheric attenuation can limit DNA damage in an

F-type climatological habitable zone to lower levels, and therefore even the planets or exomoons in the inner part of F-type climatological habitable zones should not be excluded from candidates for habitable objects on the grounds of exposure to higher stellar UV radiation than Earth.

One of the next steps in the studies of F-type circumstellar habitability from the perspective of DNA damage due to UV radiation will be inclusion of plausible planetary chemistry models by approximating the ability of UV attenuation by ATT. Cockell (2002) provides the information on flux reaching the planetary surface for various assumptions of atmospheric compositions of Archean Earth including 1 bar CO_2, sulfur haze with a column abundance of 1.5×10^{17} cm^{-2}, and organic aldehyde haze as well as the atmosphere containing 40 mb CO_2, which I have traced with ATT functions in this study. Also, the attenuation function can be obtained through the analysis of theoretical exoplanetary atmospheric models. Meadows & Seager (2011) and Kaltenegger et al. (2012) investigate the theoretical atmospheres inspired by the results from Kepler mission. Moreover, I could explore the UV conditions in water by including the attenuation functions provided by, for example, Smith & Baker (1981).

In addition to F-type stars, UV habitability around G, K, and M-type stars can be investigated by using the same method. One of the interesting features of these late type main-sequence stars is magnetic evolution, which is insignificant for F-type and earlier type stars. Especially, K-type stars are thought to have very favorable UV conditions to organisms, but how the conditions change as the stars evolve has not been studied very well. Also, we have an idea of relating biological damage to alternate independent variables such as the stellar rotation period or the photospheric magnetic density.

Bibliography

Baines, E. K., McAlister, H. A., Theo, A., et al. 2008, The Astrophysical Journal, 680, 728

Bains, W. 2004, Astrobiology, 4, 137

Balachandran, S. 1990, The Astrophysical Journal, 354, 310

Barnes, R., Greenberg, R., Quinn, T. R., McArthur, B. E., & Benedict, G. F. 2011, The Astrophysical Journal, 726, 71

Bennett, J. O. & Shostak, S. 2006, Life in the Universe, 2nd edn. (Pearson Addison Wesley)

Bernkopf, J. 1998, Astronomy and Astrophysics, 332, 127

Berry, D. 2009, Comparative Life Zones of Stars, `http://kepler.nasa.gov/multimedia/artwork/diagrams/?ImageID=29`, [Online; accessed 29-March-2014]

Blackwell, D. E. & Shallis, M. J. 1977, Monthly Notices of the Royal Astronomical Society, 180, 177

Blecic, J., Harrington, J., Madhusudhan, N., et al. 2013, The Astrophysical Journal, 779, 5

Boesgaard, A. M. & Tripicco, M. J. 1986, The Astrophysical Journal, 302, L49

Böhm-Vitense, E. 2004, The Astronomical Journal, 128, 2435

Buccino, A. P., Lemarchand, G. A., & Mauas, P. J. 2006, Icarus, 183, 491

Butler, R. P., Wright, J. T., Marcy, G. W., et al. 2006, The Astrophysical Journal, 646, 505

Cardini, D. & Cassatella, A. 2007, The Astrophysical Journal, 666, 393

Cernicharo, J. & Crovisier, J. 2005, Space Science Reviews, 119, 29

Claret, A. 2004, Astronomy and Astrophysics, 424, 919

Cockell, C. S. 1998, Journal of Theoretical Biology, 193, 717

Cockell, C. S. 1999, Icarus, 141, 399

Cockell, C. S. 2002, The ultraviolet radiation environment of Earth and Mars: past and present, ed. G. Horneck & C. Baumstark-Khan (Springer Berlin Heidelberg), 219–232

Cuntz, M., Rammacher, W., Ulmschneider, P., Musielak, Z. E., & Saar, S. H. 1999, The Astrophysical Journal, 522, 1053

Curiel, S., Cantó, J., Georgiev, L., Chávez, C. E., & Poveda, A. 2010, Astronomy and Astrophysics, 525, A78

Deleuil, M., Deeg, H. J., Alonso, R., et al. 2008, Astronomy and Astrophysics, 491, 889

Demarque, P., Woo, J.-H., Kim, Y.-C., & Yi, S. K. 2004, Astrophysical Journal Supplement Series, 155, 667

Des Marais, D. J., Nuth, III, J. A., Allamandola, L. J., et al. 2008, Astrobiology, 8, 715

Diffey, B. L. 1991, Physics in Medicine and Biology, 36, 299

Donahue, A. R. 1993, PhD thesis, New Mexico State University

Dotter, A., Chaboyer, B., Jevremović, D., et al. 2008, Astrophysical Journal Supplement Series, 178, 89

Eggleton, P. P. 1971, Monthly Notices of the Royal Astronomical Society, 151, 351

Eggleton, P. P. 1973, Monthly Notices of the Royal Astronomical Society, 163, 279

Eggleton, P. P., Faulkner, J., & Flannery, B. P. 1973, Astronomy and Astrophysics, 23, 325

Exoplanet TEAM. 2014, The Extrasolar Planets Encyclopaedia, `http://exoplanet.eu`, [Online; accessed 29-March-2014]

Fischer, D., Driscoll, P., Isaacson, H., et al. 2009, The Astrophysical Journal, 703, 1545

Fischer, D. A. & Valenti, J. 2005, The Astrophysical Journal, 622, 1102

Forget, F. & Pierrehumbert, R. T. 1997, Science, 278, 1273

Fuhrmann, K., Pfeiffer, M. J., & Bernkopf, J. 1998, Astronomy and Astrophysics, 336, 942

Gerriet41. 2008, Direct DNA Damage, `http://en.wikipedia.org/wiki/File:Direct_DNA_damage.png`, [Online; accessed 29-March-2014]

Gray, D. F. 2005, The Observation and Analysis of Stellar Photospheres, 2nd edn. (Cambridge: Cambridge University Press)

Green, A. & Miller, J. 1975, CIAP Monograph, 5, 2

Güdel, M. & Kasting, J. 2011, Cambridge Astrobiology, Vol. 6, The Young Sun and Its Influence on Planetary Atmospheres, ed. M. Gargaud, P. López-Garcìa, & H. Martin (Cambridge University Press), 167–182

Guinan, E. F. & Ribas, I. 2002, in ASP Conference Series, Vol. 269, The Evolving Sun and its Influence on Planetary Environments, ed. B. Montesinos, A. Gimenez, & E. F. Guinan (Astronomical Society of the Pacific), 85

Hart, M. H. 1979, Icarus, 37, 351

Hauschildt, P. H. 1992, Journal of Quantitative Spectroscopy & Radiative Transfer, 47, 433

Hauschildt, P. H., Allard, F., & Baron, E. 1999, The Astrophysical Journal, 512, 377

Hauschildt, P. H., Barman, T. S., Baron, E., & Allard, F. 2003, 288, 227

Heller, R. & Barnes, R. 2013, Astrobiology, 13, 18

Hellier, C., Anderson, D. R., Gillon, M., et al. 2009, The Astrophysical Journal, 690, L89

Henderson, S. T. 1977, Daylight and its spectrum, 2nd edn. (Bristol: Adam Hilger Ltd.)

Horneck, G. 1995, Journal of Photochemistry and Photobiology B: Biology, 31, 43

Huang, S. S. 1959, American Scientist, 47, 397

Husnoo, N., Pont, F., Hébrard, G., et al. 2011, Monthly Notices of the Royal Astronomical Society, 413, 2500

Joshi, Y. C., Pollacco, D., Cameron, A. C., et al. 2009, Monthly Notices of the Royal Astronomical Society, 392, 1532

Kaltenegger, L., Miguel, Y., & Rugheimer, S. 2012, International Journal of Astrobiology, 11, 297

Kasting, J. F., Whitmire, D. P., & Reynolds, R. T. 1993, Icarus, 101, 108

Kroupa, P. 2002, Science, 295, 82

Kurucz, R. L., Furenlid, I., Brault, J., & Testerman, L. 1984, National Solar Observatory Atlas

Kutner, M. L. 2003, Astronomy: A Physicsl Perspective, 2nd edn. (Cambridge University Press)

Lammer, H., Bredehöft, J. H., Coustenis, A., et al. 2009, Astronomy and Astrophysics Review, 17, 181

Ligi, R., Mourard, D., Lagrange, A. M., et al. 2012, Astronomy and Astrophysics, 545, A5

Lindberg, C. & Horneck, G. 1991, Journal of Photochemistry and Photobiology B: Biology, 11, 69

Lowrance, P. J., Kirkpatrick, J. D., & Beichman, C. A. 2002, The Astrophysical Journal, 572, L79

LucasVB. 2006, Morgan-Keenan spectral classification, `https://en.wikipedia.org/wiki/File:Morgan-Keenan_spectral_classification.png`, [Online; accessed 29-March-2014]

Lucianomendez. 2011, UpsilonAndromedae D moons, http://en.wikipedia.org/wiki/File:UpsilonAndromedae_D_moons.jpg, [Online; accessed 29-March-2014]

Matsumura, S., Takeda, G., & Rasio, F. A. 2008, The Astrophysical Journal, 686, L29

McArthur, B. E., Benedict, G. F., Barnes, R., et al. 2010, The Astrophysical Journal, 715, 1203

Meadows, V. & Seager, S. 2011, Terrestrial Planet Atmospheres and Biosignatures, ed. S. Seager (Tucson, AZ: University of Arizona Press), 441–470

Mischna, M. A., Kasting, J. F., Pavlov, A., & Freedman, R. 2000, Icarus, 145, 546

Mordasini, C., Alibert, Y., Benz, W., & Naef, D. 2008, in Astronomical Society of the Pacific Conference Series, Vol. 398, Extreme Solar Systems, ed. D. Fischer, F. A. Rasio, S. E. Thorsett, & A. Wolszczan, 235

Morel, P. & Lebreton, Y. 2007, Astrophysics and Space Science

Noyes, R. W., Hartmann, L. W., Baliunas, S. L., Duncan, D. K., & Vaughan, A. H. 1984, The Astrophysical Journal, 279, 763

Pace, N. R. 2001, Proceedings of the National Academy of Sciences, 98, 805

Peak, M. J. & Peak, J. G. 1991, in Conference: Biologic effects of light symposium, Vol. ANL/CP-73713; CONF-9110280–1; ON: DE92003447, Argonne National Lab., IL (United States)

Pietrinferni, A., Cassisi, S., Salaris, M., & Castelli, F. 2004, The Astrophysical Journal, 612, 168

Pols, O. R., Schröder, K.-P., Hurley, J. R., Tout, C. A., & Eggleton, P. P. 1998, Monthly Notices of the Royal Astronomical Society, 298, 525

Pols, O. R., Tout, C. A., Eggleton, P. P., & Han, Z. 1995, Monthly Notices of the Royal Astronomical Society, 274, 964

Rasool, S. I. & De Bergh, C. 1970, Nature, 226, 1037

Rüedi, I., Solanki, S. K., Mathys, G., & Saar, S. H. 1997, Astronomy and Astrophysics, 318, 429

Rye, R., Kuo, P. H., & Holland, H. D. 1995, Nature, 378, 603

Saffe, C., Gómez, M., & Chavero, C. 2005, Astronomy and Astrophysics, 443, 609

Santos, N. C., Bouchy, F., Mayor, M., et al. 2004, Astronomy and Astrophysics, 426, L19

Scharf, C. A. 2006, The Astrophysical Journal, 648, 1196

Schopf, J. W. 1993, Science, 260, 640

Schröder, K.-P. & Connon Smith, R. 2008, Monthly Notices of the Royal Astronomical Society, 386, 155

Schröder, K.-P., Pols, O. R., & Eggleton, P. P. 1997, Monthly Notices of the Royal Astronomical Society, 285, 696

Segura, A., Krelove, K., Kasting, J. F., et al. 2003, Astrobiology, 3, 689

Selsis, F., Kasting, J. F., Levrard, B., et al. 2007, Astronomy and Astrophysics, 476, 1373

Setlow, R. & Doyle, B. 1954, Biochimica et Biophysica Acta, 15, 117

Setlow, R. B. 1974, Proceedings of the National Academy of Science, 71, 3363

Shkolnik, E., Walker, G. A., & Bohlender, D. A. 2003, The Astrophysical Journal, 597, 1092

Shkolnik, E., Walker, G. A. H., Bohlender, D. A., Gu, P. G., & Kürster, M. 2005, The Astrophysical Journal, 622, 1075

Siess, L. 2006, Astronomy and Astrophysics, 448, 717

Skumanich, A. 1972, The Astrophysical Journal, 171, 565

Smith, R. C. & Baker, K. S. 1981, Applied Optics, 20, 177

Southworth, J., Dominik, M., Jørgensen, U. G., et al. 2011, Astronomy and Astrophysics, 527, A8

Tinney, C. G., Butler, R. P., Marcy, G. W., et al. 2001, The Astrophysical Journal, 551, 507

Toupance, G., Bossard, A., & Raulin, F. 1977, Origins of Life and Evolution of Biospheres, 8, 259

Ulmschneider, P. 1990, in ASP Conference Series, Vol. 9, Cool Stars, Stellar Systems, and the Sun: Sixth Cambridge Workshop, ed. G. Wallerstein (Astronomical Society of the Pacific), 3–14

Underwood, D. R., Jones, B. W., & Sleep, P. N. 2003, International Journal of Astrobiology, 2, 289

VandenBerg, D. A., Bergbusch, P. A., & Dowler, P. D. 2006, The Astrophysical Journal Supplement Series, 162, 375

Walker, J. C. G. 1985, Origins of Life and Evolution of the Biosphere, 16, 117

Williams, D. M. & Kasting, J. F. 1997, Icarus, 129, 254

Williams, D. M., Kasting, J. F., & Wade, R. A. 1997, Nature, 385, 234

Williams, D. M. & Pollard, D. 2002, International Journal of Astrobiology, 1, 61

Wittenmyer, R. A., Endl, M., & Cochran, W. D. 2007, The Astrophysical Journal, 654, 625

Wolszczan, A. & Frail, D. A. 1992, Nature, 355, 145

Biographical Statement

Satoko Sato was born in Tochigi, Japan in 1986, and raised in Nara, Japan until moving to Arlington, Texas in 2004. She received her B.S. in Physics from the University of Texas at Arlington in December 2009. She received her Ph.D. in Physics from the University of Texas at Arlington in May 2014. She became interested in astrobiology while taking an astrobiology class from Dr. Cuntz in her junior year at UTA. Also, she began to take an interest in stellar evolution during the course of her research for Ph.D. dissertation. Another field of her interest is aerospace engineering.